Escola de Camins
Escola Tècnica Superior d'Enginyeria de Camins, Canals i Ports
UPC BARCELONATECH

Determination of groundwater flow based on temperature data

TREBALL FINAL DE MÀSTER

Treball realitzat per:
Carlos Casanovas López-Amor

Dirigit per:
Jesús Carrera Ramírez
Francisco Javier Sánchez Vila

Màster en:
Enginyeria de Camins, Canals i Ports

Barcelona, 23 de juny del 2016

Departament d'enginyeria civil i ambiental

UNIVERSITAT POLITECNICA DE CATALUNYA

Determination of groundwater flow based on temperature data

by

Casanovas López-Amor, Carlos

A thesis submitted in complete fulfillment for the
Master's Degree of Civil Engineering

in the
ETSECCPB
Escola de Camins

June 23, 2016

UNIVERSITAT POLITECNICA DE CATALUNYA

Abstract

ETSECCPB
Escola de Camins

Master's Minor Thesis

by Casanovas López-Amor, Carlos

Different techniques have been used to measure the groundwater flow velocity but they are either too invasive or too inaccurate. In the present study two analytical solutions have been developed and tested to determine the unit discharge using heat as a tracer with an optical fiber. First, an analytical solution for the thermal response of the fluctuations of sea temperature has been developed and verified. The model considers a porous medium through which water flows and a boundary with prescribed temperature representing the fluctuations of the sea. The measuring point depth and the unit discharge define the solution. A methodology is proposed to compute the unit discharge and the depth of the measuring point. Second, an analytical approach is developed for the thermal dissipation with advection from a line source. The asymptotic behavior and the final temperature for the steady state are described. Using a FEM based in Kratos, a sensitivity analysis has been carried out to understand the dependence on the unit discharge, the thermal properties of the cable and the soil. Three stages have been defined: the initial heating governed by the cable properties, the logarithmic heating defined by the thermal conductivity of the soil and the steady state defined by the unit discharge and the previous parameters. A methodology has been also proposed to estimate the unit discharge and the thermal conductivity of the soil from thermal dissipation data.

Para medir el flujo de agua subterránea se han utilizado múltiples técnicas pero resultan ser o muy invasivas o poco precisas. En el presente estudio, se han desarrollado y verificado dos soluciones analíticas para determinar el flujo subterráneo usando el calor como trazador con la ayuda de la fibra óptica. En primer lugar, se ha desarrollado y verificado una solución analítica para la respuesta térmica de las fluctuaciones de la temperatura del mar. La profundidad del punto de medida y el flujo subterráneo determinan la solución. Se propone una metodología para calcular el flujo subterráneo y la profundidad del punto de medida. En segundo lugar, se ha desarrollado una solución

analítica para la disipación térmica con advección de una fuente lineal. Se han descrito el comportamiento asintótico y la temperatura final para el estado estacionario. Con la ayuda de un programa de elementos finitos basado en Kratos, se ha llevado a cabo un análisis de sensibilidad mostrando la dependencia con el flujo, las propiedades térmicas del cable y del suelo. Se han definido tres fases: el calentamiento inicial gobernado por las propiedades del cable, el calentamiento logarítmico definido por la conductividad térmica del suelo y el estado estacionario determinado por el flujo y las propiedades precedentes. Se ha propuesto una segunda metodología para estimar el flujo subterráneo y la conductividad térmica del suelo a partir de datos de disipación térmica.

Per mesurar el flux d'aigua subterrània s'han utilitzat diverses tècniques però són molt invasives o poc precises. En el present estudi, s'han desenvolupat i verificat dues sol·lucions analítiques per a determinar el flux subterrani utilitzant la calor com a traçador amb l'ajuda de la fibra òptica. En primer lloc, s'ha desenvolupat i verificat una sol·lució analítica per a la resposta tèrmica de les fluctuacions de la temperatura del mar. La profunditat del punt de mesura i el flux subterrani determinen la sol·lució. Es proposa una metodologia per a calcular el flux subterrani i la profunditat del punt de mesura. En segon lloc, s'ha desenvolupat una sol·lució analítica per a la dissipació tèrmica amb advecció d'una font lineal. S'han descrit el comportament asimptòtic i la temperatura final per a l'estat estacionari. Amb l'ajuda d'un programa d'elements finits basat en Kratos, s'ha dut a terme una anàlisi de sensibilitat mostrant la dependència amb el flux: l'escalfament inicial governat per les propietats del cable, l'escalfament logarítmic definit per la conductivitat tèrmica del sòl i l'estat estacionari determinat pel flux i les propietats precedents. S'ha proposat una segona metodologia per a estimar el flux subterrani i la conductivitat tèrmica del sòl a partir de dades de dissipació tèrmica.

Acknowledgements

I would like to sincerely thank Jesús for his expert advice, his transmission of knowledge and his fatherly patience. I have spent ten months discovering many insights about research on hydrogeology that have contributed to my world. But hydrogeology was not the only topic, I also learned on many topics, from environmental sciences to political issues during our conversations.

I am particularly grateful for the assistance given by Enric Bonet not only for helping me with the numerical methods but also for his temple during some tough moments.

I wish to acknowledge the help provided by Sheila Fernández for her hardworking spirit and especially for her permanent availability.

I would like to thank Laura Martínez, Laura del Val and Linda Luquot for sharing their knowledge especially on field.

I would like to express my gratitude to thank Alessandro Comolli and Anatole Julian for our conversations that helped me many times to keep looking for the answer.

I would like to thank Xavier Sánchez for making this project possible.

I want to express my gratitude to Enrique Bendito for his key assistance.

I cannot forget to express my gratitude to Albert Folch for inspiring me and giving me some good advices.

I would like to thank the people from Me Distraes and

Finally, I would like to thank the CIMNE for the scholarship as well as the people that have participated in some way or other to this thoughtful research experience.

Carlos Casanovas

Contents

List of Figures

List of Tables

Chapter 1

Introduction

Management of coastal resources is an important issue because the human being has preferred to settle in coastal zones. Some resources are now in a stress situation due to the growth of the World's population, the densification of these areas and the influence of the sea level rise. Groundwater is a clear example. It is crucial to understand coastal groundwater processes and behavior because it is the safest and easiest drinking water resource in many countries.

Groundwater is part of the water cycle. Precipitation is its principal source of recharge and sea its main receiving medium in coastal regions. We encounter a mixture of saltwater and fresh water at the boundary between land and sea. Mixing may occur either in the sea or inland due to seawater intrusion. Indeed, as freshwater flows towards the sea, it floats over the sea water, which is denser. A two layer system is created: saltwater enters into the porous medium in the lower part and freshwater floats on top towards the sea. At the same time, fresh water pushes the mixture towards the sea as a result of a higher pressure, ensuring the equilibrium of the intrusion. Nevertheless, as the amount of freshwater varies over time (floods, climate cycles, pumping wells...) the system reaches a dynamic balance where the intrusion changes its nature and moves across the porous medium over time.

The description of the process is highly dependent on the nature of the system; multiple processes take place and not only the properties of the field need to be considered but also other properties of the environment. Many studies have been made with the aim of understanding seawater intrusion [1]: from creating mathematical models with a particular geomorphology ([2], [3]) to understanding the chemical behavior in the mixing zone ([4], [5]). However, it is a complex problem with multiple coupled elements. Indeed, the hydraulic conductivity of the porous medium is not the only factor that one must consider; movements caused by differences of density linked to energy transport may modify the flow pattern by creating convection cells with flow return.

Different techniques have been used to measure the flow velocity but they are either too

invasive or too inaccurate as they need internal measures of the properties of the bulk material. Over the last decades, the use of heat as a groundwater tracer has become popular. Already in the 1980s, heat was considered a potential indicator of flow velocity [6], and since then, a growing literature on this topic has been created [7]. Focusing on the latest studies, the use of distributed temperature sensing systems (DTS) to measure temperatures by means of optical fibers is one of the main innovations in this field of study [8], [9], [10]. However, as the hydraulic conductivity is very variable and heat transfer implies conduction and advection, global results were needed so that it could be applied in any global context. To this end, analytical solutions were purposed to determine the flow velocity in different contexts [11], [12], [13]. It is still needed a particular study of the analytical solutions to obtain the maximum information from them.

Being part of a global project (Mixing and dispersion in the transport of energy and solutes, ME DISTRAES), we aim to develop methods to measure the advection and other properties related with the heat transfer problem. Indeed, while studying the transport of solutes, one encounters the same Advection-Diffusion Equation (ADE) where thermal conduction is substituted by molecular solute diffusion. By sharing the same formulation one might expect that the role of heterogeneity on heat transport could be extrapolated to solute transport. However, thermal diffusion is 5 orders of magnitude faster than molecular diffusion, which makes energy transport a much more predictable phenomenon from solute transport.

Chapter 2

Field site and setting

The purpose of this chapter is to explain the procedures and techniques that have been made in the field to obtain the required data.
Section 2.1 introduces the place of study and analyses its main features. While section 2.2 presents the performed tests and its results.

2.1 Field site

The site is located in the Riera of Argentona, some 40 km North of Barcelona (Figure 2.1). It is considered a field experimental laboratory with devices to measure hydraulic, electrical, thermal and transport parameters.

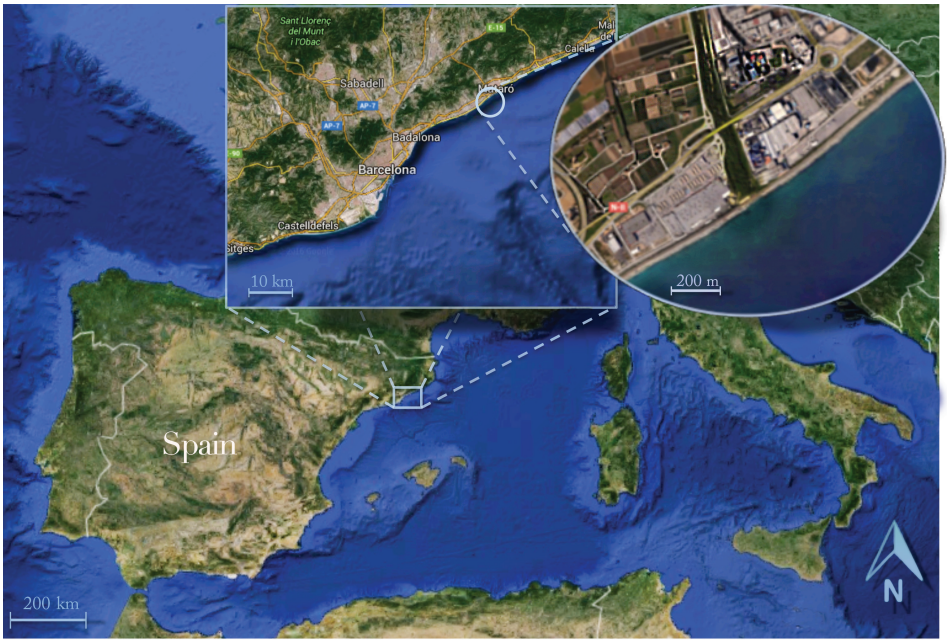

FIGURE 2.1: Site location. *Riera d'Argentona*

Climatic conditions are western Mediterranean climate conditions with moderately high temperatures in summer (average temperature of 23°C) and mild temperatures in winter

(average temperature of 10.3°C). Spring and autumn are the rainy seasons with annual precipitation ranging from 500 mm to 800 mm.
Figure 2.2 displays the regional geology of the site and its surroundings.

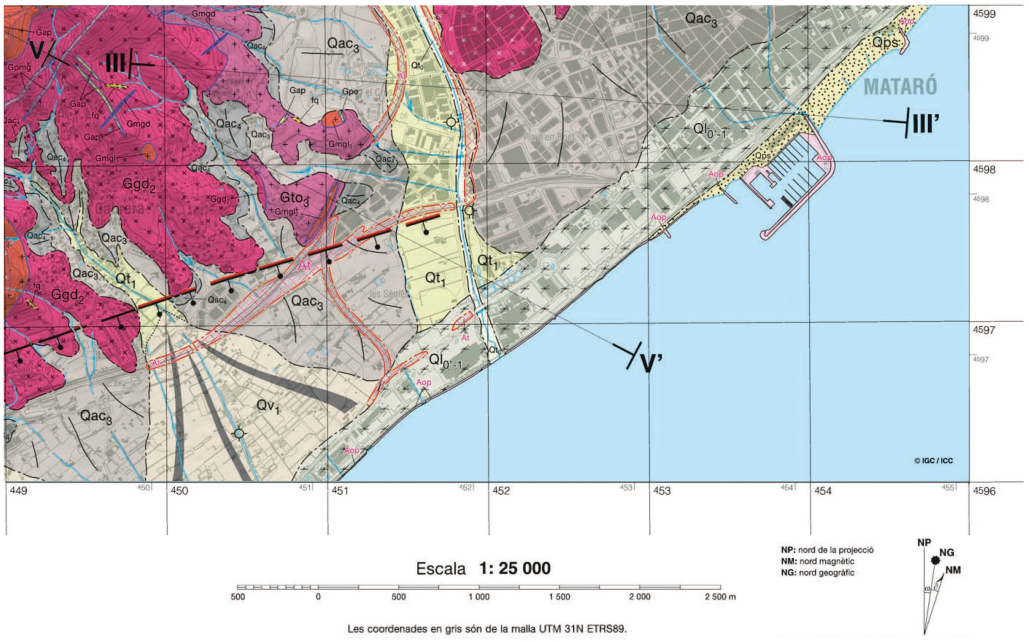

FIGURE 2.2: Geology description of the site
Modified by the author. Source: IGC and ICC, [14].

Two vertical cross sections complement the regional geology description of the zone (figures 2.4 and 2.3). They do not give accurate information of the site but they offer an approximation of what we may find.

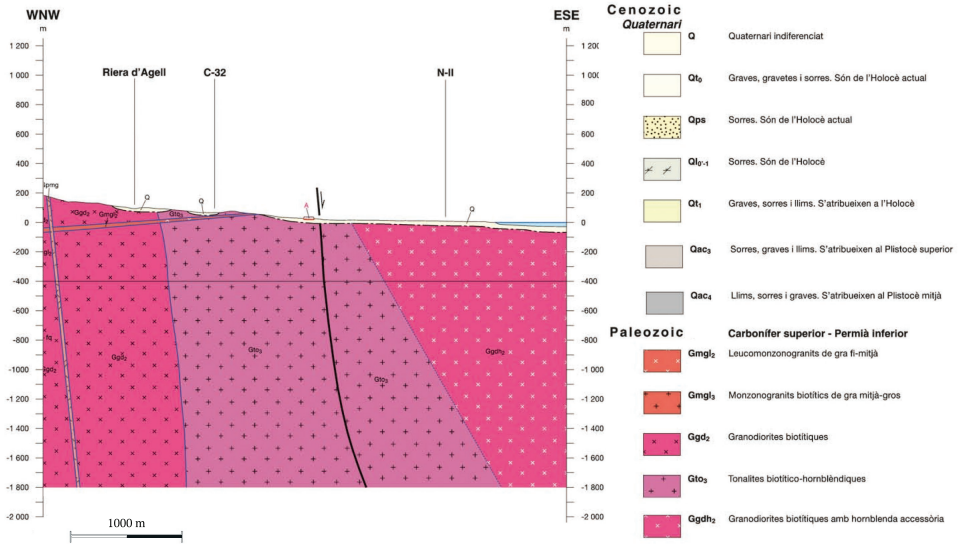

FIGURE 2.3: Vertical cross section V
(See Figure 2.2)

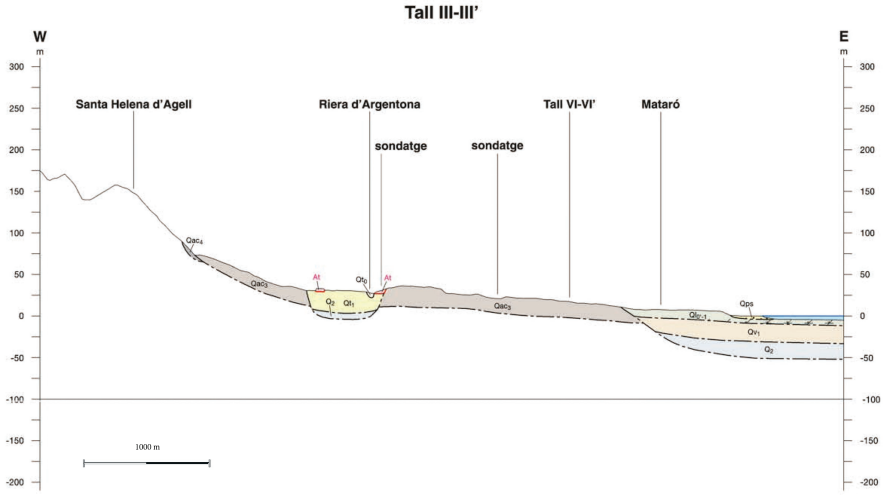

FIGURE 2.4: Vertical cross section II
(See Figure 2.2)

In a nutshell, we will find gravel, sand and silt from tonalites, granodiorites and monzogranite. All of them are considered plutonic rocks. We will find depositions of undistinguished quaternary rocks close to the surface. The studied aquifer will be considered a sandy aquifer with some silt layers.
Figure 2.5 show the dispostion of the boreholes and figure 2.6 presents the local geology of the site.

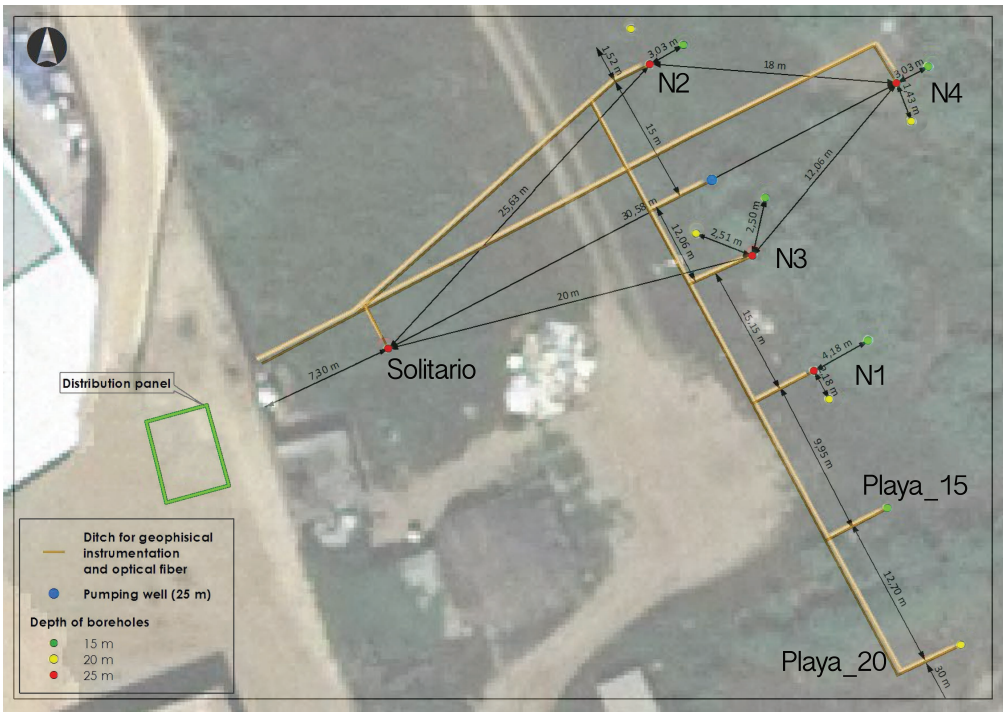

FIGURE 2.5: Site: Borehole disposition and optical fiber inland installation

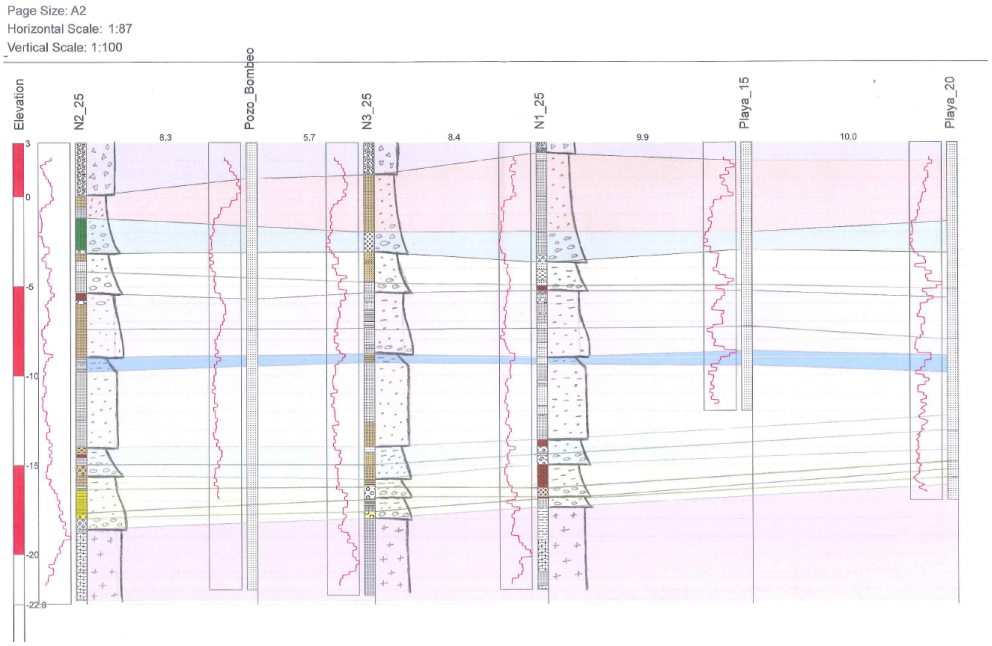

FIGURE 2.6: Local geology
(See figure 2.5)

2.2 Optical fiber

The distributed temperature sensing (DTS) system is the main measurement instrument to obtain temperature profiles. It employs light pulses in the infrared spectrum propagating in a fiber optic cable [15]. Fibre Optics Distributed Temperature Sensing (FO-DTS) employs the Raman portion of the return scattering light resulting from the reflection of a laser shot through the cable. This feature allows to obtain distributed temperature measurements at high spatial and temporal resolution. Optical fiber can measure actively and passively. The active measurement consists in injecting a heating power and studying the temperature rise during heating and its decay. Heat is applied by electrical resistance to the stainless steel tube that armors the optical fiber in our case of study (figure 2.7). On the other hand, the passive measurement consist of observing temperature without the heat source.

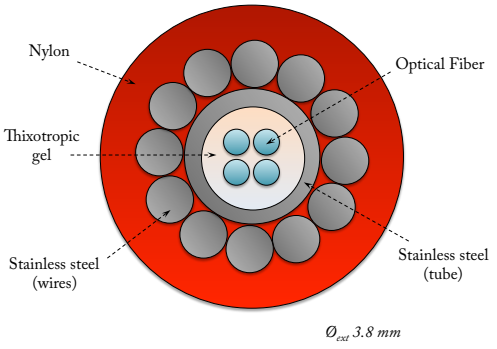

FIGURE 2.7: Optical fiber section and materials

Sixteen shallow piezometers are installed 30 m away from the seashore constituting the site. The piezometers depths range between 15 and 25 meters (figure 2.5). Twelve piezometers are put into groups of three creating four groups called *nidos* (nests). Each nest provides accurate data by combining the information of three depths.
All piezometers are equipped with optical fiber cable (Brugg Kabel AG, Switzerland) in order to perform down-hole distributed temperature measurements. Figure 2.5 shows the connection between wells and figure 2.8 describes the position of the optical fiber in a well. The optical fiber encircles the casing and covers the depth of the well. Figure 2.9 presents some data obtained from the DTS system.

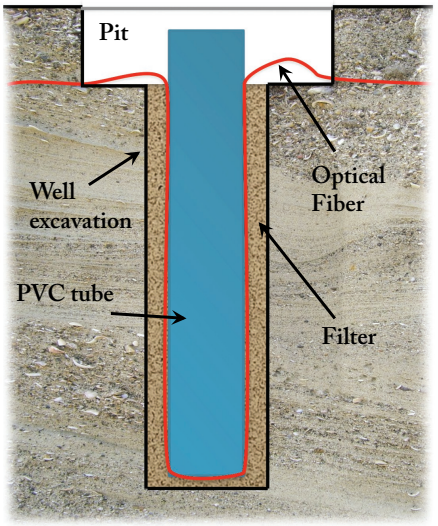

FIGURE 2.8: Optical fiber position in a well

The optical fiber is also placed offshore in the hope of characterizing groundwater discharge into the sea. It is buried some centimetres in the seafloor and it was settled in front of the site laboratory. Figure 2.10 represents the configuration of the submerged optical fiber.

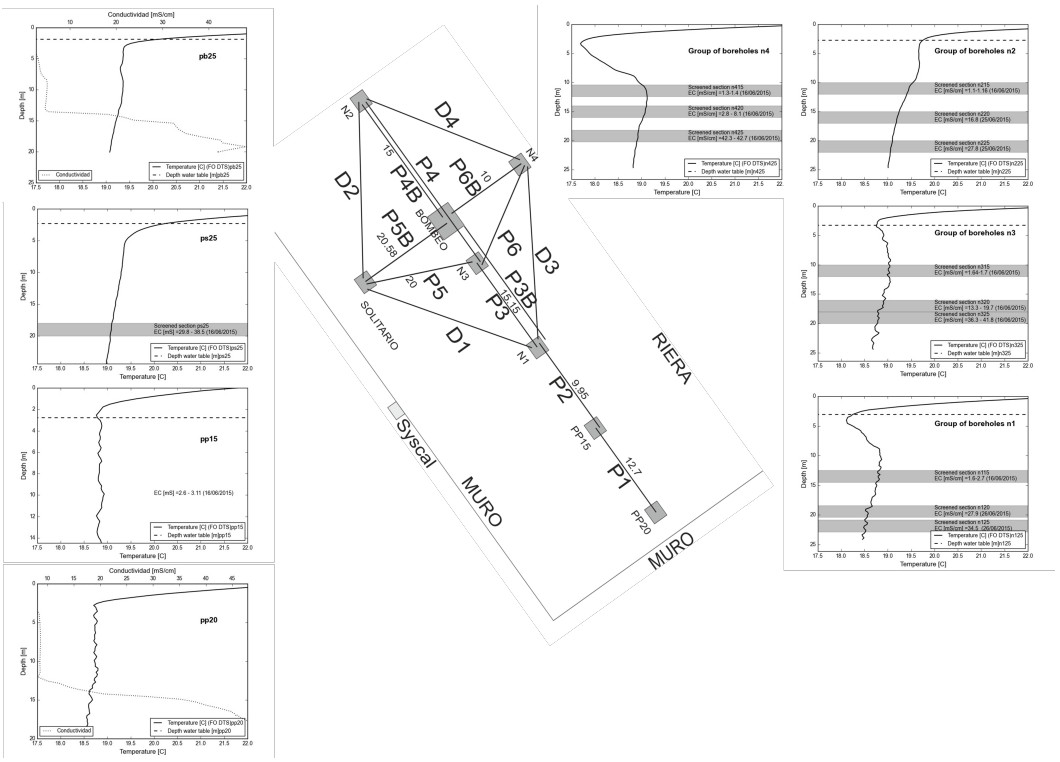

FIGURE 2.9: Fiber Optic DTS data

Data obtained from developing a optical fiber cable installed along the outer casing of each borehole (figure 2.8) in June 2015. Profiles also indicate water Electrical Conductivity measured during the same day or, if available, data from the colsest periodic manual monitoring on time. Groundwater levels are also indicated when known. The centered map indicate the distribution of the piezometers over the site.

FIGURE 2.10: Optical fiber offshore installation

Figures 2.11(a), 2.11(b), 2.11(c) and 2.11(d) show the inland equipment setting. The

picture of figure 2.11(e) was taken while the optical fiber was being settled under the seafloor.

(a) DTS central

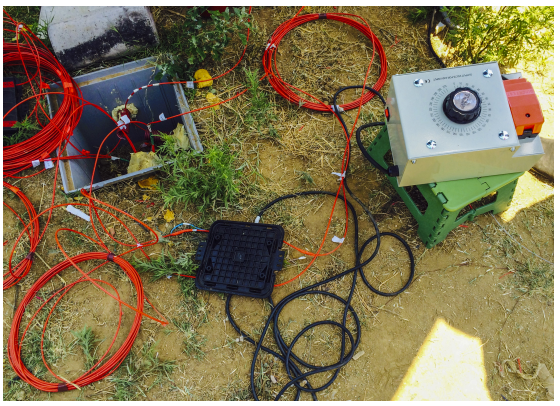

(b) Pit with piezometer and optical fiber (in red)

(c) PVC tube with optical fiber (in red)

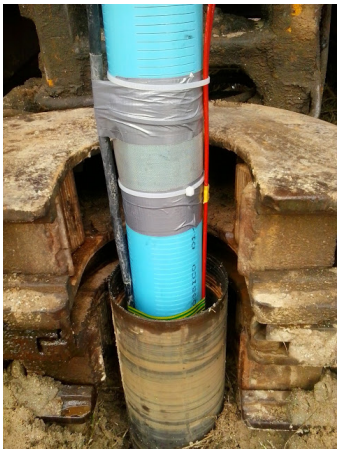

(d) Well, PVC tube and OF

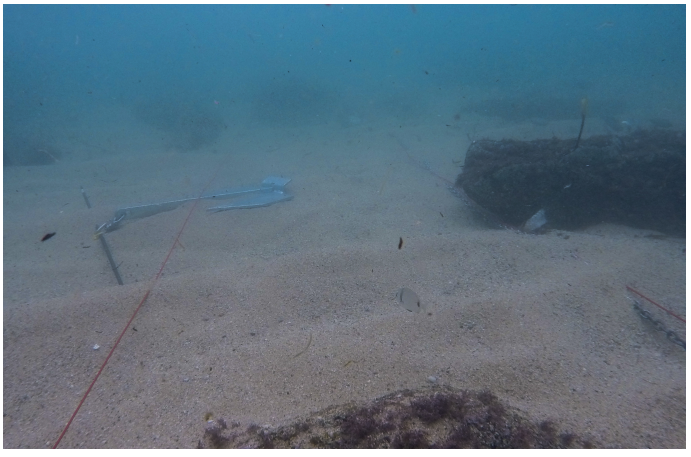

(e) Placement of the submerged optical fiber

FIGURE 2.11: Pictures of the experimental site

2.3 Material properties

Most of inputs for the model are material properties. Table 2.1 sum up the main thermal properties:

	Specific heat c (J/kg K)	**Density** ρ (kg/m^3)	**Heat capacity** $(c \cdot \rho)$ C (J/m^3 K)	**Thermal conductivity** λ (W/m K)
Water	4180	1000	$4.18 \cdot 10^6$	0.58
Solid matrix	800 – 900	2500 – 2900	$(2 – 2.61) \cdot 10^6$	3
Stainless steel	490	7850	$3.85 \cdot 10^6$	16
Nylon	1670	1140	$1.9 \cdot 10^6$	0.28
Optical fiber	754	2196	$1.66 \cdot 10^6$	1.3
Thixotropic gel	2000 – 3000	900 – 1200	$(1.8 – 3.6) \cdot 10^6$	0.2 – 0.4

TABLE 2.1: Thermal properties

The properties of the bulk are presented in table 2.2:

	Porosity ϕ (–)	**Intrinsic permeability** **k** (m^2)	**Specific storage** S_s (m^{-1})	**Dispersivity coefficients** α_L, α_T (m)
Maximum	0.3	10^{-11}	10^{-8}	0.01, 0.001
Minimum	0.1	10^{-12}	10^{-9}	-

TABLE 2.2: Bulk properties

Chapter 3

Governing equations: numerical and analytical methods

This chapter is devoted to the mathematical framework of heat transport (section 3.1) and the statement and solutions of two particular problems (section 3.2 and 3.3).

3.1 Governing equations

We consider a porous medium, defined as a continuous representation of a system composed of a solid matrix and interstitial pores typically filled with a fluid (liquid or gas). We characterise it by its porosity ϕ and the properties of its constituents (solid matrix and fluid). To study the behaviour of the porous medium, we focus on two phenomena: the movement of the fluid (3.1.1) and the energy transport (3.1.2).

3.1.1 Flow equation

To obtain the equation describing the movement of the fluid in a porous medium, we start by a mass balance of the fluid. The variation of the mass in a given volume V is due to the inflows and outflows across de boundary (∂V) and to sources and sink of fluid within the volume:

$$\frac{\partial}{\partial t}\int_V \rho_l\,\theta\,dV = \int_{\partial V} -\rho_l\,\mathbf{q}\cdot\mathbf{n}\,dS + \int_V f\,dV \tag{3.1}$$

where ρ_l $[ML^{-3}]$ is the density of the fluid; θ is the water content, i.e. a ratio between the volume of water and the volume of the porous medium, it is a dimensionless number that can range from 0 (completely dry) to the value of the materials' porosity at saturation; $\mathbf{q}$ $[MT^{-1}]$ is the water flux, $\mathbf{n}$ is the unit vector which is normal to the surface ∂V, and f $[ML^{-3}T^{-1}]$ is the sink-source term.

Using the divergence theorem[1] to get rid of boundary integrals and generalizing for any volume V,

$$\frac{\partial(\rho_l\,\theta)}{\partial t} = -\nabla\cdot(\rho_l\,\mathbf{q}) + f \tag{3.2}$$

where $\nabla\cdot$ $[L^{-1}]$ is the divergence operator. In non-saturated flow problems, the water content θ can be expressed as $\theta = \phi S_w$, where ϕ is the porosity and S_w the saturation of the porous medium.
Water flux is given by Darcy's law,

$$\mathbf{q} = -\frac{\mathbf{k}}{\mu}\cdot(\nabla\mathbf{p} + \rho_l\,\mathbf{g}) \tag{3.3}$$

where $\mathbf{q}$ $[LT^{-1}]$ is water flux (Darcy's velocity), $\mathbf{k}$ $[L^2]$ is the intrinsic permeability of the material, μ $[ML^{-1}T^{-1}]$ is the dynamic viscosity of the fluid and $\mathbf{g} = -g\mathbf{e}_z$ $[LT^{-2}]$ is the acceleration due to gravity. Darcy's law allow us to obtain the unit discharge $\mathbf{q}$ (that we call Darcy's velocity) by considering the porous medium as a continuous medium with properties of the solid matrix ($\mathbf{k}$ and ϕ) and the fluid (ρ_l and μ). Darcy's law is only valid for slow, viscous flow: Fortunately, most groundwater flow cases fall in this category. Typically any flow with a Reynolds number less than one is clearly laminar, and it would be valid to apply this law.
Substituting (3.3) into equation (3.2) yields,

$$\frac{\partial(\rho_l\,\theta)}{\partial t} = \nabla\cdot\left(\frac{\rho_l\,\mathbf{k}}{\mu}\cdot(\nabla\mathbf{p} + \rho_l\,\mathbf{g})\right) + f \tag{3.4}$$

that is the flow equation for a fluid in a porous medium considering the latter as a continuous medium after Darcy's law. In order to complete this equation, we introduce the constitutive equation, also called state function, that link the density of the fluid with the pressure, the temperature and the concentration $\rho_l(T, p, \omega)$:

$$\rho_l = \rho_{l_0}\cdot\exp\left[\alpha(T - T_0) + \beta(p - p_0) + \gamma(\omega - \omega_0)\right] \tag{3.5}$$

where α, β and γ are three parameters that depend on the nature of the fluid.

3.1.2 Heat transfer

The equation for the energy transport results from the energy balance. In our case, only thermal energy is considered. We will use the temperature as state variable. In order to link the thermal energy with the temperature, we will first introduce two physical quantities –that are related between them– :

[1] To see a more detailed process, refer to [16]

- Specific heat, c: It is defined as the change in energy stored per unit mass and per unit change in temperature. It is commonly used for pure substances.

$$c = \frac{\Delta E}{m\,\Delta T}$$

If we consider a saturated porous medium, we can compute its specific heat by taking into account both the specific heat of the mineral and water.

$$\left.\begin{aligned} m_b &= \left[\phi\rho_w + (1-\phi)\rho_s\right] V_b \\ \Delta E &= \underbrace{\phi\rho_w c_w V_b\,\Delta T}_{\Delta E_s} + \underbrace{(1-\phi)\rho_s c_s V_b\,\Delta T}_{\Delta E_l} \end{aligned}\right\} c_b = \frac{\Delta E}{m_b \Delta T} = \frac{\phi\rho_w c_w + (1-\phi)\rho_s c_s}{\phi\rho_w + (1-\phi)\rho_s} \tag{3.6}$$

where "$_s$" stands for solid, "$_b$" stands for bulk and "$_w$" stands for water.

- Volumetric heat capacity, C: It is defined as the change in energy stored per unit volume and per unit change in temperature. Typically used for mixtures, for example soil and water in a porous medium.

$$C = \frac{\Delta E}{V\,\Delta T}$$

The specific heat c and the volumetric heat capacity C are linked via the density ρ:

$$C = \rho c \tag{3.7}$$

Thermal energy can be computed on any finite volume as follows:

$$E = \int_V C_b\,T\,dV \tag{3.8}$$

Focusing again on the terms of the thermal energy balance, four processes can vary the thermal energy of the considered finite volume: two related with the surroundings (incoming and outgoing energy) and two related with internal processes (source and sink of energy):

$$\Delta E = E_{In} - E_{Out} + E_{Source} - E_{Sink} \tag{3.9}$$

Both incoming and outgoing thermal energy can be computed as the flux of energy crossing the boundary ∂V of the volume considered. The variation of energy over time can be expressed as follows:

$$\frac{dE}{dt} = \underbrace{\Phi_{In} - \Phi_{Out}}_{\partial V} + \underbrace{P_{Source} - P_{Sink}}_{V} = \Phi + P \tag{3.10}$$

where, Φ represents the heat transfer across the boundary while P represents the creation-disappearance of thermal energy within the volume.

Heat transfer can occur through three main mechanisms: advection, conduction and radiation. On the other hand, we have to consider the dispersion by the fact that we are dealing with an heterogeneous medium even if we are treating it as homogeneous. All mechanisms cause energy transfer across the boundary. Hence, to compute the flow of energy through the boundary we have;

$$\Phi = -\int_{\partial V} \mathbf{J} \cdot \mathbf{n} \, dS \tag{3.11}$$

where $\mathbf{J}$ is the local heat flux vector that represents the flow of energy per unit of area and per unit of time in $[MT^{-3}]$ and $\mathbf{n}$ is the normal to ∂V.

Advection is the transport mechanism of any attribute that can be dragged by the fluid. In our case, we consider the dragging of energy, so the advection heat flux[2] is:

$$\mathbf{J_A} = \mathbf{q} C_w \Delta T \tag{3.12}$$

where $\mathbf{q}$ $[LT^{-1}]$ is the discharge per unit of surface that in our case is the Darcy's velocity, and $C_w \Delta T$ is the energy per unit volume of flowing water.

Conduction is the flow of internal energy from a region of higher temperature to one of lower temperature by the interaction of the adjacent particles (atoms, molecules, ions, electrons, etc.) in the intervening space. The conduction flux described by Fourier's law reads:

$$\mathbf{J_C} = -\lambda \cdot \nabla \mathbf{T} \tag{3.13}$$

where λ $[MLT^{-3}\theta^{-1}]$ represents the thermal conductivity which is a second order tensor, normally isotropic, so that it is a scalar, and $\nabla \mathbf{T}$ is the temperature gradient. Note that the flux has the same direction but opposite sense of the temperature gradient, that means that heat flows from higher to lower temperatures, as one can expect.

Radiation is the transfer of internal energy by means of electromagnetic waves. For most bodies on the Earth, this radiation lies in the infrared region of the electromagnetic spectrum. The radiation flux reads:

$$\mathbf{J_R} = \epsilon \sigma T^4 \mathbf{e}_r \tag{3.14}$$

where ϵ represents the emissivity, a dimensionless measure of a material's effective ability to emit or absorb thermal radiation from its surface; ranges from 0 (none) to 1 (maximal) and σ is the Stefan's constant[3] in $[MT^{-3}\theta^{-4}]$. However, within a porous medium the transfer of energy by radiation is usually neglected as we are working in low temperature differences, so that the net radiation flux can be considered as part of the conduction flux.

[2] Also called the local heat flux as it is energy per unit of area and per unit of time. (I.S.: $\mathrm{W/m^2}$)
[3] Stefan's constant $5.6570 \cdot 10^{-8}$ $\mathrm{W/m^2K^4}$.

Dispersion is the mechanism of transport caused by the fluctuations of the velocity relative to the average velocity of the fluid, which is the one included in the advection flux. Dispersion results from fluid turbulences, from the heterogeneity of the medium or from both. In any case, it is proportional to the dispersion tensor $\mathbf{D_p}$ $[L^2T^{-1}]$. Dispersion is highly anisotropic, i.e. the longitudinal dispersion is typically much greater than the transversal dispersion[4]. The dissipative heat flux is given by:

$$\mathbf{J_D} = -C_w \mathbf{D_p} \cdot \nabla \mathbf{T} \tag{3.15}$$

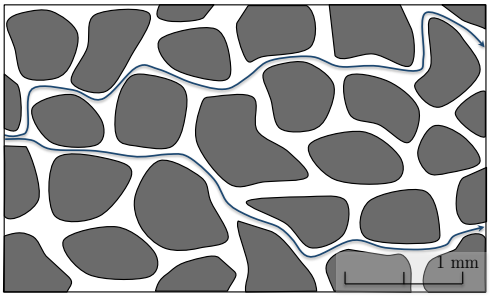

FIGURE 3.1: Dispersion caused by heterogeneity

The dispersion due to heterogeneity depends on the velocity of the flow and on a dispersion coefficient. We note α_L for the longitudinal dispersion coefficient and α_T for the transversal.

$$D_{pL} = \alpha_L \cdot |\mathbf{q}|\,, \qquad D_{pT} = \alpha_T \cdot |\mathbf{q}| \tag{3.16}$$

Furthermore, the sink-source term P, in equation 3.10, represents the source (or sink) of thermal energy coming from chemical reactions, mechanical frictions or any other internal process contributing in the variation of thermal energy. Defining the volumetric power η as follows:

$$P = \int_V \eta \; dV \tag{3.17}$$

Finally, replacing the different terms of the equation (3.10) with the equations (3.8), (3.11) and (3.17):

$$\frac{d}{dt} \int_V C_b \, T \, dV = - \int_{\partial V} \mathbf{J} \cdot \mathbf{n} \; dS + \int_V \eta \; dV \qquad \forall V(t) \tag{3.18}$$

Using the divergence theorem,

$$\frac{d}{dt} \int_V C_b \, T \, dV = - \int_V \nabla \cdot \mathbf{J} \; dV + \int_V \eta \; dV \qquad \forall V(t) \tag{3.19}$$

[4] As the dispersion depends on the direction of the flow, the eigenvalues of the dispersivity tensor are different between them. The highest eigenvalue corresponds to the eigenvector that is parallel to the flow direction.

If the volume V does not depend on time, using the Reynolds transport theorem (cf. [17]) we have:

$$\int_V C_b \frac{\partial T}{\partial t}\, dV = -\int_V \nabla\cdot\mathbf{J}\; dV + \int_V \eta\; dV \qquad \forall V \tag{3.20}$$

This equation is valid for any volume, so we have the differential equation:

$$C_b \frac{\partial T}{\partial t} = -\nabla\cdot\mathbf{J} + \eta \tag{3.21}$$

As it has been seen, $\mathbf{J} = \mathbf{J_A} + \mathbf{J_C} + \mathbf{J_D}$, so we have:

$$C_b \frac{\partial T}{\partial t} = -\nabla\cdot(\mathbf{J_A} + \mathbf{J_C} + \mathbf{J_D}) + \eta \tag{3.22}$$

Replacing each heat flux term with (3.12), (3.13) and (3.15), respectively, the equation reads:

$$C_b \frac{\partial T}{\partial t} = -\nabla\cdot(\mathbf{q}\, C_w T - \lambda\cdot\nabla\mathbf{T} - C_w\mathbf{D_p}\cdot\nabla\mathbf{T}) + \eta \tag{3.23}$$

Rearranging the equation we have:

$$C_b \frac{\partial T}{\partial t} = \nabla\cdot((\lambda + C_w\mathbf{D_p})\cdot\nabla\mathbf{T}) - \nabla\cdot(\mathbf{q}\, C_w T) + \eta \tag{3.24}$$

that is a partial differential equation of second order. If all the parameters are constant, the equation is a parabolic linear equation.

If we want to estimate the speed of the heat front, we consider the material derivate of the temperature T:

$$\frac{DT}{Dt} = \frac{\partial T}{\partial t} + \mathbf{v}\cdot\nabla\mathbf{T} \tag{3.25}$$

this derivative describes the time rate of change of temperature for a material element subjected to a space-and-time-dependent macroscopic velocity field, that is the case of the fluid of the porous medium. Considering $\mathbf{q}$ and C_w constant, we rewrite the equation (3.24) so that we can find a material derivative term:

$$C_b \overbrace{\left(\frac{\partial T}{\partial t} + \frac{C_w}{C_b}\mathbf{q}\cdot\nabla\mathbf{T}\right)}^{\frac{DT}{Dt}} = \nabla\cdot((\lambda + C_w\mathbf{D_p})\cdot\nabla\mathbf{T}) + \eta \tag{3.26}$$

$$\frac{DT}{Dt} = \frac{\partial T}{\partial t} + \frac{C_w}{C_b}\mathbf{q}\cdot\nabla\mathbf{T} = \frac{\partial T}{\partial t} + \mathbf{v}\cdot\nabla\mathbf{T} \tag{3.27}$$

where $\mathbf{v}$ is the velocity of the heat front. As we want to compare this velocity with the velocity of the fluid itself, we will use the relation

$$q = \phi\, v_w$$

that links the unit discharge with the real velocity of the fluid v_w. Working with norms instead of vectors and using the relation $C_b = \phi\, C_w + (1-\phi)\, C_s$ we have:

$$\frac{C_w}{C_b} q = \frac{v_w}{R} = \frac{q}{\phi R} \quad \Rightarrow \quad R = \frac{C_b}{C_w\, \phi} = \frac{\phi\, C_w + (1-\phi)\, C_s}{C_w\, \phi} = 1 + \frac{1-\phi}{\phi} \frac{C_s}{C_w} \tag{3.28}$$

where R is called the thermal delay as it shows the difference between the velocity of the fluid and the velocity of the advected heat front; being the latter slower[5].
Once the system of equations has been properly defined, appropriate boundary conditions need to be prescribed. Various types of boundary conditions can be assigned to a given problem but we will here restrict ourselves to two different problems with two different boundary conditions. For every problem, the choice of the boundary conditions will be justified as well as other assumptions.

3.2 Thermal response to fluctuations of sea temperature

3.2.1 Problem statement

Our first problem is to find an analytical expression for the temperature fluctuations inside a porous medium through which water flows towards (or from) a boundary with prescribed fluctuating temperature. This statement is relevant for a large number of problems in groundwater including (1) estimation of inflow/outflow at the sea from temperature measurements at some depth given the seawater daily temperature fluctuations; (2) same for river inflow/outflow, (3) estimation of recharge at soil from yearly temperature fluctuations. Figure 3.2 represents the physical situation.

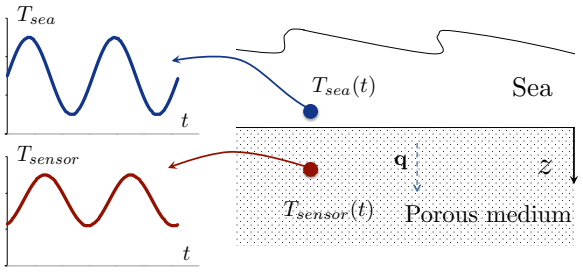

FIGURE 3.2: Sketch of the problem statement 1

To solve this problem, we make some simplifying assumptions to the heat equation 3.24:

- We decouple the heat equation from the flow equation. In fact, we assume $\mathbf{q}$ to be known and constant. We consider a uniform flow with a unit discharge $\mathbf{q} = q\, \mathbf{e}_z$. If $q > 0$, the flow enters the porous medium. On the contrary, if $q < 0$, the flow leaves the porous medium discharging into the sea. Finally, if $q = 0$, we are in a simple conduction problem as there is no movement of the fluid. This uniform

[5]Note that this velocity does not consider heat conduction.

assumption is also justified as the variation of the underground flow velocity is small compared to its mean value.

- We consider a one dimensional problem and we call z our spatial variable. This means that advection and diffusion will only work in the z direction and thus, $T(\mathbf{x}, t) = T(z, t)$. This assumption can be justified as it is close to the natural situation.
- Our domain of study does not have sinks or sources of energy, so we consider $\eta = 0$.
- The boundary condition on $z = 0$ is defined by the temperature of the sea. In order to simplify this boundary condition, we consider the following description:

$$T(0, t) = T_c + \Delta T \sin(\omega_0 t) \tag{3.29}$$

where T_c is the centred temperature of the sea, ΔT the maximum variation of the temperature over time and ω_0 is the pulsatance or angular frequency of the sea temperature. This angular frequency may represent one of three different cycles: a year, a day or a wave cycle.for the equation

- The other boundary condition it is an infinite boundary condition ($z \to +\infty$). We admit that the porous medium has an infinite length and the temperature remains constant as we move far away from the sea. Mathematically, it can be expressed as follows:

$$\lim_{z \to +\infty} T(z, t) = T_\infty \tag{3.30}$$

where T_∞ is the temperature at infinite.

- We do not have an initial time, i.e. $t \in [-\infty, +\infty]$.

With all this assumptions the problem can be stated:

$$\begin{cases} C_b \dfrac{\partial T}{\partial t} = (\lambda + C_w D_p) \dfrac{\partial^2 T}{\partial z^2} - q C_w \dfrac{\partial T}{\partial z} & \text{[PDE]} \\ \\ \begin{cases} T(0, t) = T_c + \Delta T \sin(\omega_s t) \\ \\ \lim\limits_{z \to +\infty} T(z, t) = T_\infty \end{cases} & \text{[BC]} \end{cases} \tag{3.31}$$

3.2.2 Solution

The equation 3.31 was solved using the Fourier transform and finding the eigenvalues and eigenfunctions of the transformed equation. Appendix A offers a detailed resolution for the stated problem. To compute the analytical solution, first we have to compute the following values:

- Dimensionless depth z_D:

$$z_D = \frac{z}{L} \tag{3.32}$$

where L is the characteristic length, it is chosen arbitrarily and it does not modify the final global solution.

- Global diffusion D:

$$D = \frac{\lambda}{C_b} + \frac{D_p}{\phi R} \qquad \text{with} \quad \begin{cases} C_b = \phi\, C_w + (1-\phi)\, C_s \\ D_p = \alpha_L\, q \\ R = 1 + \dfrac{(1-\phi)}{\phi}\dfrac{C_s}{C_w} \end{cases} \tag{3.33}$$

- Péclet number in a porous medium Pe_s:

$$\mathrm{Pe}_s = \frac{Lq}{D\phi R} \tag{3.34}$$

- Characteristic time t_c and reduced frequency ω_s:

$$t_c = \frac{L\phi R}{q}, \qquad \omega_s = t_c\, \omega_o \tag{3.35}$$

- Damping function γ_+ and phase function γ_-:

$$\gamma_\pm(\omega_s) = \sqrt{\frac{1}{2}\left(\sqrt{1 + \frac{16\,\omega_s^2}{\mathrm{Pe}_s^2}} \pm 1\right)} \tag{3.36}$$

The analytical solution depends on the direction of the flow.

- Case $\mathbb{A}$: For an outgoing flow ($q < 0$ and thus $\mathrm{Pe}_s < 0$ and $\omega_s < 0$) the analytical solution reads:

$$\begin{aligned} T(z,t) \quad &= (T_m - T_\infty)\, e^{-|\mathrm{Pe}_s| z_D} + T_\infty \\ &+ \Delta T\, \exp\left(-\frac{|\mathrm{Pe}_s|}{2}\,(1+\gamma_+(\omega_s))\, z_D\right) \sin\left(-\frac{|\mathrm{Pe}_s|}{2}\gamma_-(\omega_s) z_D + \omega_o t\right) \end{aligned} \tag{3.37}$$

- Caso $\mathbb{B}$: For an incoming flow ($q > 0$ and thus $\mathrm{Pe}_s > 0$ and $\omega_s > 0$) the analytical solution reads:

$$T(z,t) = T_m + \Delta T\, \exp\left(-\frac{|\mathrm{Pe}_s|}{2}\,(\gamma_+(\omega_s) - 1)\, z_D\right) \sin\left(-\frac{|q|}{2D\phi R}\gamma_-(\omega_s) z_D + \omega_o t\right) \tag{3.38}$$

Two approximations are presented: for small and large unit discharges.

3.2.2.1 Small unit discharge approximation

Considering a small unit discharge $|q| \ll 1$, we get the following asymptotic expressions:

- Case $\mathbb{A}$: Outgoing Flow ($\mathrm{Pe}_s < 0\,,\ \omega_s < 0$, i.e. $q < 0$) with $|q| \ll 1$:

$$\begin{aligned} T(z,t) \simeq \quad &(T_m - T_\infty) \exp\left(-\frac{|q|}{D\phi R} z\right) + T_\infty \\ &+ \Delta T\, \exp\left(-\sqrt{\frac{\omega_o}{2D}}\, z\right) \sin\left(-\sqrt{\frac{\omega_o}{2D}}\, z + \omega_o t\right) \end{aligned} \tag{3.39}$$

- Caso $\mathbb{B}$: Incoming Flow ($\mathrm{Pe}_s > 0\,,\ \omega_s > 0$, i.e. $q > 0$) with $|q| \ll 1$:

$$T(z,t) \simeq T_m + \Delta T \exp\left(-\sqrt{\frac{\omega_o}{2D}}\, z\right) \sin\left(-\sqrt{\frac{\omega_o}{2D}}\, z + \omega_o t\right) \tag{3.40}$$

3.2.2.2 Large unit discharge approximation

Considering a large unit discharge $|q| \gg 1$, we get the following asymptotic expressions:

- Case $\mathbb{A}$: Outgoing Flow ($\mathrm{Pe}_s < 0\,,\ \omega_s < 0$, i.e. $q < 0$) with $|q| \gg 1$:

$$\begin{aligned} T(z,t) \quad &= (T_m - T_\infty) \exp\left(-\frac{|q|}{D\phi R} z\right) + T_\infty \\ &+\Delta T \exp\left(-\frac{|q|}{D\phi R} z\right) \sin\left(-\frac{\phi R}{|q|}\omega_o z + \omega_o t\right) \end{aligned} \tag{3.41}$$

- Caso $\mathbb{B}$: Incoming Flow ($\mathrm{Pe}_s > 0\,,\ \omega_s > 0$, i.e. $q > 0$) with $|q| \gg 1$:

$$T(z,t) = T_m + \Delta T \exp\left(-D\left(\frac{\phi R}{|q|}\right)^3 z\right) \sin\left(-\frac{\phi R}{|q|}\omega_o z + \omega_o t\right) \tag{3.42}$$

3.3 Thermal dissipation from a line source

3.3.1 Problem statement

Our second problem is to find an analytical expression for the temperature created by a line source inside a porous medium through which water flows. This statement is relevant for the quantification of the groundwater flow in terms of unit discharge and material properties. Figure 3.3(a) represents the physical situation.

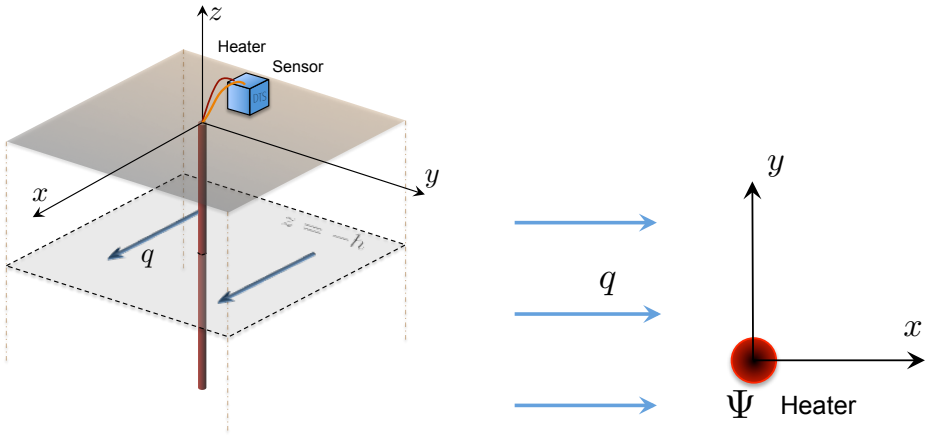

(a) 3D sketch (b) 2D sketch at $z = -h$

FIGURE 3.3: Sketch of the problem statement 2

To solve this problem, we make some simplifying assumptions to the heat equation 3.24:

- We decouple the heat equation from the flow equation. In fact, we assume q to be known and constant. We consider a uniform flow with a unit discharge $\mathbf{q} = q\,\mathbf{e_x}$ (figure 3.3). This uniform assumption is also justified as the variation of the underground flow velocity is small compared to its mean value.

- We consider a two dimensional problem and we call x and y our spatial variables. This means that all heat transfer processes will happen simultaneously at any depth z and thus they will not depend on the z component, $T(\mathbf{x}, t) = T(x, y, t)$. This assumption can be justified as it is close to the natural situation.
- Our domain of study has a source of energy in $(x, y) = (0, 0)$. As it is a point source, $\eta = \Psi\, \delta(x, y)$, $\delta(x, y)$ being the Dirac delta function.
- The domain is infinite, $(x, y) \in \mathbb{R}^2$, and the boundary conditions are imposed at infinity.
- We start applying the heat point source at $t = 0$. Our problem is valid for $t > 0$ and we have a constant initial condition at $t = 0$: $T(x, y, 0) = T_0$.

With all this assumptions the problem can be stated:

$$C_b \frac{\partial T}{\partial t} = (\lambda + C_w\, D_{pL}) \frac{\partial^2 T}{\partial x^2} + (\lambda + C_w\, D_{pT}) \frac{\partial^2 T}{\partial y^2} - q C_w \frac{\partial T}{\partial x} + \Psi\, \delta(x, y) \qquad \text{[PDE]}$$

$$T(x, y, 0) = T_0 \qquad \text{[IC]} \tag{3.43}$$

For our problem, we will use the following notation:

- Final temperature $\forall (x, y) \in \mathbb{R}^2$:

$$\lim_{t \to +\infty} T(x, y, t) \overset{\text{not.}}{=} T_f(x, y) \tag{3.44}$$

- Final temperature for $(x, y) = (0, 0)$:

$$\lim_{t \to +\infty} T(0, 0, t) = T_f(0, 0) \overset{\text{not.}}{=} T_f \tag{3.45}$$

- Temperature evolution for $(x, y) = (0, 0)$:

$$T(0, 0, t) \overset{\text{not.}}{=} T(t) \tag{3.46}$$

3.3.2 Solution

The equation 3.43 was solved using the Fourier transform and finding the eigenvalues and eigenfunctions of the transformed equation. Appendix B offers a detailed resolution for the stated problem. To compute the integral analytical solution, first we have to compute the following values:

- Dimensionless spatial variables x_D and y_D:

$$x_D = \frac{x}{L}, \qquad y_D = \frac{y}{L} \tag{3.47}$$

  where L is the characteristic length.

- Longitudinal and transversal diffusion D_L and D_T:

$$\begin{aligned} D_L &= \frac{\lambda}{C_b} + \frac{D_{pL}}{\phi R} \\ D_T &= \frac{\lambda}{C_b} + \frac{D_{pT}}{\phi R} \end{aligned} \qquad \text{with} \quad \begin{cases} C_b = \phi\, C_w + (1-\phi)\, C_s \\ D_{pL} = \alpha_L\, q \\ D_{pT} = \alpha_T\, q \\ R = 1 + \dfrac{(1-\phi)}{\phi}\dfrac{C_s}{C_w} \end{cases} \tag{3.48}$$

- Characteristic time t_c:

$$t_c = \frac{L\phi R}{q} \tag{3.49}$$

- Two Péclet numbers (for the longitudinal and transversal dispersion) Pe_L and Pe_T:

$$\mathrm{Pe}_L = \frac{Lq}{D_L\phi R} \overset{\text{not.}}{=} \frac{1}{A}, \qquad \mathrm{Pe}_T = \frac{Lq}{D_T\phi R} \overset{\text{not.}}{=} \frac{1}{B} \tag{3.50}$$

- Characteristic temperature T_c:

$$T_c = \frac{\Psi L\phi R}{C_b q} \tag{3.51}$$

The global solution reads,

$$T(x_D, y_D, t_D) = \frac{T_c}{4\pi\sqrt{AB}} e^{x_D/2A} W_H\left(\frac{Bx_D^2 + Ay_D^2}{16ABt_D}, \sqrt{\frac{Bx_D^2 + Ay_D^2}{4A^2B}}\right) \tag{3.52}$$

where,

$$W_H(u,\beta) = \int_u^{+\infty} \frac{1}{\xi} \exp\left(-\xi - \frac{\beta^2}{4\xi}\right) d\xi \tag{3.53}$$

Custodio and Llamas [16] discuss some interesting properties of this function. In particular, the asymptotic behavior when $t_D \to +\infty$ that is:

$$W_H(0,\beta) = K_0(\beta) \approx \sqrt{\frac{\pi}{2\beta}}\left(1 - \frac{1}{8\beta}\right) e^{-\beta} \qquad \text{when } \beta > 5 \tag{3.54}$$

where K_0 is the modified Bessel function of second kind and order zero.
Another possible description is:

$$T(x_D, y_D, t_D) = T_0 + \frac{T_c}{(2\pi)^2} \int_{\mathbb{R}^2} \frac{1}{\xi(k_x, k_y)} e^{ik_y y_D + ik_x x_D} \left(1 - e^{-\xi(k_x,k_y)t_D}\right) dk_y dk_x \tag{3.55}$$

where $\xi(k_x, k_y) \overset{\text{not.}}{=} \dfrac{k_x^2}{\mathrm{Pe}_L} + \dfrac{k_y^2}{\mathrm{Pe}_T} + ik_x = Ak_x^2 + Bk_y^2 + ik_x$.
An important solution is the rate of growth of the temperature for the point $(x, y) = (0, 0)$. Indeed, when we measure the evolution of temperature of the source point we

obtain[6],

$$\frac{dT}{dt} = \frac{T_c}{4\pi\sqrt{AB}} \frac{e^{-\frac{t}{4At_c}}}{t} \tag{3.56}$$

$$\frac{dT}{d(\ln t)} = \frac{T_c}{4\pi\sqrt{AB}} e^{-t/4At_c} \tag{3.57}$$

and using series expansion we can distinguish $dT/d(\ln t)$ for different cases depending on t:

$$\frac{dT}{d(\ln t)} \approx \begin{cases} \dfrac{T_c}{4\pi\sqrt{AB}} & \text{for } t \ll 4At_c \\ \dfrac{T_c}{4\pi\sqrt{AB}} \left(1 - \dfrac{t}{4At_c}\right) & \text{for } t \ll 16A^2t_c^2 \end{cases} \tag{3.58}$$

We observe that for small values of $t/4At_c$, the derivative is approximately constant and with a slope of $T_c/4\pi\sqrt{AB}$. In addition, as t increases, the slope begins to decrease (as the the first order term is negative) which leads to a stabilisation of the temperature. Considering the case where t tends to infinity:

$$\lim_{t\to+\infty} \frac{dT}{dt} = \lim_{t\to+\infty} \frac{T_c}{4\pi\sqrt{AB}} \frac{e^{-\frac{t}{4At_c}}}{t} = 0 \tag{3.59}$$

This result shows that the growth rate cancels out for $t \to +\infty$.
This final temperature is given by (3.54) and it is what will allow us to obtain the flux after obteining $\sqrt{AB}$ from (3.58).

3.4 Numerical methods

3.4.1 Computing framework and workflow

This section presents the numerical approach to the problems presented in sections 3.2 and 3.3. It consist in a Finite Element Method (FEM) based in Kratos framework [18], [19]. The application called *Flow transport application* was developed by Sheila Fernández López. It was used to model the coupling between the flow of water in a porous medium with the heat transfer within it. The geometry and discretization of the domain was made with GiD [20].
Figure 3.4 presents the process of information followed to solve both numerical problems. First, we created the geometry and generated the mesh in GiD. The results were exported and treated to create two different files (*.mdpa* and *.py*). Once the parameters had been defined and the conditions had been settled, we ran the *.py* file with Python. The solving process was done by the *Flow transport application* that uses Kratos framework. A *.res* file was created during the computing process. It collected the computed temperature

[6]The equation (3.57) is a useful equation to analyse the slope of the temperature evolution for a log-lin plot, i.e. with semi-logarithm scale (lin – Temperature; log – Time).

and pressure for the nodes of our grid at different times. Finally, the results were displayed with GiD where we could extract the information needed.

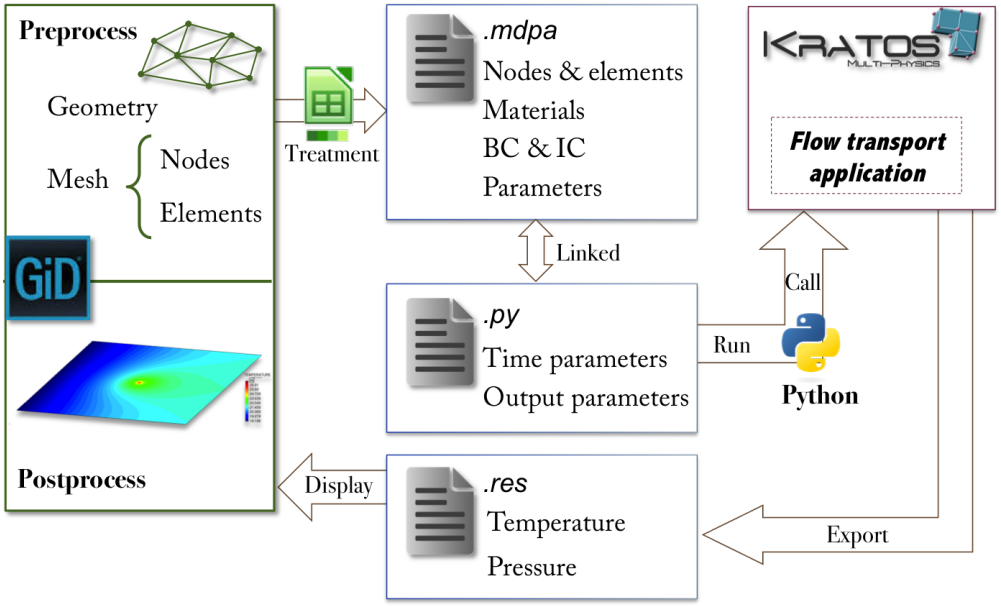

FIGURE 3.4: Process of the information for the numerical method

3.4.2 Numerical model of temperature fluctuations of the sea

We consider the domain meshed in figure 3.5: $5\,\text{m} \times 0.1\,\text{m}$

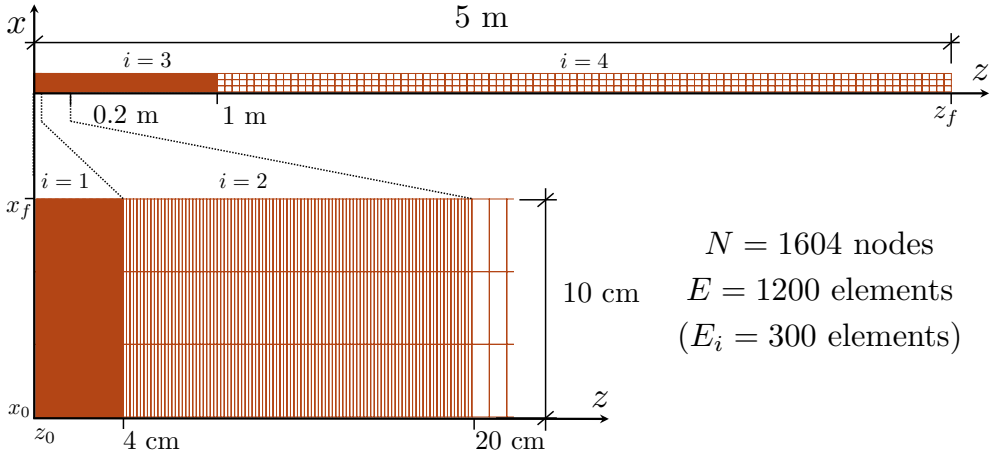

FIGURE 3.5: Mesh for the thermal response to sea thermal fluctuations

We note $\Omega \overset{\text{not.}}{=} [x_0, x_f] \times [z_0, z_f] = [0, 0.1] \times [0, 5]\ \text{m}^2$ the discretised domain and $\partial\Omega$ the boundary of the domain. We expose the boundary and initial conditions for the numerical model:

- Boundary condition for the pressure $p(x, z, t)$, $\forall t > 0$:

$$(x_0, z) = (0, z): \qquad q = -\frac{\mathbf{k}}{\mu} \left.\frac{\partial p}{\partial x}\right|_{(x_0,z)} = 0\,\mathrm{m/s} \tag{3.60}$$

$$(x_f, z) = (0.1, z): \qquad q = -\frac{\mathbf{k}}{\mu} \left.\frac{\partial p}{\partial x}\right|_{(x_f,z)} = 0\,\mathrm{m/s} \tag{3.61}$$

$$(x, z_0) = (x, 0): \qquad q = -\frac{\mathbf{k}}{\mu} \left.\frac{\partial p}{\partial z}\right|_{(x,z_0)} = q^* \tag{3.62}$$

$$(x, z_f) = (x, 5): \qquad p(x, z_f) = 49\,\mathrm{kPa} \tag{3.63}$$

  The natural condition is imposed in both boundaries (x_0, z) and (x_f, z) to avoid the flow crossing these boundaries. At (x, z_0) we impose a flow with an unit discharge q^*, i.e. a Neumann boundary condition. And at (x, z_f) we fix the pressure to 49 kPa (Dirichlet boundary condition).

- Boundary condition for the temperature $T(x, z, t)$, $\forall t > 0$:

$$(x_0, z) = (0, z): \qquad -\lambda \left.\frac{\partial T}{\partial x}\right|_{(x_0,z)} = 0\,\mathrm{W/m^2} \tag{3.64}$$

$$(x_f, z) = (0.1, z): \qquad -\lambda \left.\frac{\partial T}{\partial x}\right|_{(x_f,z)} = 0\,\mathrm{W/m^2} \tag{3.65}$$

$$(x, z_0) = (x, 0): \qquad T(x, 0, t) = \Delta T \sin \omega t \qquad t \in \mathbb{R}^+ \tag{3.66}$$

$$(x, z_f) = (x, 5): \qquad T(x, 5) = 0\,^{\mathrm{o}}\mathrm{C} \tag{3.67}$$

  The natural condition is imposed in both boundaries (x_0, z) and (x_f, z) to avoid heat transfer across the boundaries. At (x, z_0) we impose a sinusoidal temperature where ΔT is the maximum temperature reached by the boundary and ω is the angular frequency of the condition. To compute ω we use the following expression:

$$\omega = \frac{2\pi}{\tau}$$

  where τ is the period[7] of the boundary condition, for example $\tau = 1$ day if we consider the daily fluctuations of the sea. The desired condition would be at $z_f \to \infty$, but we are not able to model an infinite domain with FEM. To solve this problem, (x, z_f) we fix the temperature far from the thermal fluctuations. We consider z_f large enough to get away this boundary (x, z_f) from the thermal fluctuations.

[7] Normally, we use T for the period but in our case T represents the temperature.

- Initial condition for the pressure $p(x, z, t)$, $\forall (x, z) \in \Omega$ (at $t = 0$):

$$p(x, z, 0) = 49\,\text{kPa} \tag{3.68}$$

- Initial condition for the temperature $T(x, z, t)$, $\forall (x, z) \in \Omega$ (at $t = 0$):

$$T(x, z, 0) = 0\,^{\text{o}}\text{C} \tag{3.69}$$

3.4.3 Numerical model of the thermal dissipation of a line source

We consider the domain meshed in figure 3.6: $0.4\,\text{m} \times 0.4\,\text{m}$

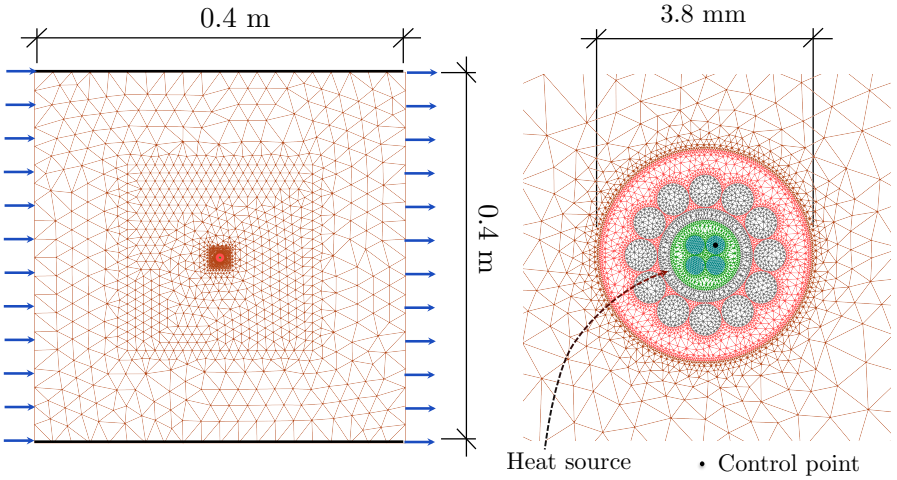

FIGURE 3.6: Mesh for the thermal dissipation of a line source

We note $\Omega \overset{\text{not.}}{=} [x_l, x_r] \times [y_d, y_u] = [-20, 20] \times [-20, 20]$ cm^2 the discretised domain and $\partial\Omega$ the boundary of the domain. We expose the boundary and initial conditions for the numerical model:

- Boundary condition for the pressure $p(x, y, t)$, $\forall t > 0$:

$$(x_l, y) = (-0.2, y): \qquad q = -\frac{\mathbf{k}}{\mu} \frac{\partial p}{\partial x}\bigg|_{(x_l, y)} = q^* \tag{3.70}$$

$$(x_r, y) = (0.2, y): \qquad p(x_r, y) = 9.81\,\text{kPa} \tag{3.71}$$

$$(x, y_d) = (x, -0.2): \qquad q = -\frac{\mathbf{k}}{\mu} \frac{\partial p}{\partial z}\bigg|_{(x, y_d)} = 0\,\text{m/s} \tag{3.72}$$

$$(x, y_u) = (x, 0.2): \qquad q = -\frac{\mathbf{k}}{\mu} \frac{\partial p}{\partial z}\bigg|_{(x, y_d)} = 0\,\text{m/s} \tag{3.73}$$

- The natural condition is imposed in all boundaries for the temperature.

- Initial condition for the pressure $p(x, y, t)$, $\forall (x, z) \in \Omega$ (at $t = 0$):

$$p(x, y, 0) = 9.81\,\text{kPa} \tag{3.74}$$

- Initial condition for the temperature $T(x, z, t)$, $\forall (x, z) \in \Omega$ (at $t = 0$):

$$T(x, y, 0) = 18\,^{\text{o}}\text{C} \tag{3.75}$$

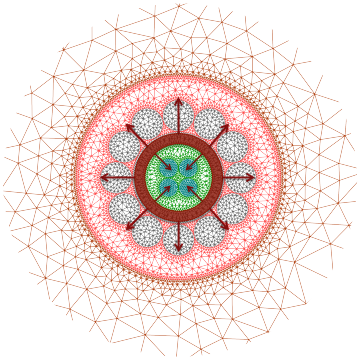

FIGURE 3.7: Source of heat

Two other elements had been considered. As the heat extends over all the domain, the boundary condition imposed at the boundaries does not fix the temperature. We have imposed a condition called *Energy Flow* to fix the temperature of the incoming flow. On the other hand, a source of heat has been fixed at the optical fiber. The tube made in metal placed in the optical fiber cable (figure 3.7) has an associated power $\eta = P^*$. As we are considering a 2D model, the units will be W/m (per unit of depth).

Chapter 4

Results

Sections 4.1 and 4.2 present the results of the two problem introduced in sections 3.2 and 3.3.

4.1 Sensitivity analysis of solutions to sea thermal fluctuations

4.1.1 Verification of the numerical code

In order to verify both the analytical and the numerical solutions for the thermal response of the medium to sea thermal fluctuations, a comparison between is needed. In the present work, the application *Flow transport application* based on Kratos framework (see section 3.4) was used to model the response of a thermal fluctuation.

The transient part of the solution is verified by imposing $T_m = T_\infty = 0\,°\text{C}$ to the analytical solutions (equations (3.37) y (3.38)). The thermal and intrinsic properties of the bulk can be found in Table 2.1 and 2.2.

Figures 4.1 and 4.2 compare the numerical and analytical solutions for outgoing and incoming flow, respectively.

Notice that the initial condition of the two models is different. The analytical model does not consider an initial condition as it was integrated $\forall t \in \mathbb{R}$. The numerical model has a constant inital condition that modifies the result during the begining of the simulation. However, it converges to the dynamic equilibrum of the analytical solution after a relatively short relaxation time. In practice, this implies that when a numerical solution is used for calibrating the model against field data (i.e., for complex cases), then a few cycles should be considered prior to actual fitting.

4.1.2 Influence of depth and unit discharge

To highlight the fact that temperature depends on depth z, Figures 4.3 and 4.4 display the evolution of temperature for different depths for an outgoing and an incoming flow,

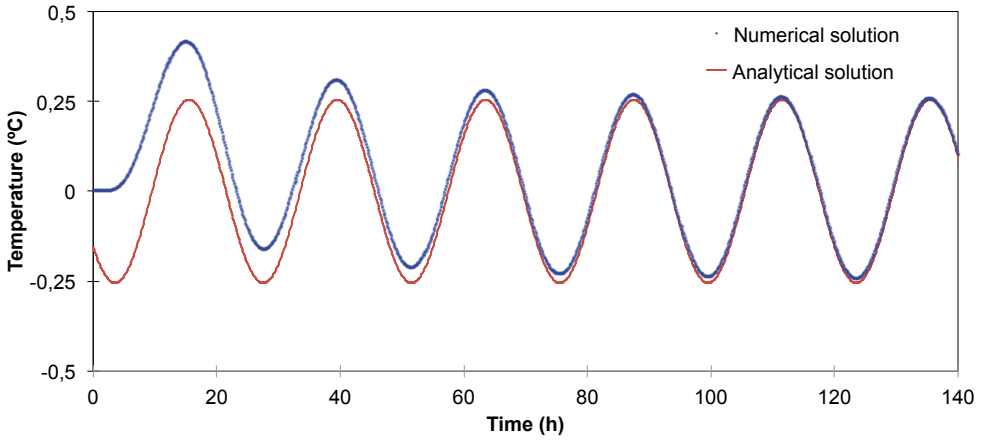

FIGURE 4.1: Comparison of the analytical and numerical model (outgoing flow)
Evolution of temperature at $z = 0.3$ m, with $q^* = -10\,\text{cm/day}$, $\Delta T = 5\,^\circ\text{C}$ and $\omega = 7.272 \cdot 10^{-5}\,\text{s}^{-1}$ ($\tau = 1\,\text{day}$). Convergence after stabilization (difference due to the initial conditions).

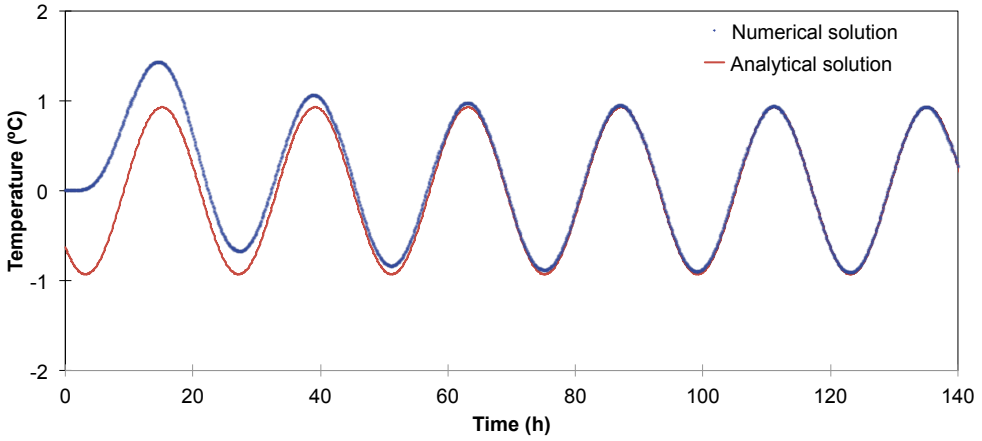

FIGURE 4.2: Comparison of the analytical and numerical model (incoming flow)
Evolution of temperature at $z = 0.3$ m, with $q^* = 20\,\text{cm/day}$, $\Delta T = 5\,^\circ\text{C}$ and $\omega = 7.272 \cdot 10^{-5}\,\text{s}^{-1}$ ($\tau = 1\,\text{day}$). Convergence after stabilization (difference due to the initial conditions).

respectively.

Figures 4.3 and 4.4 show that the phase and amplitude of the fuctuation at depth z depends on the depth. The deeper we measure the temperature, the milder the fluctuation is (i.e. the depth reduces the amplitude fluctuation). Besides, the delay between the peak of the sea temperature and the peak of the temperature of the measured point increases as we go deeper. In other words, depth increases the phase difference of the fluctuations.

We compute the thermal response at $z = 0.1\,\text{m}$ for different unit discharges in Figure 4.5 for an outgoing flow and in Figure 4.6 for an incoming flow. Taking $0\,\text{m/s}$ as reference (pure conduction), we observe that the direction of the flow plays a major role. Indeed, for an outgoing flow, we observe an attenuation of the amplitude with an increase of the unit discharge, while the amplitude increases with the unit discharge for an incoming

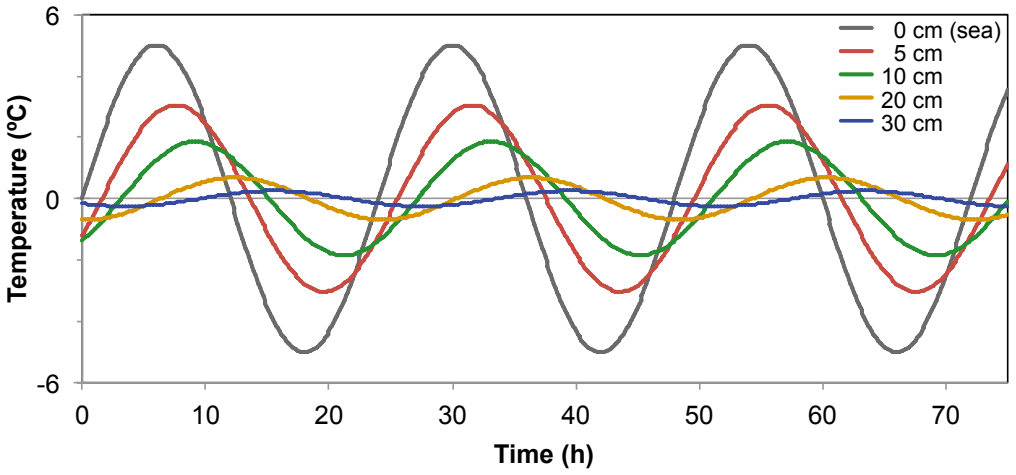

FIGURE 4.3: Evolution of temperature at different depths (outgoing flow)
Evolution of the temperature at $z = 0$ cm (grey), $z = 5$ cm (red), $z = 10$ cm (green), $z = 20$ cm (orange) and $z = 30$ cm (blue); with $q^* = -10\,\text{cm/day}$, $\Delta T = 5\,°\text{C}$ and $\omega = 7.272 \cdot 10^{-5}\,\text{s}^{-1}$ ($\tau = 1\,\text{day}$). Amplitude and phase depend on depth.

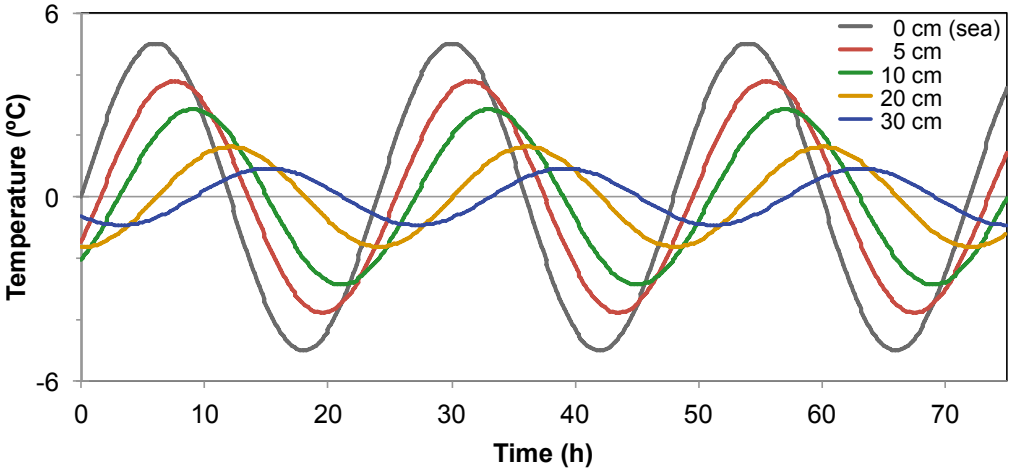

FIGURE 4.4: Evolution of temperature at different depths (incoming flow)
Evolution of the temperature at $z = 0$ cm (grey), $z = 5$ cm (red), $z = 10$ cm (green), $z = 20$ cm (orange) and $z = 30$ cm (blue); with $q^* = 20\,\text{cm/day}$, $\Delta T = 5\,°\text{C}$ and $\omega = 7.272 \cdot 10^{-5}\,\text{s}^{-1}$ ($\tau = 1\,\text{day}$). Amplitude and phase depend on depth.

flow. Both cases present a similar phase difference as they come earlier than the reference state.

To understand the effect of the unit discharge on the termal response, figure 4.7 shows the dependency of the reduced amplitud $A/A_{sea} \overset{\text{not.}}{=} A/\Delta T$ on the unit discharge q. Figure 4.8 displays the peak delay between the fluctuation of the sea and the fluctuations at a particular depth z. This delay can be measured as the elapsed time between the maximum temperature of the sea and the maximum temperature at depth z.

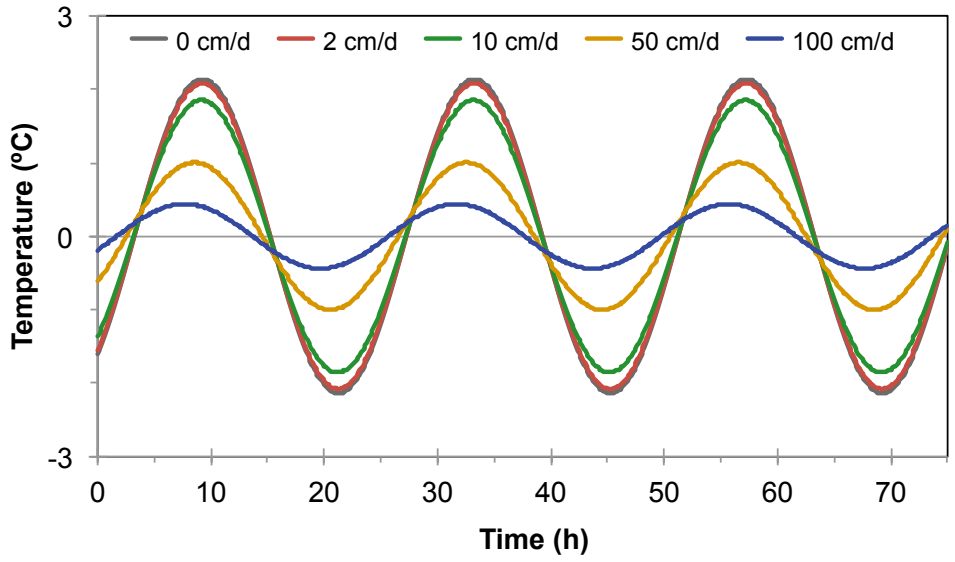

FIGURE 4.5: Temperature evolution with different unit discharges (outgoing flow)
Evolution of the temperature at $z = 10$ cm for $q^* = 0\,\text{cm/s}$ (grey), $q^* = -2\,\text{cm/s}$ (red), $q^* = -10\,\text{cm/s}$ (green), $q^* = -50\,\text{cm/s}$ (orange) and $q^* = -100\,\text{cm/s}$ (blue); with $\Delta T = 5\,°\text{C}$ and $\omega = 7.272 \cdot 10^{-5}\,\text{s}^{-1}$ ($\tau = 1\,\text{day}$). Amplitude and phase depend on unit discharge.

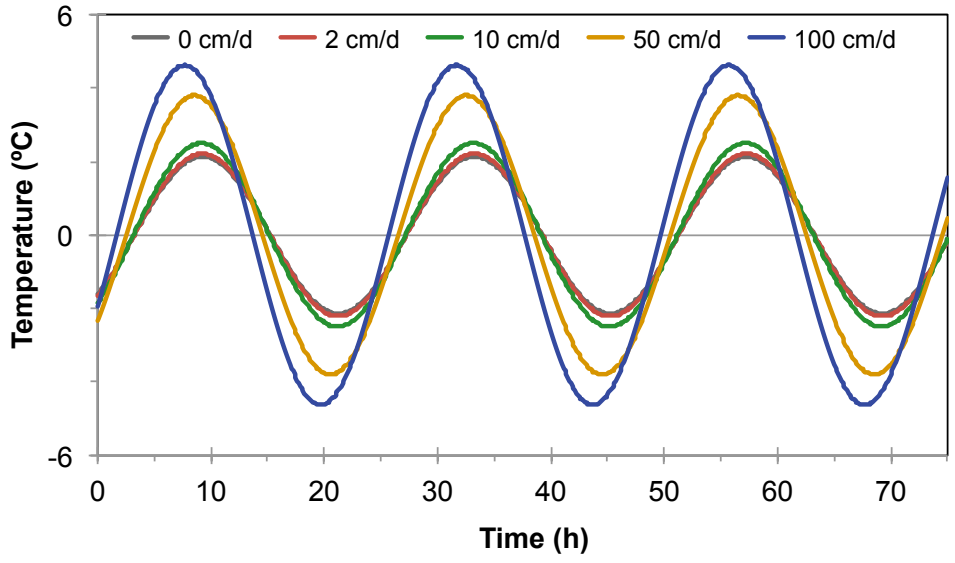

FIGURE 4.6: Temperature evolution with different unit discharges (incoming flow)
Evolution of the temperature at $z = 10$ cm for $q^* = 0\,\text{cm/s}$ (grey), $q^* = 2\,\text{cm/s}$ (red), $q^* = 10\,\text{cm/s}$ (green), $q^* = 50\,\text{cm/s}$ (orange) and $q^* = 100\,\text{cm/s}$ (blue); with $\Delta T = 5\,°\text{C}$ and $\omega = 7.272 \cdot 10^{-5}\,\text{s}^{-1}$ ($\tau = 1\,\text{day}$). Amplitude and phase depend on unit discharge.

4.1.3 Methodology to obtain the unit discharge and the depth

The aim of this subsection is to explain a methodology to compute the unit discharge and the depth of the measuring point. Appendix C contains the detailed development of this methodology.

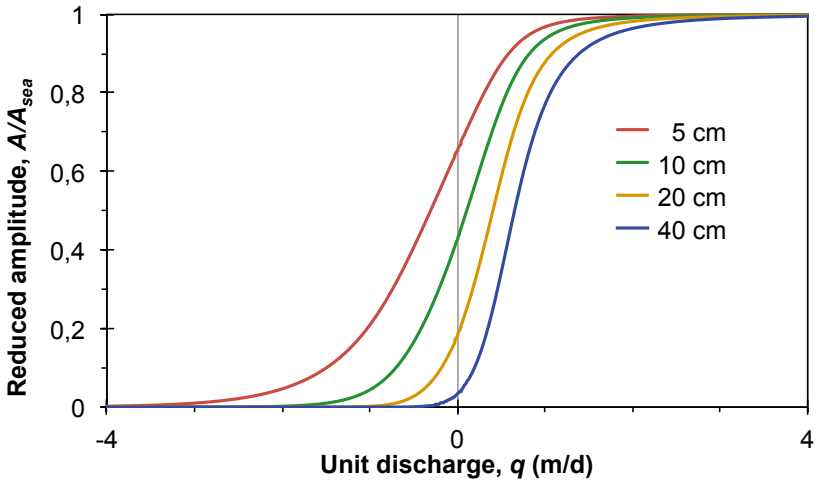

FIGURE 4.7: Amplitude dependency on unit discharge

Amplitude attenuation for an outgoing flow and amplitude intensification for an incoming flow at different depths. $z = 5$ cm (red), $z = 10$ cm (green), $z = 20$ cm (orange) and $z = 40$ cm (blue); with $\omega = 7.272 \cdot 10^{-5}\,\mathrm{s}^{-1}$ ($\tau = 1\,\mathrm{day}$).

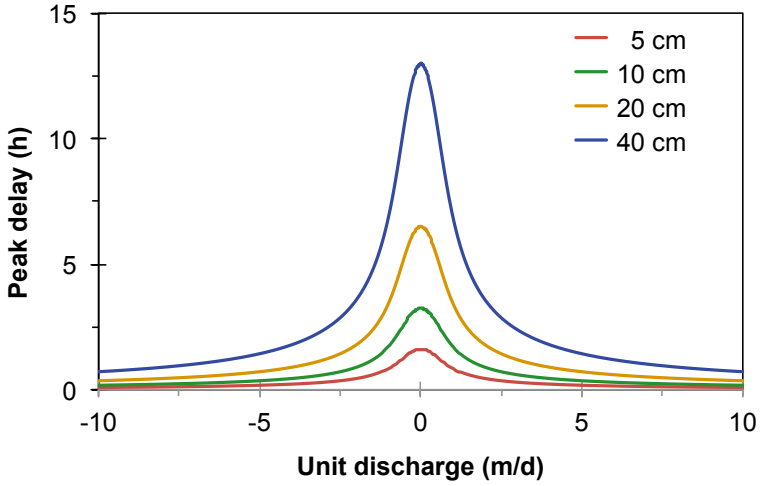

FIGURE 4.8: Peak delay dependency on unit discharge

Maximum peak delay for a pure conduction state ($q = 0\,\mathrm{m/s}$). Syncronization of the temperature fluctuations as the unit discharge increases. Amplitude attenuation for an outgoing flow and amplitude intensification for an incoming flow at different depths. $z = 5$ cm (red), $z = 10$ cm (green), $z = 20$ cm (orange) and $z = 40$ cm (blue); with $\omega = 7.272 \cdot 10^{-5}\,\mathrm{s}^{-1}$ ($\tau = 1\,\mathrm{day}$).

Once we have got the data of the evolution of the sea temperature and of the measuring point, one can find the unit discharge q and the depth z of our measuring point following the next steps:

1. We measure the period τ of our problem, i.e. the elapsed time between two peaks of the temperature. In our case, we consider the daily thermal fluctuation of the sea, so $\tau = 1$ day. We compute $\omega = 2\pi/\tau = 7.272 \cdot 10^{-5}\,\mathrm{s}^{-1}$.
2. We measure the amplitude of the sea thermal fluctuation $A_{sea} = \Delta T$ and the amplitude of the thermal response of our measuring point A_p. Then, we compute

the difference.

3. We measure the peak delay Δt: we measure the peak time for the sea temperature t_{ref} and the first peak time t_p after the reference time of our measuring point. We compute the difference: $\Delta t = t_p - t_{ref}$. We could also measure the elapsed time Δt between the peak of the sea temperature and the peak of the temperature of the measuring point, or the elapsed time between crossings of the mean temperature.
4. We compute Md:
$$\mathrm{Md} = -\frac{1}{\omega_o \Delta t} \ln\left(\frac{A_p}{\Delta T}\right) \tag{4.1}$$
where ω is the angular frequency and ln is the natural logarithm.
5. Using the figures C.3 and C.4, we find the corresponding dimensionless unit discharge r for the Md value found in step 4.
6. We compute β:
$$\beta = 2\phi R\sqrt{D\omega} \tag{4.2}$$
where $D = \lambda/C_b$ (m^2/s) is the dispersion coefficient[1], ϕ the porosity of the bulk and R the thermal delay computed as follows: $R = 1 + \frac{1-\phi}{\phi}\frac{C_s}{C_w}$ where C_s ($\mathrm{J/m^3K}$) and C_w ($\mathrm{J/m^3K}$) are the heat capacities of the solid matrix and water.
7. We compute the unit discharge q:
$$q = \beta r \tag{4.3}$$
8. The first time that we computed β, we did not consider the dispersion coefficient. We repeat steps 6 and 7 to obtain a more accurate measure. One iteration is enough to have an accurate result.
9. Once we have the unit discharge q, we compute the depth z:
$$z = \frac{\omega \Delta t \, 2D\phi R}{|q|\sqrt{\frac{1}{2}\left(\sqrt{1+\frac{\beta^2}{q^4}}-1\right)}} \tag{4.4}$$

4.2 Thermal dissipation to a line source

This section presents the sensitivity of the final temperature of the optical fiber to different properties and parameters.

[1] We will iterate in order to consider the dispersion coefficient.

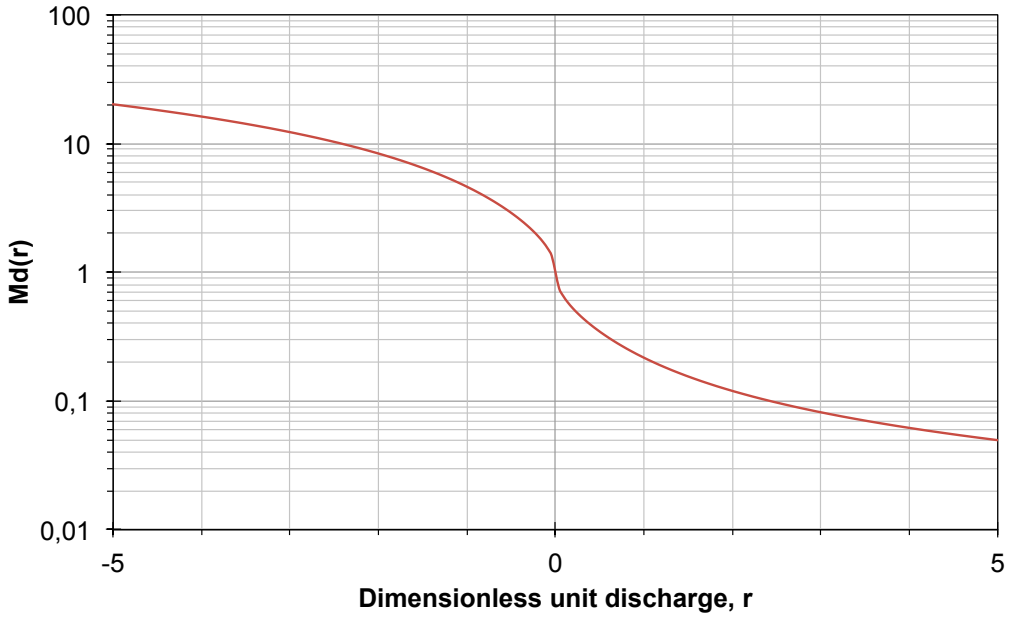

FIGURE 4.9: Md function (high values)
Lon-lin plot. The axis of abscissa represents the dimensionless variable r computed as $r = \beta q$, where $\beta = 2\phi R\sqrt{D\omega}$ and q is the demansional unit discharge.

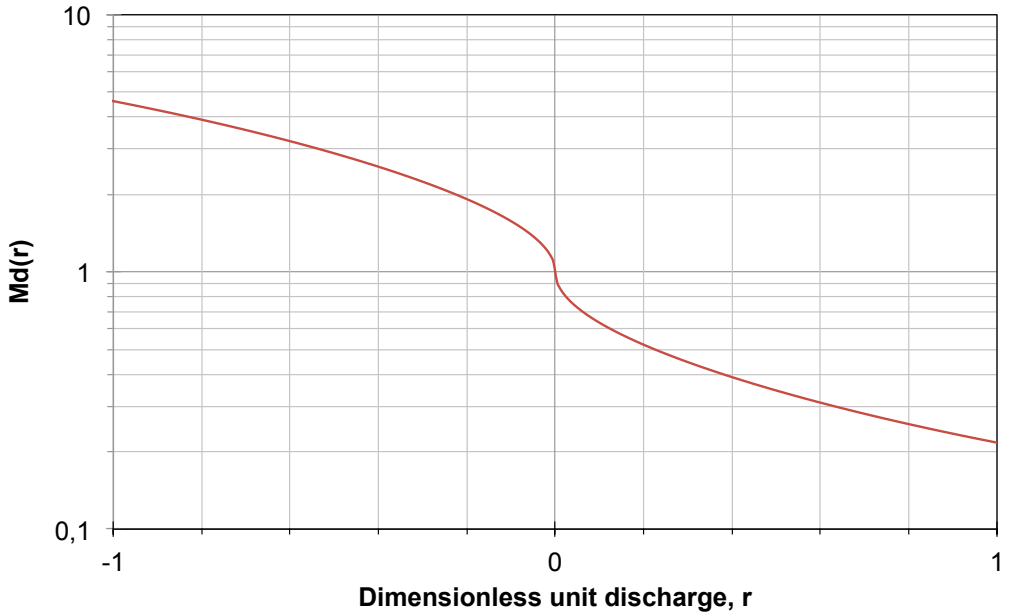

FIGURE 4.10: Md function (medium values)
Lon-lin plot. The axis of abscissa represents the dimensionless variable r computed as $r = \beta q$, where $\beta = 2\phi R\sqrt{D\omega}$ and q is the demansional unit discharge.

4.2.1 Sensitivity to the unit discharge q

The numerical results for the thermal response of a line source show the role of unit discharge during the heating process. Figure 4.12 presents the evolution of the temperature for a constant heating (supplied power) and several values of unit discharge.

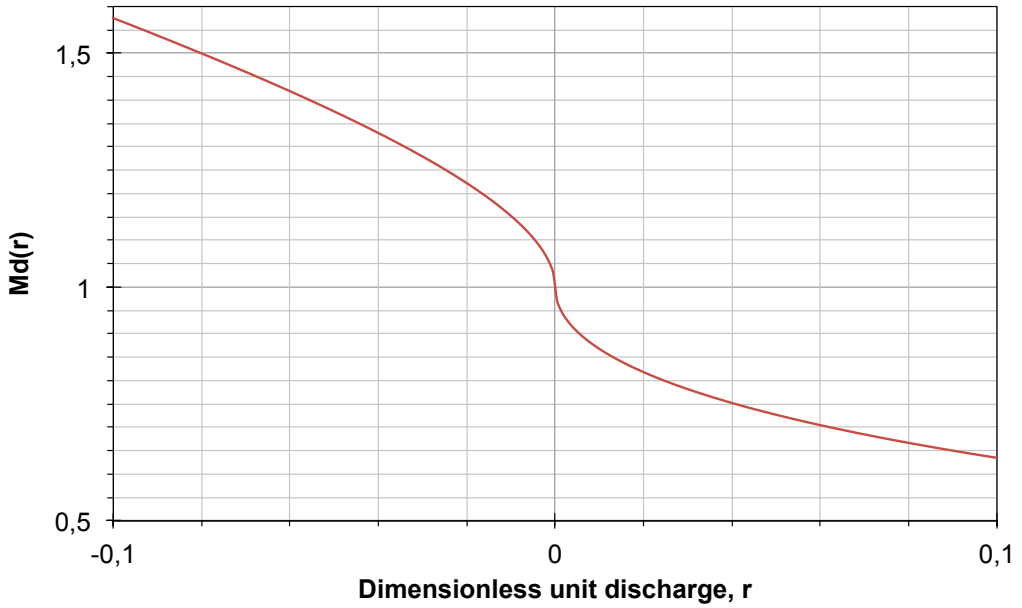

FIGURE 4.11: Md function (low values)
Lin-lin plot. The axis of abscissa represents the dimensionless variable r computed as $r = \beta q$, where $\beta = 2\phi R\sqrt{D\omega}$ and q is the demansional unit discharge.

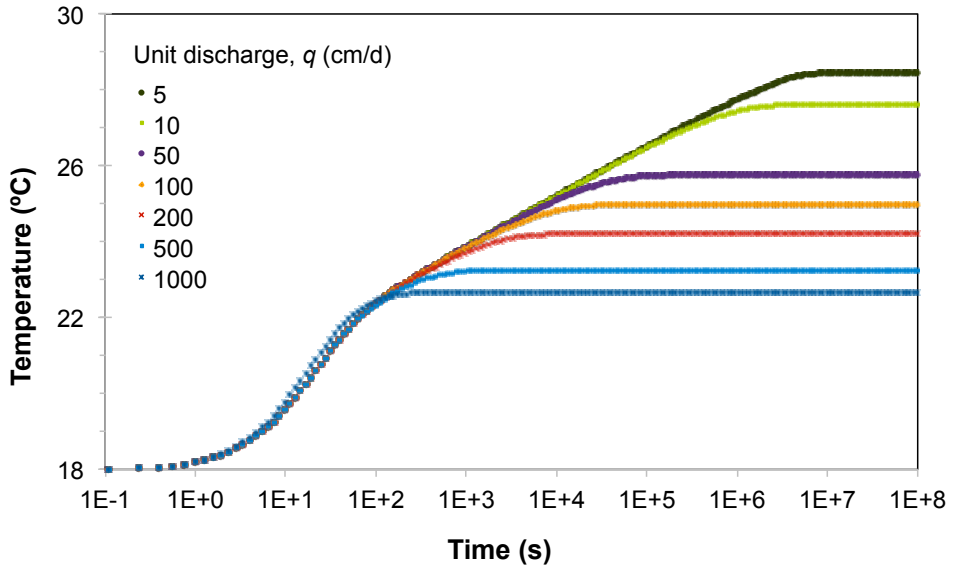

FIGURE 4.12: Evolution of the temperature for a constant heating
Temperature detected by the optical fiber for different discharges: 5 cm/d (dark green), 10 cm/d (light green), 50 cm/d (purple), 100 cm/d (orange), 200 cm/d (red), 500 cm/d (light blue), 1000 cm/d (blue). Semi-log plot.

The unit discharge has no effect on the initial heating. However, it plays an important role on the final temperature: the faster the water flows, the lower the final temperature. As expected, the flow helps energy dissipation. The final temperature is reached when the energy produced by the heating source is balanced out with the advection dissipation.

Figure 4.13 shows the dependence of the final temperature on the unit discharge.

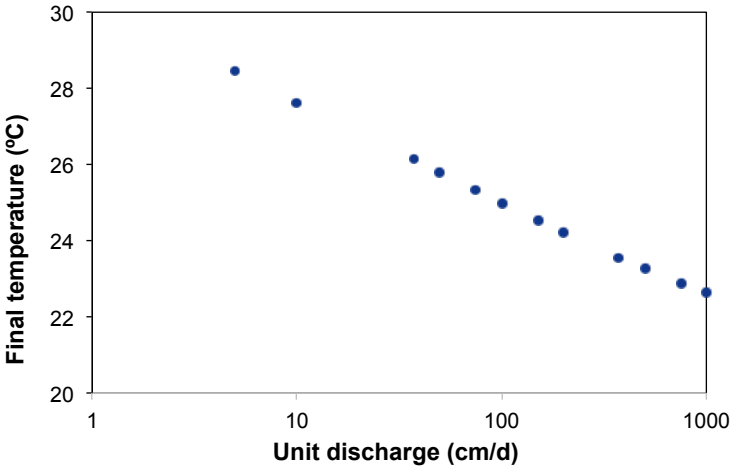

FIGURE 4.13: Dependency of the final temperature on the unit discharge. Semi-log scale.

Figure 4.14 shows the spatial distribution of the steady state temperature for four different unit discharges. The thermal plume is clearly observed in figures 4.14(c) and 4.14(d) while small boundary condition effects hinder its complete definition in figure 4.14(a). Slower flows create wider plumes. The spatial distribution of temperature solely depends on Pe.

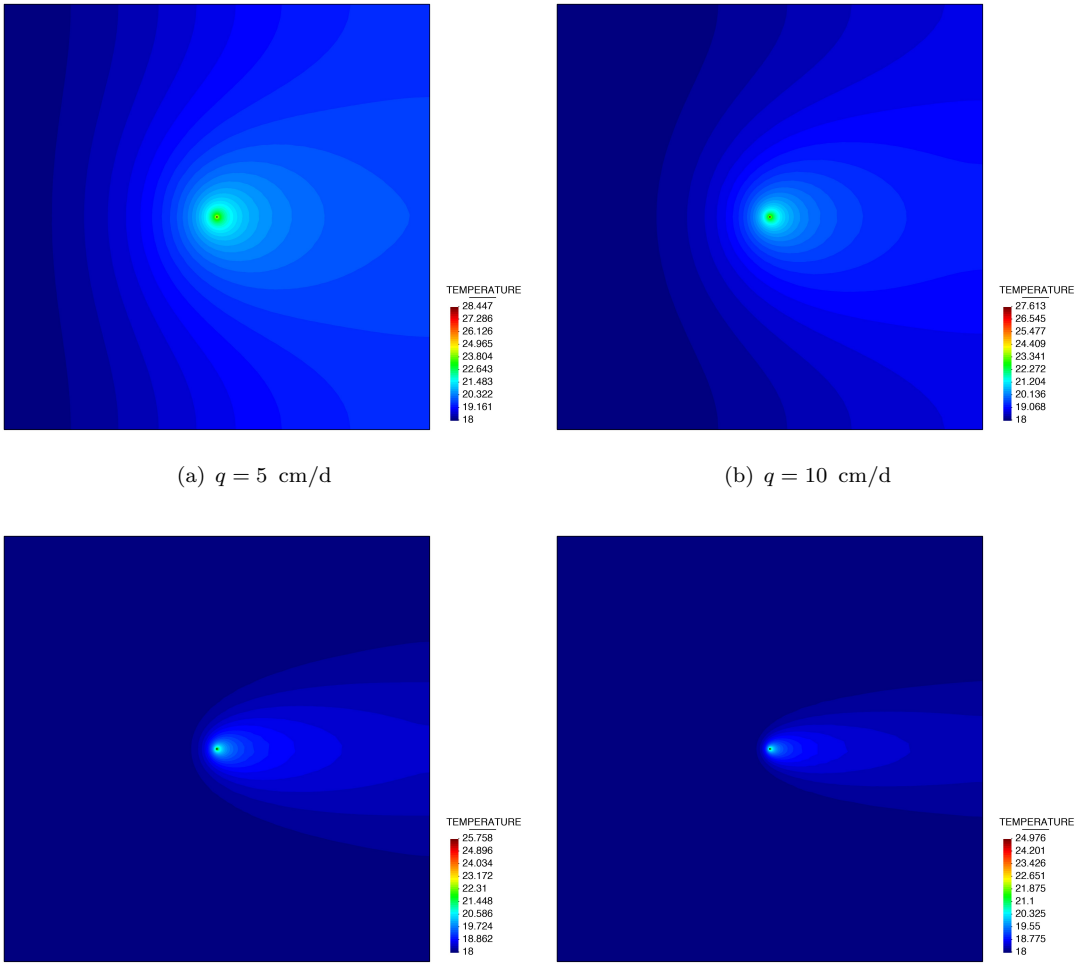

(a) $q = 5$ cm/d (b) $q = 10$ cm/d

(c) $q = 50$ cm/d (d) $q = 100$ cm/d

FIGURE 4.14: Final temperature: Snapshots for different unit discharges

4.2.2 Sensitivity to the thermal conductivity of nylon

In order to observe the effect of the properties of the optical fiber, we compare the evolution of the temperature for two different cases: An optical fiber cable covered with a high insulator material (nylon) with a low thermal conductivity, and a cable covered with a weak insulator material (decayed nylon) with a moderately high thermal conductivity for an insulator.
Figure 4.15 compares the evolution of the temperature for three different unit discharges.

Nylon's conductivity drives the evolution during the first part (initial heating). Low thermal conductivities act as a thermal barrier and hinder the heat flux to the surroundings. In terms of Fourier's law, if we have two materials (A and B) being λ_A and

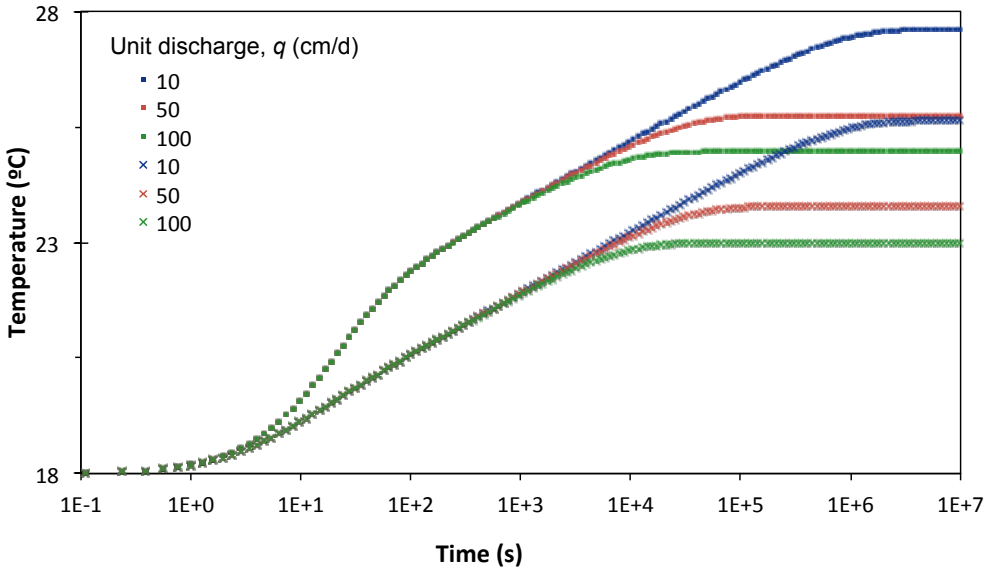

FIGURE 4.15: Evolution of the temperature for different nylon's conductivity
Temperature detected by the optical fiber for different discharges: 10 cm/d (blue), 50 cm/d (red) and 100 cm/d (green). Squares: $\lambda_{Ny} = 0.28$ W/mK. Crosses: $\lambda_{Ny} = 1$ W/mK. $P^* = 20$ W/m. Semilogarithmic plot.

λ_B their thermal conductivities, we can express the heat flux crossing both materials as,

$$\Phi_A = -\lambda_A \nabla T_A, \qquad \Phi_B = -\lambda_B \nabla T_B.$$

For the steady state, we consider the same rate of energy transfer for both materials; so we have $\Phi_A = \Phi_B$. If $\lambda_A < \lambda_B$ then the temperature gradient must be: $\nabla T_A > \nabla T_B$. For our particular problem, the thermal conductivity of the nylon layer will only change the final state by a constant shift within the fiber, but not in the soilbecause the soil will receive the same amount of thermal energy per unit of time (P^*). So if the final temperature of the soil for both situations is the same and $\nabla T_A > \nabla T_B$, then the inner final temperature must be higher for the material A, $T_A^f > T_A^f$. Figure 4.16 plots the difference of temperature over time for two different materials.
Nylon's conductivity only affects during the initial heating ($t < 5$ min). As we could expect, the difference does not depend on the unit discharge. Therefore, a preliminary calibration for the cable is needed.

4.2.3 Sensitivity to the thermal conductivity of the soil

To understand the evolution of the temperature for a constant heating, we consider different mineral conductivities. Figure 4.17 compares the evolution of the temperature for three different unit discharges in two porous media with different thermal conductivities.

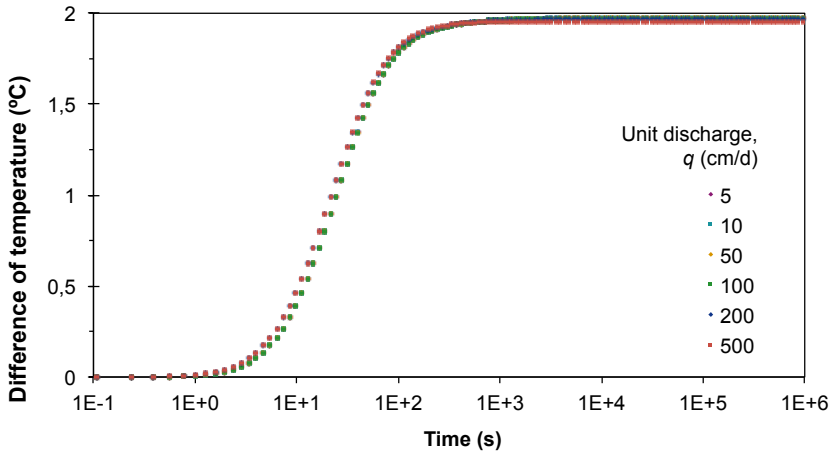

FIGURE 4.16: Temperature difference for two nylon thermal conductivities λ_{Ny} $T(\lambda_{Ny} = 0.28\,\mathrm{W/mK}) - T(\lambda_{Ny} = 1\,\mathrm{W/mK})$. The final temperature and the initial behavior during the heating process ($t < 5\,\mathrm{min}$) depend on nylon's conductivity.$P^* = 20\,\mathrm{W/m}$. Semilogaithm plot.

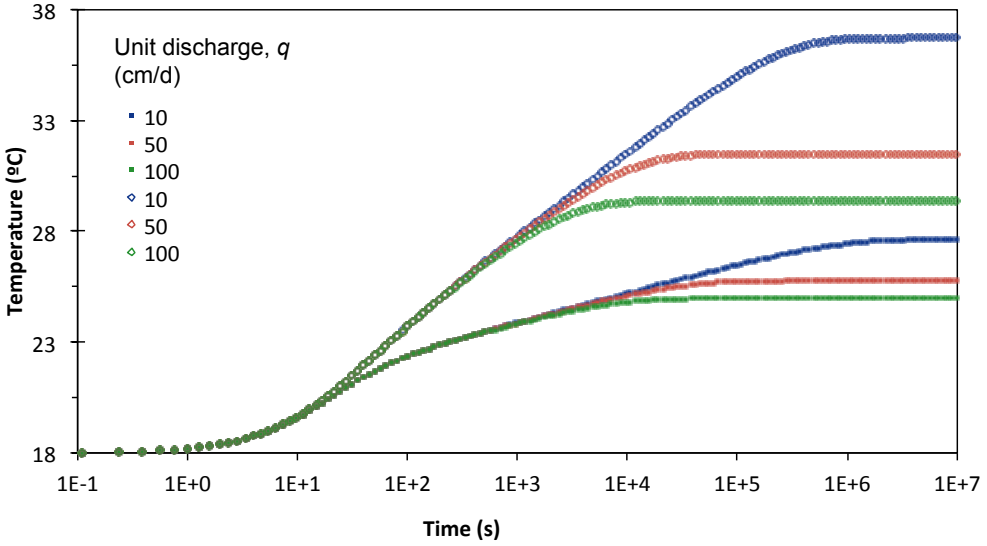

FIGURE 4.17: Evolution of the temperature for different solid matrix conductivities Temperature detected by the optical fiber for different discharges: 10 cm/d (blue), 50 cm/d (red) and 100 cm/d (green). Squares: $\lambda_s = 3\,\mathrm{W/mK}$. Empty diamonds: $\lambda_{Ny} = 1\,\mathrm{W/mK}$. $P^* = 20\,\mathrm{W/m}$. Semi-log plot.

In this case, the soil itself hinders heat dissipation, which forces the inner part to increase its temperature. This situation is similar to that of the previous analysis (nylon's conductivity) but now the soil is limitless. Figure 4.18 displays the difference of temperature of two porous media with different conductivities.

From 4.18, we observe that the conductivity of the mineral plays a crucial role after the initial heating ($t > 20\,\mathrm{s}$). The main difference is the change of the logarithmic slope.

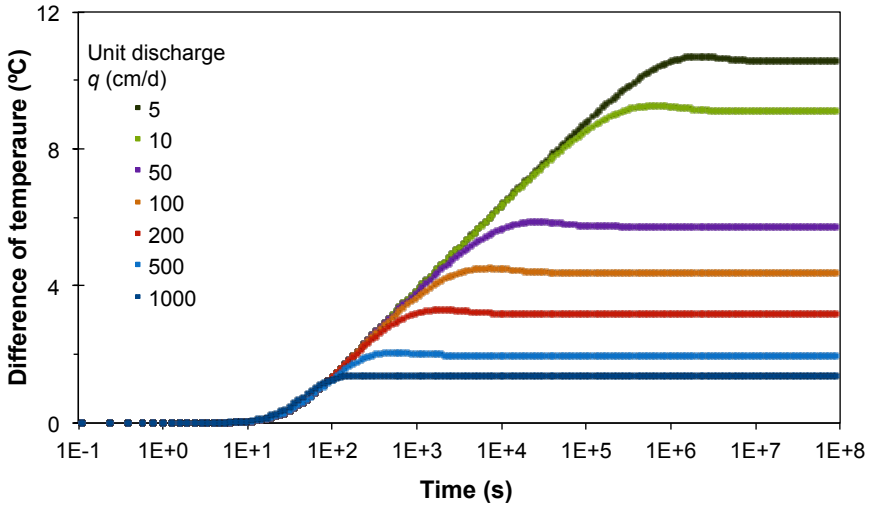

FIGURE 4.18: Temperature difference for two mineral thermal conductivities λ_s $T(\lambda_s = 1\,\mathrm{W/mK}) - T(\lambda_s = 3\,\mathrm{W/mK})$. A steeper slope for $\lambda_s = 1\,\mathrm{W/mK}$ than for $\lambda_s = 3\,\mathrm{W/mK}$. Dependency of the growth rate of the temperature on the thermal conductivity of the solid matrix. No effect detected during the initial heating ($t < 1$s). $P^* = 20\,\mathrm{W/m}$. Semilogaithm plot.

4.2.4 Sensitivity to the specific heat of the soil

Equation (3.43) shows that the specific heat of the mineral also plays a role in the evolution of the temperature. It can be considered as a time scale parameter as it only appears next to the time derivative term of the temperature. Figure 4.19 shows the difference of temperature between two porous media with different temperature.

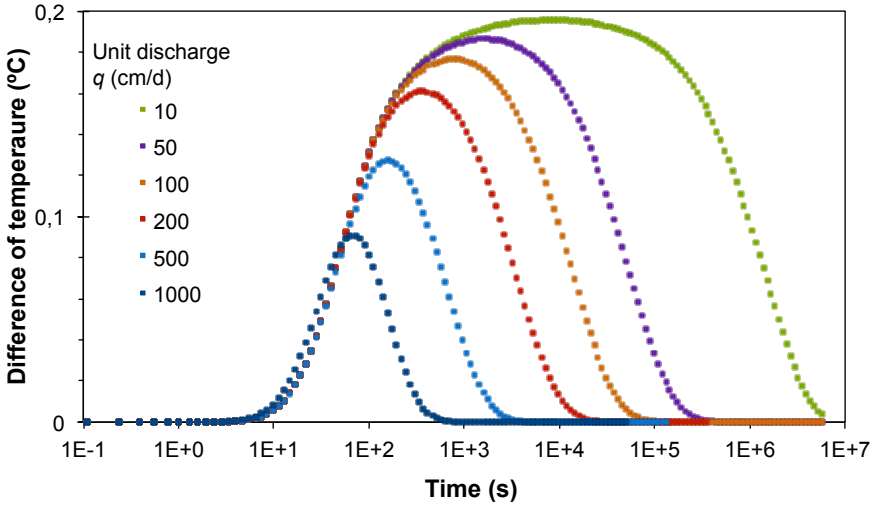

FIGURE 4.19: Temperature difference under two specific heat values of the soil c_s $T(c_s = 800\,\mathrm{J/kgK}) - T(c_s = 1200\,\mathrm{J/kgK})$. $P^* = 20\,\mathrm{W/m}$. Semi-log plot.

The effect of the specific heat only takes place after the initial heating ($t > 10\,\mathrm{s}$) and before reaching the final steady temperature. In terms of physical processes, the heat

takes longer to spread but not because the soil blocks the heat but because the soil demands more energy to increase its temperature.

4.2.5 Methodological synthesis

Summarizing the previous sensitivity analysis, the heating process consist in three different stages. Figure 4.20 illustrates the three stages.

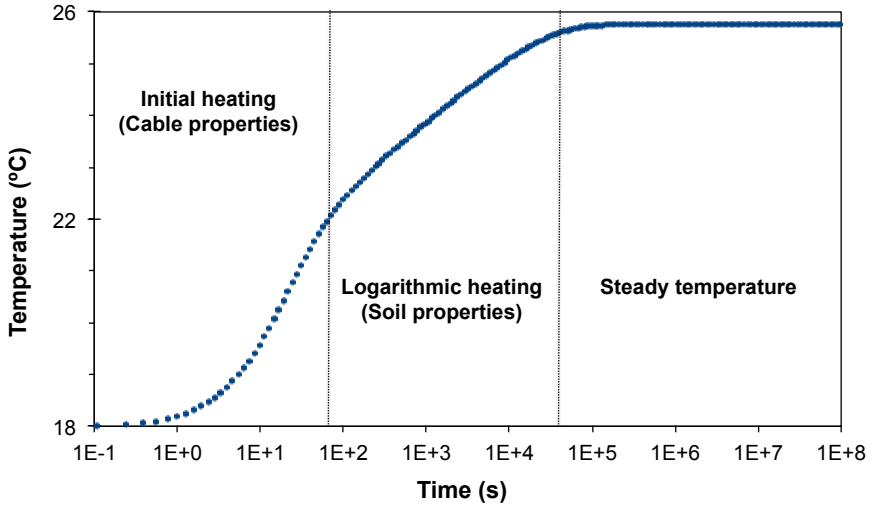

FIGURE 4.20: Three regimes of the thermal dissipation (synthesis)
$q^* = 50\,\mathrm{cm/d}$. $P^* = 20\,\mathrm{W/m}$. $\lambda_{Ny} = 0.28\,\mathrm{W/mK}$. $\lambda_s = 1\,\mathrm{W/mK}$. $c_s = 800\,\mathrm{J/kgK}$.
Cable properties govern the initial heating. Soil properties define the slope of the logarithmic heating. The steady temperature depends on the flow, and the previous properties. The supplied power escales the temperature.

Initially, during the initial heating, the evolution of the temperature depends on the cable properties. The second stage is the logarithmic heating that depends on the soil conductivity (including the dispersion term). Finally, the steady temperature is reached when the advection balances the source of heat. The final temperature of the optical fiber depends on the flow, the cable properties and the thermal conductivity of the soil. The complete heating process depends linearly on the supplied power as it scales the temperature.

Chapter 5

Conclusions

Two analytical solutions have been developed and tested against numerical models to determine groundwater unit discharge by means of temperature measurements.

First, an analytical solution for the thermal response of the fluctuations of the sea temperature has been developed and verified. The expression considers a porous medium through which water flows and a boundary with prescribed temperature representing the fluctuations of the sea. The magnitude of the impact depends mainly on the flow rate and the periodicity of the fluctuation. Two dimensionless numbers are considered to propose a non-dimensional solution: the Péclet number Pe and the reduced frequency ω_s. The response can be quantified in terms of the amplitude damping and the phase shift.

The solution can be applied to a large number of problems in groundwater. One can estimate the inflow/outflow at the sea or a river from temperature measurements at some depth given the temperature fluctuations. In fact, a methodology has been proposed to measure the unit discharge by measuring the amplitude and the peak delay with the reference. To that end, a non-dimensional function has been defined and plotted.

The approach should be able to identify not only the flow direction but also its magnitude for fluxes between a few cm/d to m/day. Still further work should be done to refine the validity limit of the model. Indeed, the solution neglects density effects and heterogeneity. Convective flow due to density instabilities in water intrusions could modify the solution. A coupled model considering not only energy transport but also solute transport would provide a more accurate model for seawater intrusion.

Second, we have also presented an analytical approach for the thermal dissipation from a line source. The global solution is expressed in terms of the well function (or exponential integral). An asymptotic behavior was found and the final temperature for the steady state was defined analytically. A Finite Element Method based in Kratos framework was used to model the problem stated. A sensitivity analysis was carried out to understand the dependency on the unit discharge, the thermal conductivity of the outer part of

the optical fiber, the thermal conductivity of the soil and the specific heat of the soil. Three stages were defined: the initial heating is controlled by the cable properties, the logarithmic heating that depends on the properties of the solid matrix and the steady temperature stage that depends on the unit discharge, the cable properties and the bulk properties. Thermal conductivity and capacity of the medium can be derived from the straight (in semi-log scale) portion of the response. Unit discharge can be estimated from the final temperature. Still, further work is required to refine this estimate by taking into account the thermal resistance of the cable and, possibly, density effects induced by heating.

Appendix A

In this appendix, we resume the resolution of the advection-conduction equation from the equation considered in section 3.2 and we solve it in detail. Therefore, we repeat some previous conclusions for the sake of clarity and continuity.

A.1 Advection-conduction equation

We rewrite the PDE equation in the equation 3.31:

$$C_b \frac{\partial T}{\partial t} = (\lambda + C_w\, D_p)\, \frac{\partial^2 T}{\partial z^2} - q C_w \frac{\partial T}{\partial z} \tag{A.1}$$

Notation (International System of Units in parentheses):

- T: temperature, $[T] = \theta$ (K)
- λ: thermal conductivity, $[\lambda] = MLT^{-3}\theta^{-1}$ (J/m s K)
- C_w: water heat capacity, $[C_w] = ML^{-1}T^{-2}\theta^{-1}$ (J/m^{3}K)
- C_b: bulk heat capacity, $[C_b] = ML^{-1}T^{-2}\theta^{-1}$ (J/m^{3}K)
- q: unit discharge (flow velocity), $[q] = LT^{-1}$ (m^3/s m^2)
- D_p: dispersivity, $[D_p] = L^2T^{-1}$ (m^2/s)

We call $D_\lambda = \dfrac{\lambda}{C_b}$ the thermal diffusivity $[D] = L^2T^{-1}$. On the other hand, bulk heat capacity can be written as follows:

$$C_b = \phi\, C_w + (1-\phi) C_s$$

where ϕ is the porosity (in a saturated porous medium) and C_s is the heat capacity of the solid matrix. If we reconsider C_w/C_b and we use R as the thermal delay:

$$\frac{C_w}{C_b} = \frac{1}{\dfrac{C_b}{C_w}} = \frac{1}{\dfrac{\phi C_w + (1-\phi)C_s}{C_w}} = \frac{1}{\phi\left(1 + \dfrac{(1-\phi)}{\phi}\dfrac{C_s}{C_w}\right)} = \frac{1}{\phi R} \;\Rightarrow\; C_w = \frac{C_b}{\phi R} \tag{A.2}$$

and if we replace it in equation A.1 as well as $\lambda = D_\lambda C_b$, we get:

$$C_b \frac{\partial T}{\partial t} = C_b \left(D_\lambda + \frac{D_p}{\phi R}\right) \frac{\partial^2 T}{\partial z^2} - q \frac{C_b}{\phi R} \frac{\partial T}{\partial z} \tag{A.3}$$

We call D the global diffusivity; it considers the thermal diffusion and the dispersion of heat. It is defined as:

$$D = D_\lambda + \frac{D_p}{\phi R} \tag{A.4}$$

and replacing it in (A.3) we obtain:

$$C_b \frac{\partial T}{\partial t} = C_b D \frac{\partial^2 T}{\partial z^2} - q \frac{C_b}{\phi R} \frac{\partial T}{\partial z} \tag{A.5}$$

A.2 Boundary conditions

As we are working in a semi-infinite domain, the boundary conditions are applied at $z = 0$ and at $z \to \infty$:

$$z = 0 : \qquad T(0,t) = T_m + \Delta T \, \sin \omega_o t \tag{A.6}$$

$$z \to \infty : \qquad \lim_{z \to \infty} T(z,t) = T_\infty \tag{A.7}$$

A.3 Dimensionless equation - Péclet number

First of all, we define the dimensionless values from the problem data:

$$T_D = \frac{T}{T_c}, \qquad t_D = \frac{t}{t_c}, \qquad z_D = \frac{z}{L} \tag{A.8}$$

We replace the dimensionless values in (A.5):

$$\frac{C_b T_c}{t_c} \frac{\partial T_D}{\partial t_D} = C_b D \frac{T_c}{L^2} \frac{\partial^2 T_D}{\partial z_D^2} - \frac{q C_b T_c}{\phi R L} \frac{\partial T_D}{\partial z_D}$$

$$\frac{\partial T_D}{\partial t_D} = D \frac{t_c}{L^2} \frac{\partial^2 T_D}{\partial z_D^2} - \frac{q}{\phi R} \frac{t_c}{L} \frac{\partial T_D}{\partial z_D} \tag{A.9}$$

And for the boundary conditions:

$$\begin{cases} T_c T_D(0,t_D) = T_m + \Delta T \, \sin\left(\omega_o t_c t_D\right) \\ \\ \lim\limits_{z_D \to \infty} T_c T_D(z_D,t_D) = T_\infty \end{cases}$$

That can be rewritten as follows:

$$\begin{cases} T_D(0,t_D) = \dfrac{T_m}{T_c} + \dfrac{\Delta T}{T_c} \sin\left(\omega_o t_c t_D\right) \\ \\ \lim\limits_{z_D \to \infty} T_D(z_D,t_D) = \dfrac{T_\infty}{T_c} \end{cases} \tag{A.10}$$

By using the dimensional analysis and Buckingham π theorem:

$$\frac{q}{\phi R}\frac{t_c}{L} = 1 \quad \Rightarrow \quad t_c = L\frac{\phi R}{q}$$

that is the advection characteristic time[1] and,

$$T_c = T_\infty$$

Replacing in (A.9) and in (A.10):

$$\begin{aligned} &\frac{\partial T_D}{\partial t_D} = D\frac{\phi R}{Lq}\frac{\partial^2 T_D}{\partial z_D^2} - \frac{\partial T_D}{\partial z_D} && \text{[EDP]} \\ &\begin{cases} T_D(0,t_D) = \dfrac{T_m}{T_\infty} + \dfrac{\Delta T}{T_\infty}\sin\left(\omega_o L\dfrac{\phi R}{q}t_D\right) \\ \lim\limits_{z_D\to\infty} T_D(z_D,t_D) = 1 \end{cases} && \text{[CC]} \end{aligned} \tag{A.11}$$

Péclet number is defined as:

$$\mathrm{Pe} = \frac{Lv}{D}$$

And we define Péclet numer for a porous medium as:

$$\mathrm{Pe}_s = \frac{Lq}{D\,\phi R} \tag{A.12}$$

We also define the dimensionless number that compares the advection time with the periodicity of the boundary condition:

$$\omega_s \overset{\text{not.}}{=} \frac{\omega_o}{\frac{q}{L\phi R}} = \frac{\omega_o L\phi R}{q} \tag{A.13}$$

se we have,

$$\begin{aligned} &\frac{\partial T_D}{\partial t_D} = \frac{1}{\mathrm{Pe}_s}\frac{\partial^2 T_D}{\partial z_D^2} - \frac{\partial T_D}{\partial z_D} && \text{[EDP]} \\ &\begin{cases} T_D(0,t_D) = \dfrac{T_m}{T_\infty} + \dfrac{\Delta T}{T_\infty}\sin\left(\omega_s t_D\right) \\ \lim\limits_{z_D\to\infty} T_D(z_D,t_D) = 1 \end{cases} && \text{[CC]} \end{aligned} \tag{A.14}$$

Note that Péclet number and the dimensionless periodicity (ω_s) can be either positive or negative depending on the direction of the flow, i.e. the sign of the unit discharge q.

[1] While $t_c = L^2/D$ is the diffusion characteristic time. We could also consider it as the characteristic time without changing the resolution of our equation.

A.4 General resolution of the PDE

A.4.1 Eigenvalues and eigenfunctions

Starting with the dimensionless equation, we aim to find its eigenfunctions:

$$\frac{\partial T_D}{\partial t_D} = \frac{1}{\mathrm{Pe}_s}\frac{\partial^2 T_D}{\partial z_D^2} - \frac{\partial T_D}{\partial z_D} \tag{A.15}$$

For the sake of clarity, we simplify the notation by writing all dimensionless variables a_D without its dimensionless symbol "$\cdot_D$". So we have:

$$\frac{\partial T}{\partial t} = \frac{1}{\mathrm{Pe}_s}\frac{\partial^2 T}{\partial z^2} - \frac{\partial T}{\partial z} \tag{A.16}$$

Considering the Fourier transform (FT) and its inverse $\forall f(t) \in \mathcal{L}^2(\mathbb{R})$:

$$\begin{aligned} \mathcal{F}\left[f(t)\right](\omega) \;:\quad \omega \;&\rightarrow\; \mathcal{F}[f(t)](\omega) \overset{\text{not.}}{=} \hat{f}(\omega) := \int_{-\infty}^{\infty} f(t)\; e^{-i\omega t} dt \\ \mathcal{F}^{-1}\left[\hat{f}(\omega)\right](t) \;:\quad t \;&\rightarrow\; \mathcal{F}^{-1}\left[\hat{f}(\omega)\right](t) = f(t) := \frac{1}{2\pi}\int_{-\infty}^{\infty} \hat{f}(\omega)\; e^{i\omega t} d\omega \end{aligned} \tag{A.17}$$

Applying the Fourier transform, $\mathcal{F}$, to the equation (A.16):

$$\mathcal{F}\left[\frac{\partial T}{\partial t}\right] = \mathcal{F}\left[\frac{1}{\mathrm{Pe}_s}\frac{\partial^2 T}{\partial z^2} - \frac{\partial T}{\partial z}\right]$$

With the notation, $\hat{T} = \mathcal{F}[T]$ we get:

$$i\omega\hat{T} = \frac{1}{\mathrm{Pe}_s}\frac{d^2\hat{T}}{dz^2} - \frac{d\hat{T}}{dz} \tag{A.18}$$

Rearranging the equation,

$$\frac{d^2\hat{T}}{dz^2} - \mathrm{Pe}_s\frac{d\hat{T}}{dz} - i\mathrm{Pe}_s\omega\hat{T} = 0 \tag{A.19}$$

This equation is a linear Ordinary Differential Equation (ODE) of second order with constant coefficients. To solve it, we use its characteristic equation:

$$\chi^2 - \mathrm{Pe}_s\chi - i\mathrm{Pe}_s\omega = 0 \tag{A.20}$$

And we get,

$$\chi_\pm = \frac{\mathrm{Pe}_s \pm \sqrt{\mathrm{Pe}_s^2 + 4\mathrm{Pe}_s\omega i}}{2} = \frac{\mathrm{Pe}_s \pm |\mathrm{Pe}_s|\sqrt{1 + \frac{4\omega}{\mathrm{Pe}_s}i}}{2} \tag{A.21}$$

Using the sign function defined as follows:

$$\operatorname{sgn} x = \begin{cases} -1 & x < 0 \\ 0 & x = 0 \\ +1 & x > 0, \end{cases}$$

the eigenvalues and eigenfunctions are presented in the next table,

$\chi_+ = \frac{\lvert \mathrm{Pe}_s \rvert}{2}\left(\operatorname{sgn}(\mathrm{Pe}_s) + \sqrt{1 + 4\frac{\omega}{\mathrm{Pe}_s}i}\right)$	$\chi_- = \frac{\lvert \mathrm{Pe}_s \rvert}{2}\left(\operatorname{sgn}(\mathrm{Pe}_s) - \sqrt{1 + 4\frac{\omega}{\mathrm{Pe}_s}i}\right)$
$\exp(\chi_+(\omega)z)$	$\exp(\chi_-(\omega)z)$

A.4.2 Particular case $\omega = 0$ – Steady problem

If $\omega = 0$, the equation (A.19) loses the 0-order term and the eigenvalues have no longer an imaginary part. On the other hand, the differential equation has the same form in both frequency and time domains. Going back to time domain[2] we find:

$$\frac{d}{dz_D}\left(\frac{dT_D}{dz_D} - \mathrm{Pe}_s T_D\right) = 0 \quad \rightarrow \quad \frac{dT_D}{dz_D} - \mathrm{Pe}_s T_D = C$$

and we can easily solve knowing that the solution is the sum of the homogeneous and particular solution:

$$T_D(z_D, t_D) = T_D(z_D) = \underbrace{T_D^h}_{\text{homogeneous}} + \underbrace{T_D^p}_{\text{particular}} \tag{A.22}$$

On the one hand, the homogeneous solution is:

$$T_D^h = Ae^{\mathrm{Pe}_s z_D}$$

And on the other hand, we obtain the particular solution by using the variation of parameters method:

$$T_D^p = \frac{C}{\mathrm{Pe}_s} = -B$$

Being the solution of the steady case:

$$for the equation T_D = Ae^{\mathrm{Pe}_s z_D} + B \tag{A.23}$$

In A.5.1 we will apply the boundary conditions to this solution.

[2] $\omega = 0$ implies steadiness in the temporal domain.

A.4.3 Real and imaginary part of the eigenvalues

Once we have the eigenfunctions, it is also of interest to split into its exponential and sinusoidal parts, implying the separation of the real and imaginary part of the eigenvalues. Analyzing the eigenvalues, we must focus on the discriminant of the characteristic equation to find its imaginary part. Being $z = 1 + 4\frac{\omega}{\mathrm{Pe}_s}i$, we compute $\sqrt{z}$:

$$z = |z|e^{i\varphi} = |z|\left(\cos\varphi + i\sin\varphi\right) = |z|\left(\frac{1}{|z|} + i\frac{4\omega}{\mathrm{Pe}_s|z|}\right) \qquad \text{donde } |z| = \sqrt{1 + \frac{16\,\omega^2}{\mathrm{Pe}_s^2}}$$

being,

$$\cos\varphi = \frac{1}{|z|}, \qquad \sin\varphi = \frac{4\omega}{\mathrm{Pe}_s|z|}$$

As $\cos\varphi > 0$, the angle φ it is defined as,

$$\varphi = \arctan\frac{4\omega}{\mathrm{Pe}_s} \qquad \varphi \in \left[-\frac{\pi}{2}, \frac{\pi}{2}\right]$$

we observe that, being $\arctan\theta$ a monotonically increasing function going through the origin of coordinates, we have,

$$\mathrm{sgn}\left(\varphi\right) = \mathrm{sgn}\left(\arctan\frac{4\omega}{\mathrm{Pe}_s}\right) = \mathrm{sgn}\left(\frac{4\omega}{\mathrm{Pe}_s}\right) = \mathrm{sgn}\left(\omega\right)\cdot\mathrm{sgn}\left(\mathrm{Pe}_s\right) \tag{A.24}$$

To compute $\sqrt{z}$, we use the root formula for an imaginary number:

$$\sqrt[n]{z} = \sqrt[n]{|z|e^{i\varphi}} = \sqrt[n]{|z|}e^{\frac{\varphi+2\pi k}{n}i}, \qquad \forall k \in \{0, 1, ..., n-1\}$$

In the case of a square root, one can write:

$$\sqrt{z} = \sqrt{|z|e^{i\varphi}} = \sqrt{|z|}e^{\frac{\varphi+2\pi k}{2}i}, \quad \forall k \in \{0, 1\}$$
$$\sqrt{z} = \sqrt{|z|}e^{\frac{\varphi}{2}i} \quad \text{or} \quad \sqrt{z} = \sqrt{|z|}e^{\left(\frac{\varphi}{2}+\pi\right)i} = -\sqrt{|z|}e^{\frac{\varphi}{2}i}$$

developing these expressions,

$$\sqrt{z} = \pm\sqrt{|z|}\left(\cos\frac{\varphi}{2} + i\sin\frac{\varphi}{2}\right) \tag{A.25}$$

We use the half-angle formula[3]:

$$\cos\frac{\varphi}{2} = \pm\sqrt{\frac{1+\cos\varphi}{2}}, \qquad \sin\frac{\varphi}{2} = \pm\sqrt{\frac{1-\cos\varphi}{2}}$$

[3]From double-angle formula: $\cos 2x = \cos^2 x - \sin^2 x$ and the Pythagorean trigonometric identity: $\sin^2 x + \cos^2 x = subfigure1$, we obtain the half-angle formula.

Since $\cos\varphi > 0$ and $\varphi \in \left[-\frac{\pi}{2}, \frac{\pi}{2}\right]$, the sign of the half-angle sine will depend on the sign of φ, while the sign of the cosine will always be positive as it belongs to the quadrant I and IV:

$$\cos\frac{\varphi}{2} = \sqrt{\frac{1+\cos\varphi}{2}}, \qquad \sin\frac{\varphi}{2} = \operatorname{sgn}(\varphi)\sqrt{\frac{1-\cos\varphi}{2}} = \operatorname{sgn}\left(\frac{\omega}{\mathrm{Pe}_s}\right)\sqrt{\frac{1-\cos\varphi}{2}}$$

Back to the square root of z,

$$\begin{aligned}
\sqrt{z} &= \pm\sqrt{|z|}\left(\cos\frac{\varphi}{2} + i\sin\frac{\varphi}{2}\right) = \pm\sqrt{|z|}\left(\sqrt{\frac{1+\cos\varphi}{2}} + i\ \operatorname{sgn}\left(\frac{\omega}{\mathrm{Pe}_s}\right)\sqrt{\frac{1-\cos\varphi}{2}}\right) \\
&= \pm\sqrt{|z|}\left(\sqrt{\frac{|z|+1}{2|z|}} + i\ \operatorname{sgn}\left(\frac{\omega}{\mathrm{Pe}_s}\right)\sqrt{\frac{|z|-1}{2|z|}}\right) \\
&= \pm\sqrt{\frac{1}{2}(|z|+1)} \pm i\ \operatorname{sgn}\left(\frac{\omega}{\mathrm{Pe}_s}\right)\sqrt{\frac{1}{2}(|z|-1)} \\
&= \pm\sqrt{\frac{1}{2}\left(\sqrt{1+\frac{16\,\omega^2}{\mathrm{Pe}_s^2}}+1\right)} \pm i\ \operatorname{sgn}\left(\frac{\omega}{\mathrm{Pe}_s}\right)\sqrt{\frac{1}{2}\left(\sqrt{1+\frac{16\,\omega^2}{\mathrm{Pe}_s^2}}-1\right)}
\end{aligned}$$

For simplicity, we define $\gamma_\pm(\omega)$ as follows:

$$\gamma_\pm(\omega) = \sqrt{\frac{1}{2}\left(\sqrt{1+\frac{16\,\omega^2}{\mathrm{Pe}_s^2}} \pm 1\right)} \tag{A.26}$$

so we have,

$$\sqrt{z} = \pm\gamma_+(\omega) \pm i\ \operatorname{sgn}(\omega)\,\gamma_-(\omega) \tag{A.27}$$

Before proceeding with the PDE resolution, some properties of the functions $\gamma_+(\omega)$ and $\gamma_-(\omega)$ are analyzed:

- When $\omega = 0$:

$$\gamma_+(0) = 1\,, \qquad \gamma_-(0) = 0 \tag{A.28}$$

- Both functions are even functions (symmetry with respect to the y-axis):

$$\gamma_+(-\omega) = \gamma_+(\omega)\,, \qquad \gamma_-(-\omega) = \gamma_-(\omega) \qquad \forall\omega \in \mathbb{R} \tag{A.29}$$

- Both functions are positive and have a minimum at $\omega = 0$:

$$\gamma_+(\omega) \geq 1, \qquad \gamma_-(\omega) \geq 0 \qquad \forall\omega \in \mathbb{R} \tag{A.30}$$

These results will be useful when considering the boundary conditions of the problem.

Rewriting the eigenvalues separating the real and imaginary parts:

$$\chi_+ = \frac{\mathrm{Pe}_s}{2}\left(1 + \mathrm{sgn}\ (\mathrm{Pe}_s)\,\gamma_+ + i\ \mathrm{sgn}\ (\omega)\,\gamma_-\right) \tag{A.31}$$

$$\chi_- = \frac{\mathrm{Pe}_s}{2}\left(1 - \mathrm{sgn}\ (\mathrm{Pe}_s)\,\gamma_+ - i\ \mathrm{sgn}\ (\omega)\,\gamma_-\right) \tag{A.32}$$

and the eigenfunctions,

$$f_+(z) = \exp\left(\frac{\mathrm{Pe}_s}{2}\left(1 + \mathrm{sgn}\ (\mathrm{Pe}_s)\,\gamma_+\right)z\right)\cdot\exp\left(i\ \mathrm{sgn}\ (\omega)\,\frac{\mathrm{Pe}_s}{2}\gamma_- z\right) \tag{A.33}$$

$$f_-(z) = \exp\left(\frac{\mathrm{Pe}_s}{2}\left(1 - \mathrm{sgn}\ (\mathrm{Pe}_s)\,\gamma_+\right)z\right)\cdot\exp\left(-i\ \mathrm{sgn}\ (\omega)\,\frac{\mathrm{Pe}_s}{2}\gamma_- z\right). \tag{A.34}$$

The general solution of the ODE can be written as a linear combination of the eigenfunctions $f_+(z)$ and $f_-(z)$:

$$\begin{aligned}\hat{T}(z,\omega) = {} & C_+ \exp\left(\frac{\mathrm{Pe}_s}{2}\left(1 + \mathrm{sgn}\ (\mathrm{Pe}_s)\,\gamma_+\right)z\right)\exp\left(i\ \mathrm{sgn}\ (\omega)\,\frac{\mathrm{Pe}_s}{2}\gamma_- z\right) \\ & + C_- \exp\left(\frac{\mathrm{Pe}_s}{2}\left(1 - \mathrm{sgn}\ (\mathrm{Pe}_s)\,\gamma_+\right)z\right)\exp\left(-i\ \mathrm{sgn}\ (\omega)\,\frac{\mathrm{Pe}_s}{2}\gamma_- z\right)\end{aligned} \tag{A.35}$$

where $C_+(\omega)$ and $C_-(\omega)$ are the coefficients of the linear combination of the eigenfunctions and they may depend on ω. The general solution can be expressed as the inverse Fourier transform of the previous function (equation A.35):

$$T(z,t) = \mathcal{F}^{-1}\left[\hat{T}(z,\omega)\right](t) \tag{A.36}$$

To have the complete expression of this solution we first need $C_+(\omega)$ y $C_-(\omega)$. For this purpose, boundary conditions must be imposed.

A.5 Imposition of the boundary conditions

Once we have the global solution of the dimensionless and transformed PDE, we turn to solve the boundary equations so that we can find $C_+(\omega)$ and $C_-(\omega)$. To this end, we divide the problem into two using the linearity of the stated problem.

$$T(z,t) = \underbrace{T^s(z)}_{\text{steady}} + \underbrace{T^t(z,t)}_{\text{transient}} \tag{A.37}$$

so that both verify the PDE (A.16):

$$\text{Steady:} \qquad 0 = \frac{1}{\mathrm{Pe}_s}\frac{d^2T_D^s}{dz_D^2} - \frac{dT_D^s}{dz_D} \tag{A.38}$$

$$\text{Transient:} \qquad \frac{\partial T_D^t}{\partial t_D} = \frac{1}{\text{Pe}_s}\frac{\partial^2 T_D^t}{\partial z_D^2} - \frac{\partial T_D^t}{\partial z_D} \tag{A.39}$$

This separation of the solution helps the resolution of the boundary condition problem. Note that the behavior of the steady term is simpler then the transient term. Indeed, being a time-independent solution, the temporal term disappears and spatial partial derivatives become total derivatives for the steady problem. Taking the [BC] of (A.14), we separate them as follows:

$$\begin{cases} T_D(0,t_D) = \underbrace{\dfrac{T_m}{T_\infty}}_{\text{steady}} + \underbrace{\dfrac{\Delta T}{T_\infty}\sin(\omega_s t_D)}_{\text{transient}} = T_D^s(0) + T_D^t(0,t_D) \\ \lim\limits_{z_D\to+\infty} T_D(z_D,t_D) = \underbrace{1}_{\text{steady}} + \underbrace{0}_{\text{transient}} = \lim\limits_{z_D\to+\infty} T_D^s(z_D) + \lim\limits_{z_D\to+\infty} T_D^t(z_D,t_D) \end{cases} \tag{A.40}$$

Now, we can proceed to the resolution.

A.5.1 Steady boundary conditions

Omitting the dimensionless symbol "$\cdot_D$" to simplify the notation:

$$\frac{d^2T^s}{dz^2} - \text{Pe}_s\frac{dT^s}{dz} = 0 \qquad \text{[ODE]}$$

$$\begin{cases} T^s(0) = \dfrac{T_m}{T_\infty} \\ \lim\limits_{z\to+\infty} T^s(z) = 1 \end{cases} \qquad \text{[BC]} \tag{A.41}$$

The general solution of (A.41)-[ODE] is found in section A.4.2. By imposing the boundary conditions (equation (A.41)-[BC]) to the equation (A.23), we will meet the steady solution.

$$T^s(x) = Ae^{\text{Pe}_s x} + B \qquad \text{[GS]}$$

$$\begin{cases} T^s(0) = \dfrac{T_m}{T_\infty} \\ \lim\limits_{z_D\to+\infty} T^s(x) = 1 \end{cases} \qquad \text{[BC]} \tag{A.42}$$

Regarding the general solution [GS], the sign of the Péclet number plays a crucial role when imposing the boundary conditions. Hence, we will differentiate two different cases:

$$\text{Case } \mathbb{A}: \quad \text{Pe}_s < 0 \qquad \text{Outgoing flow } q < 0$$

$$\text{Case } \mathbb{B}: \quad \text{Pe}_s > 0 \qquad \text{Incoming flow } q > 0$$

- Case $\mathbb{A}$ ($\mathrm{Pe}_s < 0$, i.e. $q < 0$):
  As $\mathrm{Pe}_s < 0$, we can write $-|\mathrm{Pe}_s|$ instead of Pe_s in equation (A.42)-[GS], so the equation reads:

$$T^s(z) = Ae^{-|\mathrm{Pe}_s|z} + B \qquad \text{[GS]}$$

$$\begin{cases} T^s(0) = A + B = \dfrac{T_m}{T_\infty} \\ \lim\limits_{z\to+\infty} T^s(z) = \lim\limits_{z\to+\infty} Ae^{-|\mathrm{Pe}_s|z} + B = B = 1 \end{cases} \qquad \text{[BC]} \tag{A.43}$$

  leading to,

$$\left.\begin{array}{l} A = \dfrac{T_m}{T_\infty} - 1 \\ B = 1 \end{array}\right\} \rightarrow \boxed{T^s(z) = \left(\frac{T_m}{T_\infty} - 1\right) e^{-|\mathrm{Pe}_s|z} + 1} \tag{A.44}$$

- Case $\mathbb{B}$ ($\mathrm{Pe}_s > 0$, i.e. $q > 0$):
  Rewriting (A.42)-[SG] we have:

$$T^s(z) = Ae^{|\mathrm{Pe}_s|z} + B \qquad \text{[SG]}$$

$$\begin{cases} T^s(0) = A + B = \dfrac{T_m}{T_\infty} \\ \lim\limits_{z\to+\infty} T^s(z) = \lim\limits_{z\to+\infty} Ae^{|\mathrm{Pe}_s|z} + B = 1 \end{cases} \qquad \text{[CC]} \tag{A.45}$$

  As the function has a finite value when $x \to +\infty$, A must be equal to 0. When we impose $A = 0$, we only have one unknown (B) and the first equation of the [BC]:

$$T^s(0) = B = \frac{T_m}{T_\infty}, \tag{A.46}$$

  therefore,

$$\left.\begin{array}{l} A = 0 \\ B = \dfrac{T_m}{T_\infty} \end{array}\right\} \rightarrow \boxed{T^s(z) = \frac{T_m}{T_\infty}} \tag{A.47}$$

A.5.2 Transient boundary conditions (or time-dependent)

Omitting the dimensionless symbol "$\cdot_D$" to simplify the notation:

$$\begin{aligned} &\frac{\partial T^t}{\partial t} = \frac{1}{\mathrm{Pe}_s}\frac{\partial^2 T^t}{\partial z^2} - \frac{\partial T^t}{\partial z} && \text{[PDE]} \\ &\begin{cases} T^t(0,t) = \dfrac{\Delta T}{T_\infty}\sin(\omega_s t) \\ \lim\limits_{z_D\to\infty} T^t(z,t) = 0 \end{cases} && \text{[BC]} \end{aligned} \tag{A.48}$$

Applying Fourier transform to (A.48), the equation reads,

$$\begin{aligned} &\frac{d^2\hat{T}^t}{dz^2} - \mathrm{Pe}_s\frac{d\hat{T}^t}{dz} - i\omega\mathrm{Pe}_s\hat{T}^t = 0 && \text{[ODE]} \\ &\begin{cases} \hat{T}^t(0,\omega) = \dfrac{\Delta T}{T_\infty}\dfrac{\pi}{i}\left[\delta(\omega-\omega_s) - \delta(\omega+\omega_s)\right] \\ \lim\limits_{z_D\to\infty} \hat{T}^t(z,\omega) = 0 \end{cases} && \text{[BC]} \end{aligned} \tag{A.49}$$

As one can see, the Fourier transform has not only been applied to the PDE but also to the boundary conditions. Indeed, as we are working in the frequency domain, the boundary conditions must be expressed as well in the same domain. In the case of the sine function, its Fourier transform is expressed through Dirac delta function[4] δ defined as follows,

$$\delta(\omega) = \begin{cases} +\infty & \omega = 0 \\ 0 & \omega \neq 0 \end{cases} \qquad \int_{-\infty}^{+\infty} \delta(\omega)\, d\omega = 1 \tag{A.50}$$

Or it can be defined as,

$$\delta(\omega) = \lim_{\sigma\to 0} \frac{1}{\sigma\sqrt{2\pi}} \exp\left(-\frac{\omega^2}{2\sigma^2}\right)$$

Dirac delta function has the following property that will be useful to solve inverse Fourier transforms:

$$\int_{-\infty}^{+\infty} \delta(\omega-\omega_0)\, f(\omega)\, d\omega = f(\omega_0) \tag{A.51}$$

Taking the general solution of the PDE (A.35), solved in section A.4.3, we first impose the boundary condition at $z = 0$:

$$C_+(\omega) + C_-(\omega) = \frac{\Delta T}{T_\infty}\frac{\pi}{i}\left[\delta(\omega-\omega_s) - \delta(\omega+\omega_s)\right] \tag{A.52}$$

[4] Properly, it is a distribution, i.e. an object that generalize the classical notion of function.

In order to apply the infinite boundary condition, we must consider two different cases:

$$\text{Case } \mathbb{A}: \quad \text{Pe}_s < 0\,,\ \omega_s < 0 \qquad \text{Outgoing flow } q < 0$$

$$\text{Case } \mathbb{B}: \quad \text{Pe}_s > 0\,,\ \omega_s > 0 \qquad \text{Incoming flow } q > 0$$

- Case $\mathbb{A}$ ($\text{Pe}_s < 0\,,\ \omega_s < 0$, i.e. $q < 0$, outgoing flow):
  Taking the general solution presented in equation (A.35), and considering the case $\text{Pe}_s < 0$ (writing $\text{Pe}_s = -|\text{Pe}_s|$ and $\text{sgn}\,(\text{Pe}_s) = -1$), the boundary condition reads:

$$\lim_{z\to+\infty} \hat{T}^t(z,\omega) = \lim_{z\to+\infty} \left[C_+(\omega)\, \exp\left(\frac{|\text{Pe}_s|}{2}\,(\gamma_+ - 1)\, z\right) \exp\left(-i\ \text{sgn}\,(\omega)\frac{|\text{Pe}_s|}{2}\gamma_- z\right) + \right.$$
$$\left. + C_-(\omega)\, \exp\left(-\frac{|\text{Pe}_s|}{2}\,(\gamma_+ + 1)\, z\right) \exp\left(i\ \text{sgn}\,(\omega)\frac{|\text{Pe}_s|}{2}\gamma_- z\right)\right] = 0 \quad \text{(A.53)}$$

  To solve this equation, first, we must recall that ω is different than 0; and second, $\gamma_+ - 1 > 0$ and $\gamma_- > 0$, after equation (A.30). This means that all parameters accompanying z in the exponent argument are different than 0. Focusing on the sign, the real exponential argument of the first addent is positive, implying that the addend tends to infinity when z tends to infinity. However, the real exponential argument of the second addend is negative, carrying this second addend to tend to zero when z tends to infinity. We thus deduce:

$$C_+(\omega) = 0$$

  And from equation (A.52) we can determine C_-:

$$\begin{cases} C_+ = 0 \\ C_- = \dfrac{\Delta T}{T_\infty}\dfrac{\pi}{i}\left[\delta(\omega - \omega_s) - \delta(\omega + \omega_s)\right] \end{cases} \quad \text{(A.54)}$$

  being $\hat{T}^t(z,\omega)$:

$$\hat{T}^t(z,\omega) = \frac{\Delta T}{T_\infty}\frac{\pi}{i}\left[\delta(\omega - \omega_s) - \delta(\omega + \omega_s)\right] \exp\left(-\frac{|\text{Pe}_s|}{2}\,(1 + \gamma_+)\, z\right)$$
$$\exp\left(i\ \text{sgn}\,(\omega)\frac{|\text{Pe}_s|}{2}\gamma_- z\right) \quad \text{(A.55)}$$

Applying the inverse Fourier transform and taking into account the property detailed in (A.51) we have:

$$\mathcal{F}^{-1}\left[\hat{T}^t(z,\omega)\right](t) = T^t(z,t) = \frac{1}{2\pi}\int_{-\infty}^{\infty} \hat{T}^t(z,\omega)\; e^{i\omega t} d\omega =$$

$$= \frac{\Delta T}{T_\infty}\frac{1}{2i}\int_{-\infty}^{\infty} \left[\delta(\omega-\omega_s) - \delta(\omega+\omega_s)\right] \exp\left(-\frac{|\mathrm{Pe}_s|}{2}\left(1+\gamma_+(\omega)\right) z\right) \cdot$$
$$\exp\left(i\ \mathrm{sgn}\,(\omega)\frac{|\mathrm{Pe}_s|}{2}\gamma_-(\omega) z\right) e^{i\omega t} d\omega$$

$$= \frac{\Delta T}{T_\infty}\frac{1}{2i}\left[\int_{-\infty}^{\infty} \delta(\omega-\omega_s)\ \exp\left(-\frac{|\mathrm{Pe}_s|}{2}\left(1+\gamma_+(\omega)\right) z\right) \cdot \right.$$
$$\exp\left(i\ \mathrm{sgn}\,(\omega)\frac{|\mathrm{Pe}_s|}{2}\gamma_-(\omega) z\right)\ e^{i\omega t} d\omega$$

$$\left. - \int_{-\infty}^{\infty} \delta(\omega+\omega_s)\ \exp\left(-\frac{|\mathrm{Pe}_s|}{2}\left(1+\gamma_+(\omega)\right) z\right) \cdot \right.$$
$$\left. \exp\left(i\ \mathrm{sgn}\,(\omega)\frac{|\mathrm{Pe}_s|}{2}\gamma_-(\omega) z\right)\ e^{i\omega t} d\omega\right]$$

$$= \frac{\Delta T}{T_\infty}\frac{1}{2i}\left[\exp\left(-\frac{|\mathrm{Pe}_s|}{2}\left(1+\gamma_+(\omega_s)\right) z\right) \exp\left(i\ \mathrm{sgn}\,(\omega_s)\frac{|\mathrm{Pe}_s|}{2}\gamma_-(\omega_s) z\right)\ e^{i\omega_s t}\right.$$

$$\left. - \exp\left(-\frac{|\mathrm{Pe}_s|}{2}\left(1+\gamma_+(-\omega_s)\right) z\right) \exp\left(i\ \mathrm{sgn}\,(-\omega_s)\frac{|\mathrm{Pe}_s|}{2}\gamma_-(-\omega_s) z\right)\ e^{-i\omega_s t}\right] \tag{A.56}$$

Taking into account the even symmetry of $\gamma(\omega)$ seen in equation (A.29), knowing that $\mathrm{sgn}\,(\omega_s) = -1$ and $\mathrm{sgn}\,(-\omega_s) = 1$ (as ω_s considers the direction of the flow as seen in equation (A.13)) and using the definition of the sine function[5]:

$$T^t(z,t) = \frac{\Delta T}{T_\infty}\frac{1}{2i}\exp\left(-\frac{|\mathrm{Pe}_s|}{2}\left(1+\gamma_+(\omega_s)\right) z\right) \cdot$$
$$\left[\exp\left(i\left(-\frac{|\mathrm{Pe}_s|}{2}\gamma_-(\omega_s) z + \omega_s t\right)\right) - \exp\left(-i\left(-\frac{|\mathrm{Pe}_s|}{2}\gamma_-(\omega_s) z + \omega_s t\right)\right)\right]$$

$$= \boxed{\frac{\Delta T}{T_\infty}\exp\left(-\frac{|\mathrm{Pe}_s|}{2}\left(1+\gamma_+(\omega_s)\right) z\right) \sin\left(-\frac{|\mathrm{Pe}_s|}{2}\gamma_-(\omega_s) z + \omega_s t\right)} \tag{A.57}$$

- Case $\mathbb{B}$ ($\mathrm{Pe}_s > 0$, $\omega_s > 0$, i.e. $q > 0$ incoming flow):

[5] $\sin x = \frac{1}{2i}\left(e^{ix} - e^{-ix}\right)$

Taking the general solution presented in equation (A.35), and considering the case $\mathrm{Pe}_s > 0$ (writing $\mathrm{sgn}\,(\mathrm{Pe}_s) = 1$ and $\mathrm{Pe}_s = |\mathrm{Pe}_s|$), the boundary condition reads:

$$\lim_{z\to+\infty} \hat{T}^t(z,\omega) = \lim_{z\to+\infty} \left[C_+(\omega)\, \exp\left(\frac{|\mathrm{Pe}_s|}{2}\,(1+\gamma_+)\,z\right) \exp\left(i\ \mathrm{sgn}\,(\omega)\frac{|\mathrm{Pe}_s|}{2}\gamma_- z\right) + \right.$$
$$\left. + C_-(\omega)\, \exp\left(-\frac{|\mathrm{Pe}_s|}{2}\,(\gamma_+ - 1)\,z\right) \exp\left(-i\ \mathrm{sgn}\,(\omega)\frac{|\mathrm{Pe}_s|}{2}\gamma_- z\right)\right] = 0 \quad \text{(A.58)}$$

With an analogous reasoning as done for the case $\mathbb{A}$, as ω is different than 0 and as $\gamma_+ - 1 > 0$ and $\gamma_- > 0$ (after (A.30)) we see that, all exponential arguments are different than 0 once again. The real exponential argument of the first addend is positive when z tends to infinity, while the real exponential argument of the second addend is negative when z tends to infinity. Therefore,

$$C_+(\omega) = 0$$

And from equation (A.52) we can determine C_-:

$$\begin{cases} C_+ = 0 \\ C_- = \dfrac{\Delta T}{T_\infty}\dfrac{\pi}{i}\left[\delta(\omega-\omega_s) - \delta(\omega+\omega_s)\right] \end{cases} \quad \text{(A.59)}$$

being $\hat{T}^t(z,\omega)$:

$$\hat{T}^t(z,\omega) = \frac{\Delta T}{T_\infty}\frac{\pi}{i}\left[\delta(\omega-\omega_s) - \delta(\omega+\omega_s)\right] \exp\left(-\frac{|\mathrm{Pe}_s|}{2}\,(\gamma_+ - 1)\,z\right)$$
$$\exp\left(-i\ \mathrm{sgn}\,(\omega)\frac{|\mathrm{Pe}_s|}{2}\gamma_- z\right) \quad \text{(A.60)}$$

Applying the inverse Fourier transform and taking into account the property detailed in (A.51) we have:

$$\mathcal{F}^{-1}\left[\hat{T}^t(z,\omega)\right](t) = T^t(z,t) = \frac{1}{2\pi}\int_{-\infty}^{\infty} \hat{T}^t(z,\omega)\; e^{i\omega t} d\omega =$$

$$= \frac{\Delta T}{T_\infty}\frac{1}{2i}\int_{-\infty}^{\infty} \left[\delta(\omega-\omega_s) - \delta(\omega+\omega_s)\right] \exp\left(-\frac{|\mathrm{Pe}_s|}{2}\left(\gamma_+(\omega)-1\right)z\right)\cdot$$
$$\exp\left(-i\;\mathrm{sgn}\,(\omega)\frac{|\mathrm{Pe}_s|}{2}\gamma_-(\omega)z\right) e^{i\omega t} d\omega$$

$$= \frac{\Delta T}{T_\infty}\frac{1}{2i}\left[\int_{-\infty}^{\infty} \delta(\omega-\omega_s)\; \exp\left(-\frac{|\mathrm{Pe}_s|}{2}\left(\gamma_+(\omega)-1\right)z\right)\cdot\right.$$
$$\exp\left(-i\;\mathrm{sgn}\,(\omega)\frac{|\mathrm{Pe}_s|}{2}\gamma_-(\omega)z\right)\; e^{i\omega t} d\omega$$

$$\left. - \int_{-\infty}^{\infty} \delta(\omega+\omega_s)\; \exp\left(-\frac{|\mathrm{Pe}_s|}{2}\left(\gamma_+(\omega)-1\right)z\right)\cdot\right.$$
$$\left.\exp\left(-i\;\mathrm{sgn}\,(\omega)\frac{|\mathrm{Pe}_s|}{2}\gamma_-(\omega)z\right)\; e^{i\omega t} d\omega\right]$$

$$= \frac{\Delta T}{T_\infty}, i.e. \text{q¿0}) : \tfrac{1}{2i}\left[\exp\left(-\frac{|\mathrm{Pe}_s|}{2}\left(\gamma_+(\omega_s)-1\right)z\right)\exp\left(-i\;\mathrm{sgn}\,(\omega_s)\frac{|\mathrm{Pe}_s|}{2}\gamma_-(\omega_s)z\right)\; e^{i\omega_s t}\right.$$

$$\left. - \exp\left(-\frac{|\mathrm{Pe}_s|}{2}\left(\gamma_+(-\omega_s)-1\right)z\right)\exp\left(-i\;\mathrm{sgn}\,(-\omega_s)\frac{|\mathrm{Pe}_s|}{2}\gamma_-(-\omega_s)z\right)\; e^{-i\omega_s t}\right] \tag{A.61}$$

Taking into account the even symmetry of $\gamma(\omega)$ seen in equation (A.29), knowing that $\mathrm{sgn}\,(\omega_s) = 1$ and $\mathrm{sgn}\,(-\omega_s) = -1$ and using the definition of the sine function:

$$T^t(z,t) = \frac{\Delta T}{T_\infty}\frac{1}{2i}\exp\left(-\frac{|\mathrm{Pe}_s|}{2}\left(\gamma_+(\omega_s)-1\right)z\right)\cdot$$
$$\left[\exp\left(i\left(-\frac{|\mathrm{Pe}_s|}{2}\gamma_-(\omega_s)z+\omega_s t\right)\right) - \exp\left(-i\left(-\frac{|\mathrm{Pe}_s|}{2}\gamma_-(\omega_s)z+\omega_s t\right)\right)\right]$$

$$= \boxed{\frac{\Delta T}{T_\infty}\exp\left(-\frac{|\mathrm{Pe}_s|}{2}\left(\gamma_+(\omega_s)-1\right)z\right)\sin\left(-\frac{|\mathrm{Pe}_s|}{2}\gamma_-(\omega_s)z+\omega_s t\right)} \tag{A.62}$$

A.6 Global solution

Once the steady case and the transient case have been solved, we are able to formulate the global solution as it is the sum of the previous two, as seen in (A.37). The dimensionless solution is:

- Case $\mathbb{A}$ ($\mathrm{Pe}_s < 0\,,\ \omega_s < 0$, i.e. $q < 0$, outgoing flow):

$$\begin{aligned} T_D(z_D, t_D) &= \left(\frac{T_m}{T_\infty} - 1\right) e^{-|\mathrm{Pe}_s| z_D} + 1 \\ &+ \frac{\Delta T}{T_\infty} \exp\left(-\frac{|\mathrm{Pe}_s|}{2}\left(1 + \gamma_+(\omega_s)\right) z_D\right) \sin\left(-\frac{|\mathrm{Pe}_s|}{2}\gamma_-(\omega_s) z_D + \omega_s t_D\right) \end{aligned} \tag{A.63}$$

- Case $\mathbb{B}$ ($\mathrm{Pe}_s > 0\,,\ \omega_s > 0$, i.e. $q > 0$ incoming flow):

$$\begin{aligned} T_D(z_D, t_D) &= \frac{T_m}{T_\infty} \\ &+ \frac{\Delta T}{T_\infty} \exp\left(-\frac{|\mathrm{Pe}_s|}{2}\left(\gamma_+(\omega_s) - 1\right) z_D\right) \sin\left(-\frac{|\mathrm{Pe}_s|}{2}\gamma_-(\omega_s) z_D + \omega_s t_D\right) \end{aligned} \tag{A.64}$$

Note: $\omega_s t_D = \omega_o t$.

And the dimensional global solution:

- Case $\mathbb{A}$: Outgoing Flow ($\mathrm{Pe}_s < 0\,,\ \omega_s < 0$, i.e. $q < 0$):

$$\begin{aligned} T(z,t) &= (T_m - T_\infty) \exp\left(-\frac{|q|}{D\phi R} z\right) + T_\infty \\ &+ \Delta T \exp\left(-\frac{|q|}{2D\phi R}\left(1 + \gamma_+(\omega_s)\right) z\right) \sin\left(-\frac{|q|}{2D\phi R}\gamma_-(\omega_s) z + \omega_o t\right) \end{aligned} \tag{A.65}$$

- Caso $\mathbb{B}$: Incoming Flow ($\mathrm{Pe}_s > 0\,,\ \omega_s > 0$, i.e. $q > 0$):

$$T(z,t) = T_m + \Delta T \exp\left(-\frac{|q|}{2D\phi R}\left(\gamma_+(\omega_s) - 1\right) z\right) \sin\left(-\frac{|q|}{2D\phi R}\gamma_-(\omega_s) z + \omega_o t\right) \tag{A.66}$$

Where,

$$\omega_s = \frac{L\phi R}{q}\omega_o\,, \qquad \gamma_\pm(\omega) = \sqrt{\frac{1}{2}\left(\sqrt{1 + \frac{16\,\omega^2}{\mathrm{Pe}_s^2}} \pm 1\right)}\,, \qquad \mathrm{Pe}_s = \frac{Lq}{D\phi R}$$

$$D = D_\lambda + \frac{D_p}{\phi R}\,, \qquad R = 1 + \frac{(1-\phi)}{\phi}\frac{C_s}{C_w}$$

A.7 Approximations with expansions

In some situations, we may simplify the solutions by using an asymptotic or Taylor expansion. For example, we may have a small unit discharge q and we can use an asymptotic expansion to compute γ_+.

Calling $s = \dfrac{4\omega_s}{\mathrm{Pe}_s}$ we have:

$$s = \frac{4\omega_s}{\mathrm{Pe}_s} = \frac{4\frac{L\phi R}{q}\omega_o}{\frac{Lq}{D\phi R}} = \frac{4\omega_o D}{\left(\frac{q}{\phi R}\right)^2} \tag{A.67}$$

A.7.1 Small unit discharge

If $|q| \ll 1$ then $|s| \gg 1$ so we have:

$$\gamma_\pm(s) = \sqrt{\frac{1}{2}\left(\sqrt{1+s^2} \pm 1\right)} \sim \sqrt{\frac{1}{2}\left(\sqrt{s^2} \pm 1\right)} \sim \sqrt{\frac{1}{2}\left(s \pm 1\right)} \sim \sqrt{\frac{s}{2}} \tag{A.68}$$

and with the same reasoning we have that $\gamma_+ \pm 1 = \gamma_+$. While using these expressions in some of the arguments of the global solutions seen on A.6 we have:

$$\frac{|\mathrm{Pe}_s|}{2}\left(\gamma_+(s) \pm 1\right) \overset{|s|\gg 1}{\sim} \frac{|\mathrm{Pe}_s|}{2}\sqrt{\frac{s}{2}} = \frac{|\mathrm{Pe}_s|}{2}\sqrt{\frac{2\omega_s}{\mathrm{Pe}_s}}\sqrt{\omega_s \mathrm{Pe}_s} = \frac{\sqrt{2}}{2}\sqrt{\omega_s \mathrm{Pe}_s}$$

$$\frac{|\mathrm{Pe}_s|}{2}\gamma_-(s) \overset{|s|\gg 1}{\sim} \frac{\sqrt{2}}{2}\sqrt{\omega_s \mathrm{Pe}_s}$$

and replacing Pe_s and ω_s,

$$\frac{\sqrt{2}}{2}\sqrt{\omega_s \mathrm{Pe}_s} = L\sqrt{\frac{\omega_o}{2D}}$$

so the dimensional global solution reads:

- Case $\mathbb{A}$: Outgoing Flow ($\mathrm{Pe}_s < 0\,,\ \omega_s < 0$, i.e. $q < 0$) with $|q| \ll 1$:

$$\boxed{\begin{aligned} T(z,t) \quad &= (T_m - T_\infty)\exp\left(-\frac{|q|}{D\phi R}z\right) + T_\infty \\ &\quad + \Delta T\ \exp\left(-\sqrt{\frac{\omega_o}{2D}}\,z\right)\sin\left(-\sqrt{\frac{\omega_o}{2D}}\,z + \omega_o t\right) \end{aligned}} \tag{A.69}$$

- Caso $\mathbb{B}$: Incoming Flow ($\mathrm{Pe}_s > 0\,,\ \omega_s > 0$, i.e. $q > 0$) with $|q| \ll 1$:

$$\boxed{T(z,t) = T_m + \Delta T\ \exp\left(-\sqrt{\frac{\omega_o}{2D}}\,z\right)\sin\left(-\sqrt{\frac{\omega_o}{2D}}\,z + \omega_o t\right)} \tag{A.70}$$

A.7.2 Large unit discharge

If $|q| \gg 1$ then $|s| \ll 1$ so we have:

$$\gamma_{\pm}(s) = \sqrt{\frac{1}{2}\left(\sqrt{1+s^2} \pm 1\right)} \approx \sqrt{\frac{1}{2}\left(1 + \frac{s^2}{2} \pm 1\right)} \tag{A.71}$$

$$\gamma_{+}(s) \approx \sqrt{1 + \frac{s^2}{4}} \approx 1 + \frac{s^2}{8} \tag{A.72}$$

$$\gamma_{-}(s) \approx \sqrt{\frac{s^2}{4}} = \frac{|s|}{2} \tag{A.73}$$

and then,

$$\begin{aligned}
\frac{|\mathrm{Pe}_s|}{2}\left(\gamma_+(s)+1\right) &\approx \frac{|\mathrm{Pe}_s|}{2}(1+\frac{s^2}{8}+1) \approx |\mathrm{Pe}_s| \\
\frac{|\mathrm{Pe}_s|}{2}\left(\gamma_+(s)-1\right) &\approx \frac{|\mathrm{Pe}_s|}{2}(1+\frac{s^2}{8}-1) \approx \frac{|\mathrm{Pe}_s|}{16}\frac{16\omega_s^2}{\mathrm{Pe}_s^2} = \frac{\omega_s^2}{|\mathrm{Pe}_s|} \\
\frac{|\mathrm{Pe}_s|}{2}\gamma_-(s) &\approx \frac{|\mathrm{Pe}_s|}{2}\frac{|s|}{2} = \frac{|\mathrm{Pe}_s|}{4}\frac{4|\omega_s|}{|\mathrm{Pe}_s|} = |\omega_s|
\end{aligned}$$

and replacing Pe_s and ω_s,

$$\begin{aligned}
\frac{|\mathrm{Pe}_s|}{2}\left(\gamma_+(s)+1\right) &\approx \frac{L|q|}{D\phi R} \\
\frac{|\mathrm{Pe}_s|}{2}\left(\gamma_+(s)-1\right) &\approx \frac{LD}{\left(\frac{|q|}{\phi R}\right)^3} \\
\frac{|\mathrm{Pe}_s|}{2}\gamma_-(s) &\approx \frac{L\phi R}{|q|}\omega_o
\end{aligned}$$

The global solution reads:

- Case $\mathbb{A}$: Outgoing Flow ($\mathrm{Pe}_s < 0\,,\ \omega_s < 0$, i.e. $q < 0$) with $|q| \gg 1$:

$$\boxed{\begin{aligned} T(z,t) &= (T_m - T_\infty)\exp\left(-\frac{|q|}{D\phi R}z\right) + T_\infty \\ &\quad + \Delta T\,\exp\left(-\frac{|q|}{D\phi R}z\right)\sin\left(-\frac{\phi R}{|q|}\omega_o z + \omega_o t\right) \end{aligned}} \tag{A.74}$$

- Caso $\mathbb{B}$: Incoming Flow ($\mathrm{Pe}_s > 0\,,\ \omega_s > 0$, i.e. $q > 0$) with $|q| \gg 1$:

$$\boxed{T(z,t) = T_m + \Delta T\,\exp\left(-D\left(\frac{\phi R}{|q|}\right)^3 z\right)\sin\left(-\frac{\phi R}{|q|}\omega_o z + \omega_o t\right)} \tag{A.75}$$

Appendix B

In this appendix, we resume the resolution of the advection-conduction equation from the equation considered in section 3.3 and we solve it in detail. Therefore, we repeat some previous conclusions for the sake of clarity and continuity.

B.1 Advection-conduction equation

We rewrite the PDE equation in the equation 3.43:

$$C_b \frac{\partial T}{\partial t} = (\lambda + C_w\, D_{pL}) \frac{\partial^2 T}{\partial x^2} + (\lambda + C_w\, D_{pT}) \frac{\partial^2 T}{\partial y^2} - q C_w \frac{\partial T}{\partial x} + \Psi\, \delta(x, y) \qquad \text{[PDE]}$$

$$T(x, y, 0) = T_0 \qquad \text{[IC]} \tag{B.1}$$

Notation (International System of Units in parentheses):

- T: temperature, $[T] = \theta$ (K)
- λ: thermal conductivity, $[\lambda] = MLT^{-3}\theta^{-1}$ (J/m s K)
- C_w: water heat capacity, $[C_w] = ML^{-1}T^{-2}\theta^{-1}$ (J/m^{3}K)
- C_b: bulk heat capacity, $[C_b] = ML^{-1}T^{-2}\theta^{-1}$ (J/m^{3}K)
- q: unit discharge (flow velocity), $[q] = LT^{-1}$ (m^3/s m^2)
- D_{pL}: longitudinal dispersivity, $[D_{pL}] = L^2T^{-1}$ (m^2/s)
- D_{pT}: transversal dispersivity, $[D_{pT}] = L^2T^{-1}$ (m^2/s)
- Ψ: power density, heat source (power per unit of volume), $[\Psi] = ML^{-1}T^{-3}$ (W/m^3)

We call $D_\lambda = \dfrac{\lambda}{C_b}$ the thermal diffusivity $[D] = L^2T^{-1}$. On the other hand, bulk heat capacity can be written as follows:

$$C_b = \phi\, C_w + (1 - \phi) C_s$$

where ϕ is the porosity (in a saturated porous medium) and C_s is the heat capacity of the solid matrix. If we reconsider C_w/C_b and we use R as the thermal delay:

$$\frac{C_w}{C_b} = \frac{1}{\dfrac{C_b}{C_w}} = \frac{1}{\dfrac{\phi C_w + (1-\phi)C_s}{C_w}} = \frac{1}{\phi\left(1 + \dfrac{(1-\phi)}{\phi}\dfrac{C_s}{C_w}\right)} = \frac{1}{\phi R} \;\Rightarrow\; C_w = \frac{C_b}{\phi R} \tag{B.2}$$

and if we replace it in equation (B.1) as well as $\lambda = D_\lambda C_b$, we get:

$$C_b \frac{\partial T}{\partial t} = C_b \left(D_\lambda + \frac{D_{pL}}{\phi R} \right) \frac{\partial^2 T}{\partial x^2} + C_b \left(D_\lambda + \frac{D_{pT}}{\phi R} \right) \frac{\partial^2 T}{\partial y^2} - q \frac{C_b}{\phi R} \frac{\partial T}{\partial x} + \Psi \, \delta(x, y) \quad \text{(B.3)}$$

We call D_L the longitudinal diffusivity and D_T the transversal diffusivity; they consider the thermal diffusion and the dispersion of heat. They are defined as:

$$D_L = D_\lambda + \frac{D_{pL}}{\phi R}, \qquad D_T = D_\lambda + \frac{D_{pT}}{\phi R} \quad \text{(B.4)}$$

and replacing them in (B.3) we obtain:

$$C_b \frac{\partial T}{\partial t} = C_b \, D_L \frac{\partial^2 T}{\partial x^2} + C_b \, D_T \frac{\partial^2 T}{\partial y^2} - q \frac{C_b}{\phi R} \frac{\partial T}{\partial x} + \Psi \, \delta(x, y) \quad \text{(B.5)}$$

B.2 Initial condition

As we are considering the problem for $t > 0$, the initial condition reads:

$$t = 0 : \qquad T(x, y, 0) = T_0 \quad \text{(B.6)}$$

B.3 Dimensionless equation - Péclet number

First of all, we define the dimensionless values from the problem data:

$$T_D = \frac{T}{T_c}, \qquad t_D = \frac{t}{t_c}, \qquad x_D = \frac{x}{L_x}, \qquad y_D = \frac{y}{L_y} \quad \text{(B.7)}$$

We replace the dimensionless values in (B.5):

$$\frac{C_b T_c}{t_c} \frac{\partial T_D}{\partial t_D} = C_b D_L \frac{T_c}{L_x^2} \frac{\partial^2 T_D}{\partial x_D^2} + C_b D_T \frac{T_c}{L_y^2} \frac{\partial^2 T_D}{\partial y_D^2} - \frac{q C_b T_c}{\phi R L_x} \frac{\partial T_D}{\partial z_D} + \frac{\Psi}{L_x L_y} \delta(x_D, y_D)$$

$$\frac{\partial T_D}{\partial t_D} = D_L \frac{t_c}{L_x^2} \frac{\partial^2 T_D}{\partial x_D^2} + D_T \frac{t_c}{L_y^2} \frac{\partial^2 T_D}{\partial y_D^2} - \frac{q}{\phi R} \frac{t_c}{L_x} \frac{\partial T_D}{\partial z_D} + \frac{\Psi t_c}{C_b T_c L_x L_y} \delta(x_D, y_D) \quad \text{(B.8)}$$

And for the initial condition:

$$T_D(x_D, y_D, 0) = \frac{T_0}{T_c} \quad \text{(B.9)}$$

Using the dimensional analysis and Buckingham π theorem:

$$\frac{q}{\phi R} \frac{t_c}{L_x} = 1 \quad \rightarrow \quad t_c = L_x \frac{\phi R}{q}$$

that is the advection characteristic time[6] and,

$$L_x = L_y = L$$

$$T_c = \frac{\Psi t_c}{L^2 C_b} = \frac{\Psi \phi R}{C_b L q}$$

Replacing in (B.8) and in (B.9):

$$\begin{aligned} &\frac{\partial T_D}{\partial t_D} = \frac{D_L \phi R}{qL}\frac{\partial^2 T_D}{\partial x_D^2} + \frac{D_T \phi R}{qL}\frac{\partial^2 T_D}{\partial y_D^2} - \frac{\partial T_D}{\partial z_D} + \delta(x_D, y_D) && \text{[PDE]} \\ &T_D(x_D, y_D, 0) = \frac{T_0}{T_c} && \text{[IC]} \end{aligned} \tag{B.10}$$

We define Péclet number for a porous medium. It compares the diffusion and advection times:

$$\mathrm{Pe}_s = \frac{t_d}{t_a} = \frac{\frac{L^2}{D}}{\frac{L\phi R}{q}} = \frac{Lq}{D\phi R} \tag{B.11}$$

and considering the difference between longitudinal and transversal dispersion we define:

$$\mathrm{Pe}_L = \frac{Lq}{D_L \phi R}, \qquad \mathrm{Pe}_T = \frac{Lq}{D_T \phi R} \tag{B.12}$$

Rewriting equation (B.10),

$$\begin{aligned} &\frac{\partial T_D}{\partial t_D} = \frac{1}{\mathrm{Pe}_L}\frac{\partial^2 T_D}{\partial x_D^2} + \frac{1}{\mathrm{Pe}_T}\frac{\partial^2 T_D}{\partial y_D^2} - \frac{\partial T_D}{\partial z_D} + \delta(x_D, y_D) && \text{[PDE]} \\ &T_D(x_D, y_D, 0) = \frac{T_0}{T_c} && \text{[IC]} \end{aligned} \tag{B.13}$$

B.4 General resolution of the PDE

Starting with the dimensionless equation, we aim to find its eigenfunctions:

$$\frac{\partial T_D}{\partial t_D} = \frac{1}{\mathrm{Pe}_L}\frac{\partial^2 T_D}{\partial x_D^2} + \frac{1}{\mathrm{Pe}_T}\frac{\partial^2 T_D}{\partial y_D^2} - \frac{\partial T_D}{\partial z_D} + \delta(x_D, y_D) \tag{B.14}$$

For the sake of clarity, we note:

$$A = \frac{1}{\mathrm{Pe}_L}, \qquad B = \frac{1}{\mathrm{Pe}_T} \tag{B.15}$$

[6] While $t_c = L_x^2/D_L$ is the diffusion characteristic time in x direction and $t_c = L_y^2/D_T$ is the diffusion characteristic time in y direction. We could also consider it as the characteristic time without changing the resolution of our equation.

and we simplify the notation by writing all dimensionless variables a_D without its dimensionless symbol "$\cdot_D$" and it yields,

$$\frac{\partial T}{\partial t} = A\frac{\partial^2 T}{\partial x^2} + B\frac{\partial^2 T}{\partial y^2} - \frac{\partial T}{\partial x} + \delta(x,y) \tag{B.16}$$

where A, B and are constant.
We consider Fourier's Transform (FT) on x and y defined as below:

$$\hat{T}(k_x,y,t) = \mathcal{F}_x\left[T(x,y,t)\right](k_x,y,t) = \int_{-\infty}^{+\infty} T(x,y,t)\cdot e^{-ik_x x}dx \tag{B.17}$$

$$\breve{T}(x,k_y,t) = \mathcal{F}_y\left[T(x,y,t)\right](x,k_y,t) = \int_{-\infty}^{+\infty} T(x,y,t)\cdot e^{-ik_y y}dy \tag{B.18}$$

And applying the FT on x to the equation (B.16) we get:

$$\mathcal{F}_x\left[\frac{\partial T}{\partial t}\right] = \mathcal{F}_x\left[A\frac{\partial^2 T}{\partial x^2} + B\frac{\partial^2 T}{\partial y^2} - \frac{\partial T}{\partial x} + \delta(x,y)\right] \tag{B.19}$$

$$\frac{\partial \hat{T}}{\partial t} = \mathcal{F}_x\left[A\frac{\partial^2 T}{\partial x^2}\right] + \mathcal{F}_x\left[B\frac{\partial^2 T}{\partial y^2}\right] - \mathcal{F}_x\left[\frac{\partial T}{\partial x}\right] + \mathcal{F}_x\left[\delta(x,y)\right] \tag{B.20}$$

$$\frac{\partial \hat{T}}{\partial t} = A\left(ik_x\right)^2\hat{T} + B\frac{\partial^2 \hat{T}}{\partial y^2} - \left(ik_x\right)\hat{T} + \delta(y) \tag{B.21}$$

And applying now the FT on y:

$$\mathcal{F}_y\left[\frac{\partial \hat{T}}{\partial t}\right] = \mathcal{F}_y\left[A\left(ik_x\right)^2\hat{T} + B\frac{\partial^2 \hat{T}}{\partial y^2} - \left(ik_x\right)\hat{T} + \delta(y)\right] \tag{B.22}$$

$$\frac{\partial \breve{\hat{T}}}{\partial t} = A\left(ik_x\right)^2\breve{\hat{T}} + B\left(ik_y\right)^2\breve{\hat{T}} - \left(ik_x\right)\breve{\hat{T}} + 1 \tag{B.23}$$

we note $\breve{\hat{T}} \overset{\text{not.}}{=} \tilde{T}$. Equation (B.23) reads,

$$\frac{\partial \tilde{T}}{\partial t} = \left(-Ak_x^2 - Bk_y^2 - ik_x\right)\tilde{T} + 1 \tag{B.24}$$

$$\frac{\partial \tilde{T}}{\partial t} = -\xi\tilde{T} + 1 \qquad\qquad \xi \equiv \xi(k_x,k_y) \overset{\text{not.}}{=} Ak_x^2 + Bk_y^2 + ik_x \tag{B.25}$$

Using ODE resolution method for a first order linear ordinary differential equation:

$$\left.\begin{aligned} &\tilde{T} = \tilde{T}_h + \tilde{T}_p \\ &\tilde{T}_h = Ce^{-\xi t} \\ &\tilde{T}_p = \frac{1}{\xi} \end{aligned}\right\} \quad \tilde{T} = Ce^{-\xi t} + \frac{1}{\xi} \tag{B.26}$$

B.5 Imposition of the initial condition

To determine C, we have to impose the initial condition. Before imposing it to $\tilde{T}$, first, we have to apply the FT to (B.16)[CI]:

$$\tilde{T}(x,y,0) = \mathcal{F}_y\left[\mathcal{F}_x\left[u(x,y,0)\right]\right] = \mathcal{F}_y\left[\mathcal{F}_x\left[\frac{T_0}{T_c}\right]\right] = \mathcal{F}_y\left[\frac{T_0}{T_c}\,\delta(k_x)\right] = \frac{T_0}{T_c}\,\delta(k_x,k_y) \quad \text{(B.27)}$$

So we have,

$$\tilde{T}(k_x,k_y,0) = C + \frac{1}{\xi(k_x,k_y)} = \frac{T_0}{T_c}\,\delta(k_x,k_y) \qquad \Rightarrow \qquad C = \frac{T_0}{T_c}\,\delta(k_x,k_y) - \frac{1}{\xi(k_x,k_y)} \quad \text{(B.28)}$$

And then,

$$\tilde{T}(k_x,k_y,t) = \left[\frac{T_0}{T_c}\,\delta(k_x,k_y) - \frac{1}{\xi(k_x,k_y)}\right] e^{-\xi(k_x,k_y)t} + \frac{1}{\xi(k_x,k_y)} \quad \text{(B.29)}$$

In order to obtain $u(x,y,t)$ we need to go from the frequency domain to the space domain. We consider the Inverse Fourier Transform (IFT):

$$T(x,y,t) = \mathcal{F}_x^{-1}\left[\hat{T}(k_x,y,t)\right](x,y,t) = \frac{1}{2\pi}\int_{-\infty}^{+\infty} \hat{T}(k_x,y,t)\cdot e^{ik_x x}dk_x \quad \text{(B.30)}$$

$$T(x,y,t) = \mathcal{F}_y^{-1}\left[\breve{T}(x,k_y,t)\right](x,y,t) = \frac{1}{2\pi}\int_{-\infty}^{+\infty} \breve{T}(x,k_y,t)\cdot e^{ik_y y}dk_y \quad \text{(B.31)}$$

Applying IFT on y:

$$\begin{aligned}\hat{T}(k_x,y,t) &= \mathcal{F}_y^{-1}\left[\tilde{T}(k_x,k_y,t)\right] \\ &= \frac{1}{2\pi}\int_{-\infty}^{+\infty}\left(\left[\frac{T_0}{T_c}\,\delta(k_x,k_y) - \frac{1}{\xi(k_x,k_y)}\right] e^{-\xi(k_x,k_y)t} + \frac{1}{\xi(k_x,k_y)}\right) e^{ik_y y}dk_y\end{aligned}$$

And then on x:

$$\begin{aligned} T(x,y,t) &= \mathcal{F}_x^{-1}\left[\hat{T}(k_x,y,t)\right] \\ &= \frac{1}{(2\pi)^2}\int_{\mathbb{R}^2}\left(\left[\frac{T_0}{T_c}\,\delta(k_x,k_y)-\frac{1}{\xi(k_x,k_y)}\right]e^{-\xi(k_x,k_y)t}+\frac{1}{\xi(k_x,k_y)}\right)e^{ik_y y+ik_x x}dk_y dk_x \\ &= \frac{T_0}{T_c}-\frac{1}{(2\pi)^2}\int_{\mathbb{R}^2}\left(\frac{1}{\xi(k_x,k_y)}e^{-\xi(k_x,k_y)t}\right)e^{ik_y y+ik_x x}dk_y dk_x \\ &\quad+\frac{1}{(2\pi)^2}\int_{\mathbb{R}^2}\frac{1}{\xi(k_x,k_y)}e^{ik_y y+ik_x x}dk_y dk_x \\ &= \frac{T_0}{T_c}+\frac{1}{(2\pi)^2}\int_{\mathbb{R}^2}\frac{1}{\xi(k_x,k_y)}e^{ik_y y+ik_x x}\left(1-e^{-\xi(k_x,k_y)t}\right)dk_y dk_x \end{aligned} \tag{B.32}$$

where $\xi(k_x,k_y)=Ak_x^2+Bk_y^2+ik_x$.
Resuming the dimensionless notation,

$$T_D(x_D,y_D,t_D)=\frac{T_0}{T_c}+\frac{1}{(2\pi)^2}\int_{\mathbb{R}^2}\frac{1}{\xi(k_x,k_y)}e^{ik_y y_D+ik_x x_D}\left(1-e^{-\xi(k_x,k_y)t_D}\right)dk_y dk_x \tag{B.33}$$

where $\xi(k_x,k_y)=Ak_x^2+Bk_y^2+ik_x$.

B.6 Final temperature at the source point

Computing the previous equation B.33 and substituting in $(x,y)=(0,0)$ we obtain the temperature evolution for the source point:

$$(x,y)=(0,0) \qquad \Rightarrow \qquad (x_D,y_D)=(0,0)$$

$$T_D(0,0,t_D)\overset{\text{not.}}{=}T_D(t_D)=\frac{T_0}{T_c}+\frac{1}{(2\pi)^2}\int_{\mathbb{R}^2}\frac{1}{\xi(k_x,k_y)}\left(1-e^{-\xi(k_x,k_y)t_D}\right)dk_y dk_x \tag{B.34}$$

Replacing $T_D=\frac{T}{T_c}$,

$$T(t_D)=T_0+\frac{T_c}{(2\pi)^2}\int_{\mathbb{R}^2}\frac{1}{\xi(k_x,k_y)}\left(1-e^{-\xi(k_x,k_y)t_D}\right)dk_y dk_x \tag{B.35}$$

We consider the time derivative of the function $T_D(0,0,t_D)$. Equation (B.35) is too complex to solve, therefore we will simplify the process by working with the time derivative of the temperature.

$$\frac{dT}{dt_D}(t_D)=\frac{T_c}{(2\pi)^2}\int_{\mathbb{R}^2}e^{-\left(Ak_x^2+Bk_y^2+ik_x\right)t_D}dk_y dk_x \tag{B.36}$$

separating the two integrals,

$$\frac{dT}{dt_D}(t_D) = \frac{T_c}{(2\pi)^2}\int_{-\infty}^{+\infty} e^{-Bk_y^2 t_D}dk_y \int_{-\infty}^{+\infty} e^{-\left(Ak_x^2+ik_x\right)t_D}dk_x \tag{B.37}$$

- Integral on k_y: Applying the change of variable $z = \sqrt{Bt_D}k_y$ we find the Gaussian integral:

$$\int_{-\infty}^{+\infty} e^{-Bk_y^2 t_D}dk_y = \frac{1}{\sqrt{Bt_D}}\int_{-\infty}^{+\infty} e^{-z^2}dz = \sqrt{\frac{\pi}{Bt_D}} \tag{B.38}$$

- Integral on k_x: Rearrenging the exponent,

$$\left(Ak_x^2 + ik_x\right)t_D = \left(\sqrt{At_D}\left(k_x + \frac{i}{2A}\right)\right)^2 + \frac{t_D}{4A}$$

it yields,

$$\int_{-\infty}^{+\infty} e^{-\left(Ak_x^2+ik_x\right)t_D}dk_x = \int_{-\infty}^{+\infty} e^{-\left(\sqrt{At_D}\left(x+\frac{i}{2A}\right)\right)^2 - \frac{t_D}{4A}}dk_x$$

$$= \frac{e^{-\frac{t_D}{4A}}}{\sqrt{At_D}}\int_{-\infty}^{+\infty} e^{-z^2}dz = \frac{\sqrt{\pi}e^{-\frac{t_D}{4A}}}{\sqrt{At_D}} \qquad \text{where } z = \sqrt{At_D}\left(k_x + \frac{i}{2a}\right) \tag{B.39}$$

Raplacing equations (B.38) and (B.39) into (B.37),

$$\frac{dT}{dt_D}(t_D) = \frac{T_c}{(2\pi)^2}\sqrt{\frac{\pi}{Bt_D}}\frac{\sqrt{\pi}e^{-\frac{t_D}{4A}}}{\sqrt{At_D}} = \frac{T_c}{4\pi\sqrt{AB}}\frac{e^{-\frac{t_D}{4A}}}{t_D} \tag{B.40}$$

using the dimensional time we have,

$$\frac{dT}{dt}\underbrace{\frac{dt}{dt_D}}_{t_c} = \frac{T_c}{4\pi\sqrt{AB}}t_c\frac{e^{-\frac{t}{4At_c}}}{t} \qquad \Rightarrow \qquad \frac{dT}{dt} = \frac{T_c}{4\pi\sqrt{AB}}\frac{e^{-\frac{t}{4At_c}}}{t} \tag{B.41}$$

Equation (B.41) provides valuable information. Indeed, it is the time derivative of the temperature in the source point. Its slope reports the growth rate of the temperature. If we consider the change of variable $p = \ln t$ and we compute dT/dp:

$$p = \ln\frac{t}{t_{ref}} \quad \Rightarrow \quad \frac{dT}{dt}(t) = \frac{dT}{dp}\frac{dp}{dt}(t) \quad \Rightarrow \quad \frac{dT}{d(\ln t)} = \frac{dT}{dt}\left(\frac{d(\ln t)}{dt}\right)^{-1} = \frac{dT}{dt}\cdot t \tag{B.42}$$

and it yields,

$$\frac{dT}{d(\ln t)} = \frac{T_c}{4\pi\sqrt{AB}}e^{-t/4At_c} \tag{B.43}$$

This expression will allow us to understand the plot in semilogarithm scale of the evolution of the temperature of the source point. Using series expansion for t small,

$$\frac{dT}{d(\ln t)} = \frac{T_c}{4\pi\sqrt{AB}}\left(1 - \frac{t}{4At_c} + O(t^2)\right) \tag{B.44}$$

That we can distinguish $dT/d(\ln t)$ for different cases depending on t:

$$\frac{dT}{d(\ln t)} \approx \begin{cases} \dfrac{T_c}{4\pi\sqrt{AB}} & \text{for } t \ll 4At_c \\ \dfrac{T_c}{4\pi\sqrt{AB}}\left(1 - \dfrac{t}{4At_c}\right) & \text{for } t \ll 16A^2t_c^2 \end{cases} \tag{B.45}$$

We observe that for small values of $t/4At_c$, the derivative is approximately constant and with a slope of $T_c/4\pi\sqrt{AB}$. In addition, as t increases, the slope begins to decrease (as the the first order term is negative) that could lead to a stabilisation of the temperature. Back to the time derivative of the temperature, we consider the case where t tends to infinity:

$$\lim_{t\to+\infty}\frac{dT}{dt} = \lim_{t\to+\infty}\frac{T_c}{4\pi\sqrt{AB}}\frac{e^{-\frac{t}{4At_c}}}{t} = 0 \tag{B.46}$$

This result shows that the temperature becomes constant for $t \to +\infty$. However, we still do not know if we have a finite temperature when $t \to +\infty$.
In order to define the value of the temperature at time t at the source point, we integrate the equation (B.41). We consider as hypothesis the fact that the temperature at $t \to$ is finite, i.e. $T_f < +\infty$:

$$\int_{T(t)}^{T_f} dT = \frac{T_c}{4\pi\sqrt{AB}}\int_t^{+\infty}\frac{e^{-\frac{\tau}{4At_c}}}{\tau}d\tau$$

$$T_f - T(t) = \frac{T_c}{4\pi\sqrt{AB}}\int_t^{+\infty}\frac{e^{-\frac{\tau}{4At_c}}}{\tau}d\tau$$

$$T(t) = T_f - \frac{T_c}{4\pi\sqrt{AB}}\int_t^{+\infty}\frac{e^{-\frac{\tau}{4At_c}}}{\tau}d\tau \tag{B.47}$$

Considering the exponential integral Ei as follows:

$$\mathrm{Ei}(x) = -\int_{-x}^{+\infty}\frac{e^{-s}}{s}ds \tag{B.48}$$

We apply the change of variable $s = \frac{\tau}{4At_c}$ to the equation (B.47):

$$T(t) = T_f - \frac{T_c}{4\pi\sqrt{AB}}\int_{\frac{t}{4At_c}}^{+\infty}\frac{e^{-s}}{s}ds = T_f + \frac{T_c}{4\pi\sqrt{AB}}\,\mathrm{Ei}\left(-\frac{t}{4At_c}\right) \tag{B.49}$$

Replacing $T_f = T_0 + \Delta T$ we have,

$$T(t) = T_0 + \Delta T + \frac{T_c}{4\pi\sqrt{AB}} \operatorname{Ei}\left(-\frac{t}{4At_c}\right) \tag{B.50}$$

and evaluating $T(0)$ we should obtain T_0:

$$T(0) = T_0 = T_0 + \Delta T + \frac{T_c}{4\pi\sqrt{AB}} \operatorname{Ei}(0) \tag{B.51}$$

$$\Delta T = -\frac{T_c}{4\pi\sqrt{AB}} \operatorname{Ei}(0) \to +\infty \tag{B.52}$$

So the hypothesis made on T_f is not valid as we encounter an infinite increase of temperature ΔT. We conclude that equation B.50 is consistent with the rate of growth, but the absolute temperature is infinite. Physically, we are giving a finite energy to a single point, so we are imposing an infinite energy density carrying the point to increase infinitely its temperature.
In order to have the slope in dimensional terms, we replace T_c, A and B:

$$\frac{T_c}{4\pi\sqrt{AB}} = \frac{\Psi}{4\pi C_b\sqrt{D_L D_T}} = \frac{\Psi}{4\pi\sqrt{(\lambda + C_w D_{pL})(\lambda + C_w D_{pT})}}$$

and if $D_\lambda \gg D_{pL}$ (and so it is $D_\lambda \gg D_{pT}$) then we have,

$$\frac{T_c}{4\pi\sqrt{AB}} \approx \frac{\Psi}{4\pi\lambda} \tag{B.53}$$

B.7 Final temperature

Using the dimensional temperature for the equation B.33, we have

$$T(x_D, y_D, t_D) = T_0 + \frac{T_c}{(2\pi)^2} \int_{\mathbb{R}^2} \frac{1}{\xi(k_x, k_y)} e^{ik_y y_D + ik_x x_D} \left(1 - e^{-\xi(k_x,k_y)t_D}\right) dk_y dk_x \tag{B.54}$$

where $\xi(k_x, k_y) = Ak_x^2 + Bk_y^2 + ik_x$. And its time derivative,

$$\frac{\partial T}{\partial t}(x_D, y_D, t_D) = \frac{T_c}{(2\pi)^2} \int_{\mathbb{R}^2} \exp\left(ik_y y_D + ik_x x_D - \xi(k_x, k_y)t_D\right) dk_y dk_x \tag{B.55}$$

separating the two integrals,

$$\frac{\partial T}{\partial t}(x_D, y_D, t_D) = \frac{T_c}{(2\pi)^2} \int_{-\infty}^{+\infty} e^{-Bk_y^2 t_D + ik_y y_D} dk_y \int_{-\infty}^{+\infty} e^{-Ak_x^2 t_D + ik_x(x_D - t_D)} dk_x \tag{B.56}$$

using the identity $-ax^2 + bx = -\left(\sqrt{a}\,(x - b/2a)\right)^2 + b^2/4a$ for the exponents, we have:

- Integral on k_x:

$$I_x = \int_{-\infty}^{+\infty} e^{-Ak_x^2 t_D + ik_x(x_D - t_D)} dk_x$$
$$= \int_{-\infty}^{+\infty} \exp\left(-\left(\sqrt{At_D}\left(k_x - \frac{i(x_D - t_D)}{2At_D} \right) \right)^2 - \frac{(x_D - t_D)^2}{4At_D} \right) dk_x \quad \text{(B.57)}$$

Applying the change of variable,

$$z = \sqrt{At_D}\left(k_x - \frac{i(x_D - t_D)}{2At_D} \right), \qquad dk_x = \frac{dz}{\sqrt{At_D}}$$

we encounter the Gaussian integral:

$$I_x = \frac{e^{-(x_D - t_D)^2/4At_D}}{\sqrt{At_D}} \int_{-\infty}^{+\infty} e^{-z^2} dz = \frac{\sqrt{\pi} e^{-(x_D - t_D)^2/4At_D}}{\sqrt{At_D}} \quad \text{(B.58)}$$

- Integral on k_y:

$$I_y = \int_{-\infty}^{+\infty} e^{-Bk_y^2 t_D + ik_y y_D} dk_y = \int_{-\infty}^{+\infty} \exp\left(-\left(Bt_D\left(k_y - \frac{y_D}{2Bt_D} i \right) \right)^2 - \frac{y_D^2}{4Bt_D} \right) dk_y \quad \text{(B.59)}$$

Applying the change of variable,

$$z = \sqrt{Bt_D}\left(k_y - \frac{iy_D}{2Bt_D} \right), \qquad dk_y = \frac{dz}{\sqrt{Bt_D}}$$

we encounter the Gaussian integral:

$$I_y = \frac{e^{-y_D^2/4Bt_D}}{\sqrt{Bt_D}} \int_{-\infty}^{+\infty} e^{-z^2} dz = \frac{\sqrt{\pi} e^{-y_D^2/4Bt_D}}{\sqrt{Bt_D}} \quad \text{(B.60)}$$

back to $\partial T / \partial t_D$:

$$\frac{\partial T}{\partial t}(x_D, y_D, t_D) = \frac{T_c}{(2\pi)^2} I_x I_y = \frac{T_c}{4\pi\sqrt{AB} t_D} \exp\left(-\frac{(x_D - t_D)^2}{4At_D} - \frac{y_D^2}{4Bt_D} \right) \quad \text{(B.61)}$$

If we integrate in time,

$$\int_{T_0}^{T(t)} dT = \int_0^{t_D} \frac{T_c}{4\pi\sqrt{AB}\tau} \exp\left(-\frac{(x_D - \tau)^2}{4At_D} - \frac{y_D^2}{4Bt_D} \right) d\tau$$

$$T(t) - T_0 = \frac{T_c}{4\pi\sqrt{AB}} \int_0^{t_D} \frac{1}{\tau} \exp\left(-\frac{(x_D - \tau)^2}{4At_D} - \frac{y_D^2}{4B\tau} \right) d\tau \quad \text{(B.62)}$$

Note that at $(x_D, y_D) = (0, 0)$ we get the equation (B.47). From now on, we omit the dimensionless symbol "$\cdot_D$" for x_D, y_D and t_D. Integration is facilitated by denoting,

$$u = \frac{Bx^2 + Ay^2}{16AB\tau}$$

so that,

$$\frac{\tau}{4A} = \frac{Bx^2 + Ay^2}{16A^2Bu} = \frac{\beta^2}{4u}, \qquad \frac{d\tau}{A} = -\frac{\beta^2}{u^2}du$$

where,

$$\beta = \sqrt{\frac{Bx^2 + Ay^2}{4A^2B}}$$

Therefore,

$$T(x, y, t) = \frac{T_c}{4\pi\sqrt{AB}} e^{x/2A} \int_u^{+\infty} \frac{1}{u} \exp\left(-u - \frac{\beta^2}{4u}\right) du \tag{B.63}$$

$$= \frac{T_c}{4\pi\sqrt{AB}} e^{x/2A} W_H\left(u, \beta\right) \tag{B.64}$$

$$= \frac{T_c}{4\pi\sqrt{AB}} e^{x/2A} W_H\left(\frac{Bx^2 + Ay^2}{16AB\tau}, \sqrt{\frac{Bx^2 + Ay^2}{4A^2B}}\right) \tag{B.65}$$

Where,

$$W_H(u, \beta) = \int_u^{+\infty} \frac{1}{\xi} \exp\left(-\xi - \frac{\beta^2}{4\xi}\right) d\xi \tag{B.66}$$

Custodio and Llamas [16] discuss some interesting properties. In particular, the asymptotic behavior is:

$$W_H(0, \beta) = K_0(\beta) \approx \sqrt{\frac{\pi}{2\beta}} \left(1 - \frac{1}{8\beta}\right) e^{-\beta} \qquad \text{when } \beta > 5 \tag{B.67}$$

where K_0 is the modified Bessel function of second kind and order zero.

Appendix C

In this appendix, we summarize the procedure to obtain the unit discharge q and the depth z from temperature data. We start from the global solution presented in section 3.2.2 and developed in appendix 5.

The transient part of the global solution (equations (A.57) and (A.62)) for incoming and outgoing flow can be written as follows:

$$T^t(z,t) = \Delta T \exp\left(-\frac{|q|}{2D\phi R}\left(\gamma_+(\omega_s) - \text{sgn } q\right) z\right) \sin\left(-\frac{|q|}{2D\phi R}\gamma_-(\omega_s) z + \omega_o t\right) \quad \text{(C.1)}$$

where sgn q is the sign function, being 1 when $q > 0$ and -1 when $q < 0$. This equation includes the two cases (outgoing and incoming flow). We consider $\gamma_\pm(\omega_s) = \gamma_\pm(q)$, as Péclet number and the reduced frequency depend on q. We define the amplitude A and the phase θ:

$$A(z) = \Delta T \exp\left(-\frac{|q|}{2D\phi R}\left(\gamma_+(q) - \text{sgn } q\right) z\right) \quad \text{(C.2)}$$

$$\theta(z,t) = -\frac{|q|}{2D\phi R}\gamma_-(q) z + \omega_o t \quad \text{(C.3)}$$

As expected, $A_{ref} = A(0) = \Delta T$ and $\theta_{ref}(t) = \theta(0,t) = \omega_o t$. To measure in field, we compare the amplitude and the time lapse with a reference state (figure C.1), i.e. we measure ΔA and Δt. We only compare the amplitude of the transient solution. To that end, we would measure the amplitude in field by averaging A^+ substracting the mean value of the maximum recorded temperature, and A^-, obtained substracting the minimum T from the mean. For Δt we have,

$$\Delta\theta = \theta_{ref}(t) - \theta(z,t) = 0 \quad \Rightarrow \quad \omega_o t_{ref} - \left(-\frac{|q|}{2D\phi R}\gamma_-(q) z + \omega_o\left(t_{ref} + \Delta t\right)\right) = 0$$

$$z = \frac{\omega_o \Delta t \, 2D\phi R}{|q|\gamma_-(q)} \quad \text{(C.4)}$$

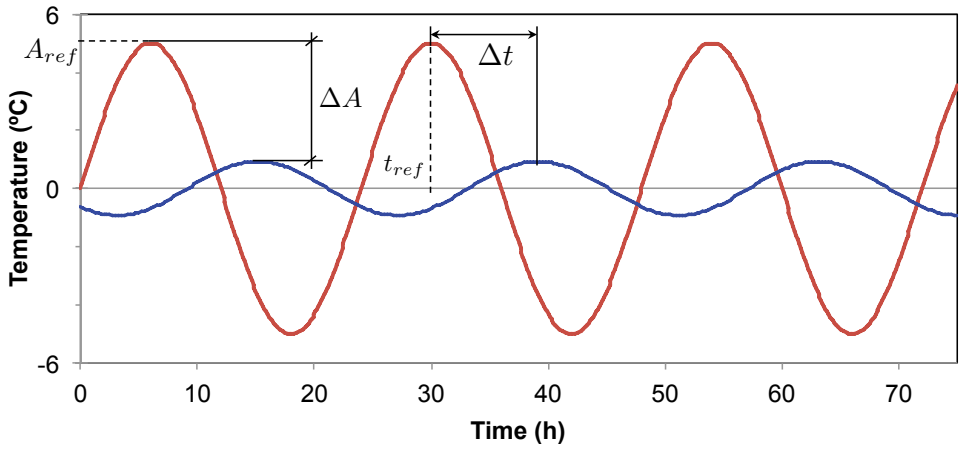

FIGURE C.1: Measured parameters in field
In red the reference curve, normally at $z = 0$, and in blue the measured curve in a particular depth z.

and for ΔA,

$$\Delta A(z) = A_{ref} - A(z) = \Delta T - \Delta T \exp\left(-\frac{|q|}{2D\phi R}\left(\gamma_+(\omega_s) - \operatorname{sgn} q\right) z\right)$$

$$\frac{\Delta T - \Delta A}{\Delta T} = \exp\left(-\frac{|q|}{2D\phi R}\left(\gamma_+(\omega_s) - \operatorname{sgn} q\right) z\right)$$

replacing the equation (C.4) yields,

$$\frac{\Delta T - \Delta A}{\Delta T} = \exp\left(-\frac{|q|}{2D\phi R}\left(\gamma_+(\omega_s) - \operatorname{sgn} q\right) \frac{\omega_o \Delta t\, 2D\phi R}{|q|\gamma_-(q)}\right) \tag{C.5}$$

$$-\frac{1}{\omega_o \Delta t} \ln\left(\frac{\Delta T - \Delta A}{\Delta T}\right) = \frac{\gamma_+(q) - \operatorname{sgn} q}{\gamma_-(q)} \tag{C.6}$$

and we note,

$$\mathrm{Md}^*(q) \overset{\text{not.}}{=} \frac{\gamma_+(q) - \operatorname{sgn} q}{\gamma_-(q)} = \frac{\sqrt{\frac{1}{2}\left(\sqrt{1+s^2}+1\right)} - \operatorname{sgn} q}{\sqrt{\frac{1}{2}\left(\sqrt{1+s^2}-1\right)}} \tag{C.7}$$

where $s = D\omega_o \left(\frac{\phi R}{q}\right)^2 = \left(\frac{\lambda}{C_b} + \frac{\alpha_L |q|}{\phi R}\right) \omega_o \left(\frac{\phi R}{q}\right)^2$
Figure C.2 displays the function $\mathrm{Md}^*(q)$.

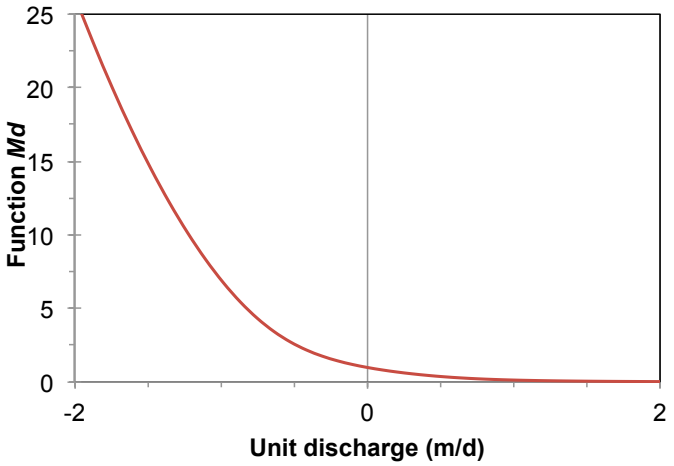

(a) Lin-lin plot of Md*

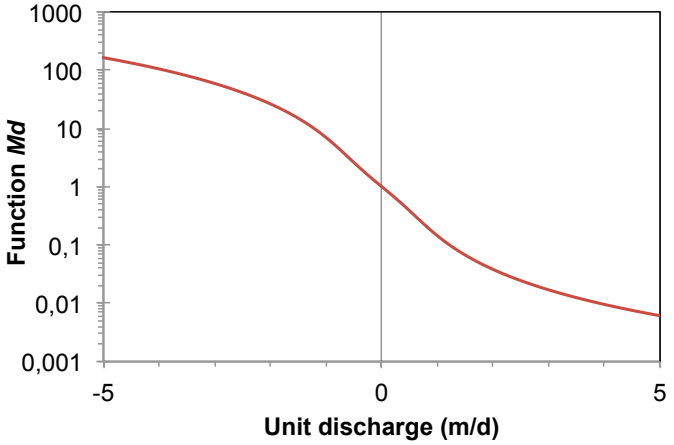

(b) Log-lin plot of Md*

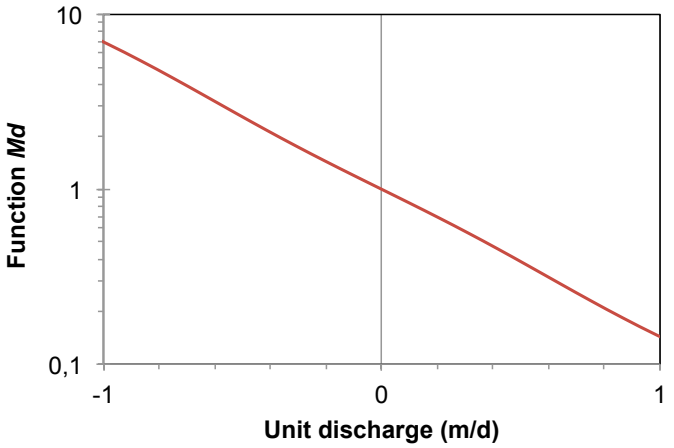

(c) Log-lin plot of Md

FIGURE C.2: Function Md* with several resolutions

With $\omega = 7.272 \cdot 10^{-5}\,\mathrm{s}^{-1}$ ($\tau = 1\,\mathrm{day}$), $\phi = 0.3$, $R = 2.492$, $D = 5.0366 \cdot 10^{-7}\,\mathrm{m}^2$

To sum up, to compute the unit discharge q and the depth z of the measuring point we follow the next steps:

1. We measure the period τ of our problem, i.e. the elapsed time between two peaks of the temperature. In our case, we consider the daily thermal fluctuation of the sea, so $\tau = 1$ day. We compute $\omega = 2\pi/\tau = 7.272 \cdot 10^{-5}\,\mathrm{s}^{-1}$.
2. We measure the amplitude of the sea thermal fluctuation $A_{sea} = \Delta T$ and the amplitude of the thermal response of our measuring point A_p. Then, we compute the difference.
3. We measure the peak delay Δt: we measure the peak time for the sea temperature t_{ref} and the first peak time t_p after the reference time of our measuring point. We compute the difference: $\Delta t = t_p - t_{ref}$. We could also measure the elapsed time Δt between the peak of the sea temperature and the peak of the temperature of the measuring point, or the elapsed time between crossings of the mean temperature.
4. We compute Md:
$$\mathrm{Md} = -\frac{1}{\omega_o \Delta t} \ln\left(\frac{A_p}{\Delta T}\right) \tag{C.8}$$
where ω is the angular frequency and ln is the natural logarithm.
5. Using the figures C.3 and C.4, we find the corresponding dimensionless unit discharge r for the Md value found in step 4.
6. We compute β:
$$\beta = 2\phi R\sqrt{D\omega} \tag{C.9}$$
where $D = \lambda/C_b$ (m^2/s) is the dispersion coefficient[7], ϕ the porosity of the bulk and R the thermal delay computed as follows: $R = 1 + \frac{1-\phi}{\phi}\frac{C_s}{C_w}$ where C_s ($\mathrm{J/m^3K}$) and C_w ($\mathrm{J/m^3K}$) are the heat capacities of the solid matrix and water.
7. We compute the unit discharge q:
$$q = \beta r \tag{C.10}$$
8. The first time that we computed β, we did not consider the dispersion coefficient. We repeat steps 6 and 7 to obtain a more accurate measure. One iteration is enough to have an accurate result.
9. Once we have the unit discharge q, we compute the depth z:
$$z = \frac{\omega \Delta t\, 2D\phi R}{|q|\sqrt{\frac{1}{2}\left(\sqrt{1 + \frac{\beta^2}{q^4}} - 1\right)}} \tag{C.11}$$

[7] We will iterate in order to consider the dispersion coefficient.

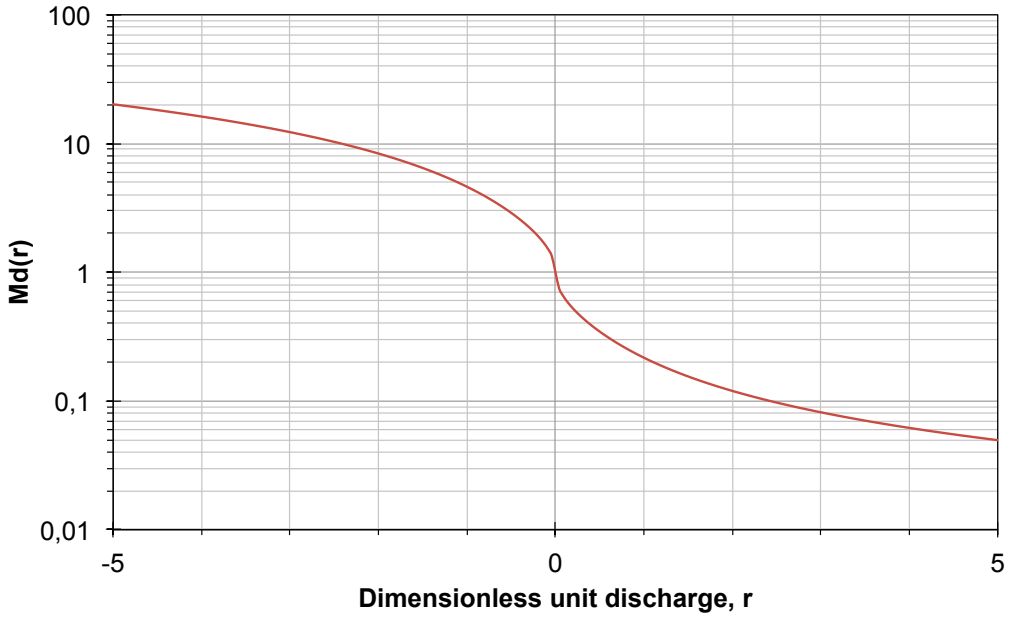

(a) Lon-lin plot of Md

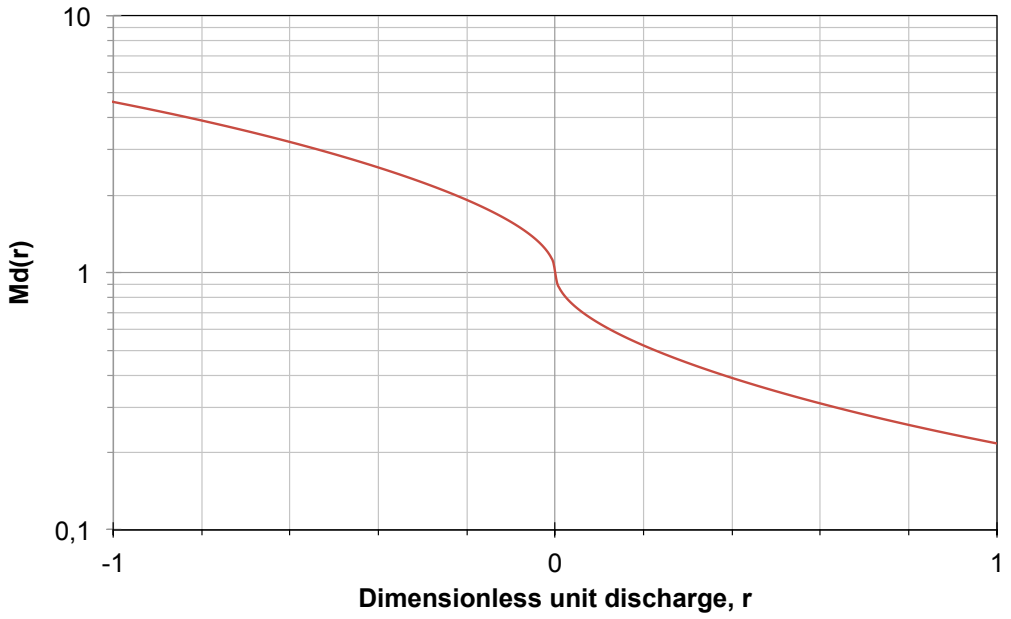

(b) Log-lin plot of Md

FIGURE C.3: Md function (high and medium values)

The axis of abscissa represents the dimensionless variable r computed as $r = \beta q$, where $\beta = 2\phi R\sqrt{D\omega}$ and q is the dimensional unit discharge.

FIGURE C.4: Md function (low values)

Lin-lin plot. The axis of abscissa represents the dimensionless variable r computed as $r = \beta q$, where $\beta = 2\phi R\sqrt{D\omega}$ and q is the dimensional unit discharge.

Bibliography

[1] Adrian D Werner, Mark Bakker, Vincent EA Post, Alexander Vandenbohede, Chunhui Lu, Behzad Ataie-Ashtiani, Craig T Simmons, and David A Barry. Seawater intrusion processes, investigation and management: recent advances and future challenges. *Advances in Water Resources*, 51:3–26, 2013.

[2] Emil O Frind. Seawater intrusion in continuous coastal aquifer-aquitard systems. *Advances in water Resources*, 5(2):89–97, 1982.

[3] Peter S Huyakorn, Peter F Andersen, James W Mercer, and Harold O White. Saltwater intrusion in aquifers: Development and testing of a three-dimensional finite element model. *Water Resources Research*, 23(2):293–312, 1987.

[4] Mohsen Rezaei, Esteban Sanz, Ezat Raeisi, Carlos Ayora, Enric Vázquez-Suné, and Jesús Carrera. Reactive transport modeling of calcite dissolution in the fresh-salt water mixing zone. *Journal of Hydrology*, 311(1):282–298, 2005.

[5] Nuria Boluda-Botella, Vicente Gomis-Yagües, and Francisco Ruiz-Beviá. Influence of transport parameters and chemical properties of the sediment in experiments to measure reactive transport in seawater intrusion. *Journal of Hydrology*, 357(1): 29–41, 2008.

[6] MJ Drury, AM Jessop, and TJ Lewis. The detection of groundwater flow by precise temperature measurements in boreholes. *Geothermics*, 13(3):163–174, 1984.

[7] Mary P Anderson. Heat as a ground water tracer. *Ground water*, 43(6):951–968, 2005.

[8] Mark Bakker, Ruben Caljé, Frans Schaars, Kees-Jan van der Made, and Sander de Haas. An active heat tracer experiment to determine groundwater velocities using fiber optic cables installed with direct push equipment. *Water Resources Research*, 51(4):2760–2772, 2015.

[9] Mark B Hausner, Levi Kryder, John Klenke, Richard Reinke, and Scott W Tyler. Interpreting variations in groundwater flows from repeated distributed thermal perturbation tests. *Groundwater*, 2015.

[10] Eddie W Banks, Margaret A Shanafield, and Peter G Cook. Induced temperature gradients to examine groundwater flowpaths in open boreholes. *Groundwater*, 52 (6):943–951, 2014.

[11] Christine E Hatch, Andrew T Fisher, Justin S Revenaugh, Jim Constantz, and Chris Ruehl. Quantifying surface water–groundwater interactions using time series analysis of streambed thermal records: Method development. *Water Resources Research*, 42(10), 2006.

[12] Jannick Kolbjørn Jensen and Peter Engesgaard. Nonuniform groundwater discharge across a streambed: Heat as a tracer. *Vadose Zone Journal*, 10(1):98–109, 2011.

[13] Nelson Molina-Giraldo, Philipp Blum, Ke Zhu, Peter Bayer, and Zhaohong Fang. A moving finite line source model to simulate borehole heat exchangers with groundwater advection. *International Journal of Thermal Sciences*, 50(12):2506–2513, 2011.

[14] J Cirés and X Berástegui. Mapa geològic de catalunya 1: 25 000-full 393-2-2 (74-31) 421-2-1 (74-31) mataró, premià de mar. *Servei Geològic de Catalunya i Institut Cartogràfic de Catalunya, Barcelona*, 1985, 2003, 2006, 2008.

[15] Javier Benitez Buelga. *Implementation of the Heated Pulsed Theory using actively heated fiber optics: measurements of soil volumetric water content and soil volumetric heat capacity.* PhD thesis, Agronomos, 2014.

[16] Emilio Custodio, Manuel Ramon Llamas, et al. *Hidrología subterránea*, volume 1. Omega Barcelona, 1976.

[17] Xavier Oliver Olivella and Carlos Agelet de Saracíbar Bosch. *Mecánica de medios continuos para ingenieros.* Univ. Politèc. de Catalunya, 2002.

[18] Pooyan Dadvand, Riccardo Rossi, and Eugenio Oñate. An object-oriented environment for developing finite element codes for multi-disciplinary applications. *Archives of computational methods in engineering*, 17(3):253–297, 2010.

[19] Rubén Otín, Javier Mora, and Eugenio Onate. Emant: integration of gid and kratos, open and flexible computational tools. In *IEEE/ACES International Conference on Wireless Communications and Applied Computational Electromagnetics, 2005.*, pages 883–886. IEEE, 2005.

[20] Ramon Ribó, MAR Pasenau, Enrique Escolano, JSP Ronda, and LF González. Gid reference manual. *CIMNE, Barcelona*, 1998.